UNIVERSITY OF
Southampton

University of Southampton Research Repository
ePrints Soton

http://eprints.soton.ac.uk

UNIVETRSITY OF SOUTHAMPTON

Faculty of Physics and Applied Sciences

School of Electronics and Computer Science

**The Effects of Crosslinking Byproducts on the Electrical Properties
of Low Density Polyethylene**

by

Nuriziani Hussin

A thesis submitted for the degree of Doctor of Philosophy

September 2011

UNIVERSITY OF SOUTHAMPTON

ABSTRACT

FACULTY OF PHYSICS AND APPLIED SCIENCES

A thesis submitted for PhD

THE EFFECT OF CROSSLINKING BYPRODUCTS ON THE ELECTRICAL
PROPERTIES OF LOW DENSITY POLYETHYLENE

By Nuriziani Hussin

Crosslinked polyethylene (XLPE) is widely used for high voltage insulation in power
transmission systems. However, it has been found that, after crosslinking with Dicumyl
Peroxide (DCP), the crosslinking byproducts such as acetophenone, α-methylstyrene and
cumyl alcohol have a significant influence on electrical properties of XLPE power cables.
This thesis distinguished the individual contribution of the crosslinking byproducts on
space charge formation, dielectric properties, dc conductivity as well as the ac breakdown
strength. Percentage weight increases as well as the Fourier Transform Infrared (FTIR)
spectrum were used to monitor the chemical level in the soaked samples. Despite high
concentration of byproducts in the LDPE film compared to practical, the measurement
results have successfully reveal the contribution of each byproduct on the electrical
properties. It should be noted that some consideration should be taken when taking the
quantitative value from the result obtained.

Space charge accumulation was measured using the pulsed electroacoustic (PEA)
technique. Homocharges are observed in acetophenone and α-methylstyrene soaked
LDPE. Meanwhile heterocharge formed in cumyl alcohol soaked LDPE. From the charge
decay profile in dc condition, these chemicals are observed to assist the transportation of
the charges in the sample bulk due to shallow traps from the byproducts. These shallow
traps assist the trapping process into deep traps when ac field is applied to the byproduct
soaked LDPE. As a result, more charges trapped in deep traps were found in soaked LDPE
compared to clean LDPE. In addition, from the space charge measurement in ac condition,

it is proved that the amount of charge trapped in deep traps also depends on the population of shallow traps in the polymer which is contradicted to the literature where the byproducts are normally associated to the deep traps.

Permittivity values of acetophenone, α-methylstyrene soaked LDPE and cumyl alcohol are slightly higher than permittivity value of the clean untreated LDPE. Cumyl alcohol soaked LDPE has higher dielectric loss at lower frequency due to Maxwell-Wagner-Sillars polarisation as well as space charge polarisation effect. In contrast, acetophenone does not change the dielectric loss value and α-methylstyrene gives very little effect. These byproducts have very high dc conductivity values. It is also proposed that the chemicals provide shallow traps that aid the charge movement and this is consistent with the mobility values that calculated from the conduction current result. The ac breakdown results however show no significant difference from the breakdown strength of clean LDPE. Based on ac space charge results and ac breakdown test results, it is concluded that the byproducts have little effects in ac condition.

Contents

List of Figures

XI

XII

List of Tables

Authors Declaration

I, Nuriziani Hussin, declare that the thesis entitled "The Effects of Crosslinking Byproducts on The Electrical Properties of Low Density Polyethylene", and the work presented in the thesis are both my own and have been generated by me as a result of my own original research. I confirm that:

1. This work was done wholly in candidature for a research degree at the University of Southampton;

2. Where any part of this thesis has previously been submitted for a degree or any other qualification at the University of Southampton or any other institution, that this has been clearly attributed;

3. Where I have consulted the published work of others, this is always clearly attributed;

4. Where the work of others has been quoted the source is always given, and with the exception of such quotations this thesis is entirely my own work;

5. I have acknowledged all main sources of help;

6. Where the thesis is based on work done by myself jointly with others, I have made clear exactly what contributions were my own; Some of this work have been published as:

- Hussin, N. and Chen, G. (2008) *The Effect of Acetophenone and alpha-Methylstyrene on the Space Charge Properties of Low Density Polyethylene*. In: *Conference on Electrical Insulation and Dielectric Phenomena*, 26-29 October 2008, Quebec, Canada. pp. 702-705. (Published)

- Hussin, N. and Chen, G. (2009) *The trapping characteristic of low density polyethylene in the presence of crosslinking by-products. Journal of Physics: Conference Series*, 183. 012007. ISSN 1742-6596 (Published)

- Hussin, N. and Chen, G. (2009) *Modification of Space Charge Pattern and Charge Mobility of Low Density Polyethylene (LDPE) in the presence of Crosslinking Byproducts*. In: *The 9th International Conference on Properties and Applications of Dielectric Materials*, 19 - 23 July 2009, Harbin, China. pp. 950-953. (Published)

- Hussin, N and Chen, G (2009) *Analysis of Space Charge Formation in LDPE in the Presence of Crosslinking Byproducts*. Submitted to IEEE *Journal of Transactions on Dielectrics and Electrical Insulation* (Accepted)

- Hussin, N and Chen, G (2010) *Space Charge Accumulation and Conductivity of Crosslinking Byproducts Soaked LDPE*. In: *Conference on Electrical Insulation and Dielectric Phenomena*, 17-20 October 2010. West Lafayette, USA. (Published)

- Hussin, N. and Chen, G. (2011) *AC Breakdown Characteristics of LDPE in the Presence of Crosslinking By-products*. In: *UHVnet 2011*, 18-19 January 2011, Winchester, UK. p. 66. (Poster presentation)

- Hussin, N., Zhau, J. and Chen, G. (2011) *Space Charge and AC Breakdown Characteristics of Crosslinking Byproducts Soaked LDPE*. In 2011 *International Symposium on Electrical Insulating Materials*, Japan. (Accepted)

Signed: _ Date: _ _ _ _ _ _ _ _ _ _ _

Acknowledgements

First and foremost, my upmost gratitude goes to God for all the blessings and mercy, which helped me cope through this research.

The preparation of this important research would not have been possible without the support, hard work and endless efforts of a large number of individuals.

I would like to give my deepest thanks to my supervisor, Dr George Chen for his continuous support in this research. George was always there to listen and advise. He guided and assisted me to solve the problems encountered. He has been friend and mentor.

I also thank my colleagues from the EPE Group, especially Wilson, Zhi Qiang, Martin, Ian, Jerry, Celia and Nikky for their help in assisting me with the lab equipments and understanding some principles of this research. They were always there to help and made this PhD life fun!

I am also grateful to my husband, Muhamad Humaizi Talib for all his love, care, patience and support. Let me say 'Thank you' to my parents Hussin Hamid and Zaliaha Supian, as well as my siblings in Malaysia for all their endless prayers and thought that motivate me to finish this research. Without you I will never be here! Thank you all!

Definitions and Abbreviations Used

Definitions

E	Electric field (V/m)
V	Voltage/potential (V)
i(t)	Current (A)
u	Velocity field
t	Time
e	Electron charge
eV	Electron volt
ε_o	Permittivity of vacuum
ε_r	Relative permittivity
ε'	Dielectric constant / real permittivity
ε''	Imaginary part of permittivity
ε^*	Complex permittivity
ε'_0	Real permittivity at zero frequency
ε'_∞	Real permittivity at limiting high frequency
$\tan \delta$	Dielectric loss tangent
ρ	Charge density (C/mm^3)
φ	Thermal activation energy (eV)
Φ	Potential barrier
μ	Mobility (m^2/Vs)
σ	Conductivity (S/m)
T	Temperature (ºK)
$e_p(t)$	Pulse voltage (V)
P(x,t)	Pressure pulse

$\rho(x,t)$	Total charge density (C/m^3)
$q(x,t)$	Total charge (C)
k	Boltzmann constant $(8.62 \times 10^{-5} \text{ eV/K})$
h	Plank's constant
f	Frequency
ω	Angular frequency
J	Current density
m	Mass
d	Thickness
D_n	Fick's diffusion coefficient
n	Number density of charge
f_{pulse}	Pulse generator frequency
f_{ac}	Alternating current frequency
E_s/V_s	Stressing Field / Voltage in PEA measurement
V_p	Pulse voltage in PEA measurement
C*	Complex capacitance
C_0	Capacitance in air gap
Z	Impedance
R	Resistance
α	Weibull scale parameter
β	Weibull shape parameter

Abbreviations

PE	Polyethylene
LDPE	Low density polyethylene
XLPE	Cross-linked polyethylene
DCP	Dicumyl peroxide
HDPE	High density polyethylene
MDPE	Medium density polyethylene
TR-XLPE	Tree retarded crosslinked polyethylene
C	Carbon

H	Hydrogen
O	Oxygen
Si	Silane
Al	Aluminium
DC or d.c	Direct current
AC or a.c	Alternating current
HV	High voltage
HVAC	High voltage alternating current
HVDC	High voltage direct current
LIMM	Laser intensity modulation method
LIPP	Laser induced pressure pulse
LLDPE	Linear low density polyethylene
PEA	Pulsed electro-acoustic
TSM	Thermal Step method
PMMA	Polyethyl methacrylate
PVDF	Polyvinylidene fluoride
SCLC	Space charge limited current
V_{TFL}	Trap-filled-limit
FFT	Fast Fourier transforms
IFFT	Inverse Fast Fourier transforms
GPIB	General Purpose interface bus
TTL	Transistor-transistor logic
GPIB	General Purpose interface bus
STP	Shielded twisted pair
BNC	Bayonet Neill concelma
FTIR	Fourier transforms infrared
OS	Open system
CS	Close system
Volt off	Measurement during short circuit
Volt on	Measurement during close circuit
a+α	acetophenone plus α-methylstyrene in LDPE
a+c	acetophenone plus cumyl alcohol in LDPE
α+c	α-methylstyrene plus cumyl alcohol in LDPE

Chapter 1   Introduction

1.1   Overview of Research

The development of underground cable started with the telegraph lines. The earliest use of continuously insulated conductor was recorded in 1812 by B. Schilling when an electrical pulse was sent through a cable insulated with strips of India rubber. It was then expanded into the electrical lighting system where a steady flow of a considerable amount of energy was needed. T. A. Edison who planned his first installation for New York City decided to have an underground system distribution. During his time, copper rods insulated with wrapping of jute were used. This design gave a pleasing performance for low voltage service. This power distribution is still limited to the area capable of being supplied from one source if the regulation did not exceed the maximum bound.

In 1882, ac distribution was employed by L. Gaulard and J. D. Gibbs and during the early installation, the cable operated at 2,000 volt, the overhead was used due to their satisfactory performance and almost universally employed. In Washington and Chicago, overhead wires were prohibited, hence a number of underground lines were emplaced. Many insulation and method of installation were tried but the successfulness was little. However, in 1890, Ferranti had successfully installed the first line insulated with paper between Deptford to London for single-phase operation at 10,000 volt and some were still in use at the original voltage after more than 50 years. The conductors were insulated with wide strips of paper applied helically around the conductor before saturated with rosin-based oil.

Impregnated paper became most universal form of insulation cable for underground transmission due to its low dielectric loss, low dissipation factor and high dielectric strength. Impregnated paper insulation consists of several layers of paper tapes, wrapped helically around the conductor. The total wall of papers is subsequently heated, vacuum dried and impregnated with an insulating fluid. The impregnating fluid used changed from time to time. Circa 1925, impregnating compound changed from rosin-based compound to mineral oil or oil blended to obtain higher viscosity. Around 1983, polybutene replaced oil as the insulating fluid. The reliability of paper insulated as the insulating material was excellent. However, it required a high degree skill for appropriate splicing and terminating.

The insulation of cable system is then shifted towards polymer, particularly polyethylene (PE), as more development and research done in that area. Low Density Polyethylene (LDPE) was mainly used in the cable insulation system for its low cost, moisture and chemicals resistance, low temperature flexibility and excellent electrical properties. However, power cables typically operate at high temperatures and hence the insulation surrounding the conductor is subjected to elevated temperatures and a temperature gradient. With a melting point approximately at 110ºC, LDPE could not operate in the temperature range for paper-oil insulated cable. During the last decade, the voltage rating for underground cable has become increased due to higher electrical usage. In the future, the electrical stress will become increase and hence, the need for a better polymer that could withstand higher electrical stress has become vital.

1.1.1   *High Voltage Cable*

It was stated by the International Electrotechnical Commission (IEC 502) that the standard for HV level is the range of 35 kV <V<230 kV [1]. A full detail on the range of different voltage level is presented in Table 1-1. Different type and thickness of insulation material is used for each operating voltage due to the thermal and mechanical properties of the material. For example, based on IEC 502 specification, at rated voltage of 20kV, the insulation thickness for XLPE cable is 5.5mm meanwhile for PVC cable is 6.4mm. However not all countries follow the IEC standard. In country like Japan, the insulation thickness specified by the national standard for XLPE insulated cables is greater than the

IEC but for export purpose, the IEC value is followed. In USA, which have different voltage rating, the IEC standard for insulation thickness is not applicable [2].

Table 1-1: Classification of the operating voltage levels [1].

System	Nominal voltage (V_r) kV
Low Voltage (LV)	$V_r < 1$
Medium Voltage (MV)	$1 < V_r < 35$
High Voltage (HV)	$35 < V_r < 230$
Extra High Voltage (EHV)	$230 < V_r < 800$

In 1955, Crosslinked polyethylene (XLPE) was first patented and with the crosslinking technique, the thermal stability of PE is improved [3]. XLPE has now been used widely in high voltage insulation system. Compared to LDPE, XLPE has slightly higher dielectric loss, lasts longer and shows less moisture sensitive [4]. Cables with XLPE insulation for operating voltage up to 132 kV have now has been established widely. The use of metallic barrier which usually an extruded sheath has been introduced to avoid the incidence of water trees in the cable. The incentive of using XLPE has allow the cable to operate at 90°C compared to 70°C for LDPE and 80°C for HDPE [2].

Despite of its ability to withstand high temperature, it is undeniable that XLPE has some other weaknesses as a cable insulator. Easy accumulation of space charge in XLPE for instance, become the main anxiety in employing this material in insulation system [5]. It was considered that the crosslinking byproducts of well used crosslinking agent, Dicumyl Peroxide (DCP), antioxidant or the crosslink polymer morphology could generate space charge in the insulation material [6]. Through research N. Hirai reported that the crosslinked structure has no distinct trapping property [7]. Sulphur-containing antioxidant in the combination effect of acetophenone creates heterocharges [8]. The antioxidant by itself cannot trap any charges in the bulk. The trapping of the free radical from the crosslinking process is sometime inevitable, due to viscosity effect. As a result, the crosslinking is not completed and the residual peroxide as well as the byproducts could become a major factor to degradation process.

3

DCP which is widely used as the crosslinking agent creates volatile crosslinking by-products such as acetophenone, cumyl alcohol, α-methylstyrene and cumene which also affect the insulation properties. These byproducts are said to cause charges trapped in the XLPE. Other than causing space charge formation in the sample, the byproducts also have an effect on other electrical properties of XLPE like increasing the tan δ value, temporary increase in breakdown strength, and so forth [3].

In practice, degassing is introduced after the crosslinking process to remove the crosslinking byproducts from the insulation by subjecting the XLPE cable to moderately high temperature for a certain period. Ideally it is possible to remove all byproducts in all sample. However the times involved are rather long even for small cable. For example, it took 500 hours for acetophenone to be degassed to 10% of its' original concentration in an average MV cable (approximately 5.5mm thick) [3]. Although degassing can occur freely from the outer surface of the insulation, the process is constrained from the inner surface. Hence the byproducts are more likely to stay in the insulation nearer to the conductor. Degassing process may take longer for a thicker sample and even much slower as the outer insulation shield (semiconductor shield) is added to the cable. Temperature could be increased to fasten the degassing process. However, without extra care, very high temperature may result to damage to the core through thermal expansion and softening the insulator. In addition, it was reported that degassing may also change the morphology of the dielectric [9].

1.2   Research Objective and Aims

It is clear that the main advantages of XLPE are its good electrical, mechanical and thermal properties. However, due to the existence of the impurities in XLPE including the crosslinking byproducts, researches have now looking for other material that could match the excellent properties of XLPE. However, the knowledge that we have on each of the impurities and how they actually cause problem is very little. It is believed that by understanding on how these individual impurities, in this case the crosslinking byproducts affect the electrical properties of XLPE, some improvement could be done on the conventional XLPE cable. Research on the effect of water molecules on the formation of water treeing in XLPE has lead to the production tree-retarded crosslinked polyethylene

(TR-XLPE). It is hope that by doing this research, comparable improvement could be made on XLPE cable.

Each and every byproduct in XLPE affect differently to the polymer's electrical properties and thus, the experiments will be conducted so that the effect of each of the byproducts can be distinguished. XLPE film consisted of a few parts which are the crosslinked chains, un-crosslinked chains, peroxides, volatile crosslinking byproducts, antioxidant as well as stabilizer. Each of the XLPE part may affect the electrical properties differently. On the basis of understanding the individual contribution of the crosslinking byproducts, it is important to have very consistent polymer base for the byproducts to reside in order to have a fair comparison between the byproducts. Due to that, instead of using XLPE as the base polymer, LDPE is chosen.

In this research, a few objectives have been outlined;

1. Crosslinking byproducts are known to be one of the major sources of space charge accumulation. It is hoped that by investigating the space charge profile of crosslinking byproducts in LDPE will give some understanding on the mechanism of charge formation in the polymer. Through space charge measurement, the trapping characteristics of polymer as well as the crosslinking byproducts could be revealed. We are hopping that by studying space charge profile during dc and ac stressing will give more understanding on how the electric field affects the trapping behaviour.

2. For any material to become a good insulator, the dielectric constant along with dielectric loss value should be low. Investigation on the dielectric spectroscopy of the crosslinking byproducts will tell us how this additives affecting these values. Also, from this measurement, the polarisation process that happens in the byproduct soaked sample could be studied.

3. An excellent insulation will have very small conductivity and most of the current is due to capacitive charging current that will decay by time. In this thesis, we aim to

study the changes in the conductivity value of LDPE in the presence of the crosslinking byproducts. From the result, we are aiming to calculate the mobility of the carriers in each byproducts soaked sample.

4. It is common to associate the space charge formation with breakdown strength of the polymer. After all, this is one of the reasons why space charge accumulation is unfavourable in cable insulation. Here, we are intended to compare the breakdown strength of the dielectrics with and without the byproducts. Hopefully we could see here to what extend these byproducts affecting the breakdown strength value.

5. From the results that obtained from all measurements stated above, we are aiming to compare the characteristics of each of the byproducts and how they individually influence the electrical properties of the LDPE.

1.3   Thesis Outline

This thesis consisted of a few chapters that are arranged as follows.

Chapter 1 outlines the overview of the research as well as the objectives of the work.

Chapter 2 presents the details about the material that will be used in this research, which is polyethylene. This chapter includes background knowledge on the crosslinking process and introduction to the crosslinking byproducts.

Since the main problem caused by the crosslinking byproducts is the space charge formation, **Chapter 3** describes the space charge phenomenon in the polymer including the conduction mechanism in polymer.

In **Chapter 4** the techniques used to measure space charge are explained and the fundamental concepts of the measurements are also presented.

In **Chapter 5**, the sample preparation which explains about the soaking process is reported. The similar procedures are applied to all samples before any measurement is conducted. In other words, this chapter will be referred by other chapters to explain on the samples that were used in the measurement.

Chapter 6 describes the space charge characteristics of the clean and soaked samples at dc and ac fields. Charge decay profiles of the samples are used to understand the trapping characteristics of the byproducts soaked LDPE.

Chapter 7 shows the dielectric spectroscopy of the liquid byproducts, clean LDPE as well as soaked LDPE. The results are compared and the polarisation effect is observed from the dielectric spectrum.

Conduction current measurement is presented in **Chapter 8**. In this chapter, the conductivity result is being related to the results obtained in space charge measurement. Also, the mobility of the carriers is calculated and compared.

Chapter 9 describes the breakdown measurement of the byproducts soaked LDPE. Results in this chapter will also be linked to the space charge results from Chapter 6.

Last but not least, **Chapter 10** presents the conclusions and future work for this research.

Chapter 2   Polyethylene

2.1   Introduction

Polyethylene is produced since 1936 and until now, it becomes the most popular material used for insulation. It is produced at pressure up to thousand atmospheres, which gives a polymer of single chain type but with short branches along the main chain. Polyethylene is created from polymerization of ethylene where in this process the double bond in ethylene between carbon atoms is opened up and forms a long carbon chain, as shown in Figure 2-1.

$$\sim CH_2 = CH_2 \sim \quad \Longrightarrow \quad \sim CH_2\text{-} CH_2\text{-} CH_2\text{-} CH_2\text{-} CH_2 \sim$$

Ethylene (gas)   **Polyethylene (solid)**
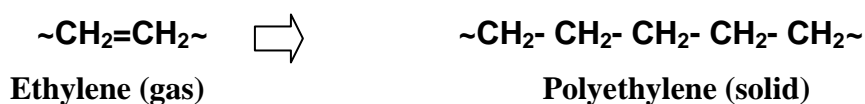
Figure 2-1: The formation of polyethylene from ethylene.

As a thermoplastic, polyethylene melts to a liquid when heated and freezes to a brittle, very glassy state when cooled sufficiently. Polyethylene is categorized into groups by its density and branching. The density of PE is actually a measure of crystallinity. In term of manufacture, PE is classified into 'high density', 'medium density', 'low density' or 'linear low density'. Method of polyethylene manufacture controls the exact chemical structure, which in turn controls the properties of PE. The polymer chain is not always linear. In polymerization, the process always leads to side chain attached to the long main chain. This is called chain branching and it contributes to the increase of molecular weight. The length and the distribution on the branches affect physical properties as well as the ability of the PE to crystallize.
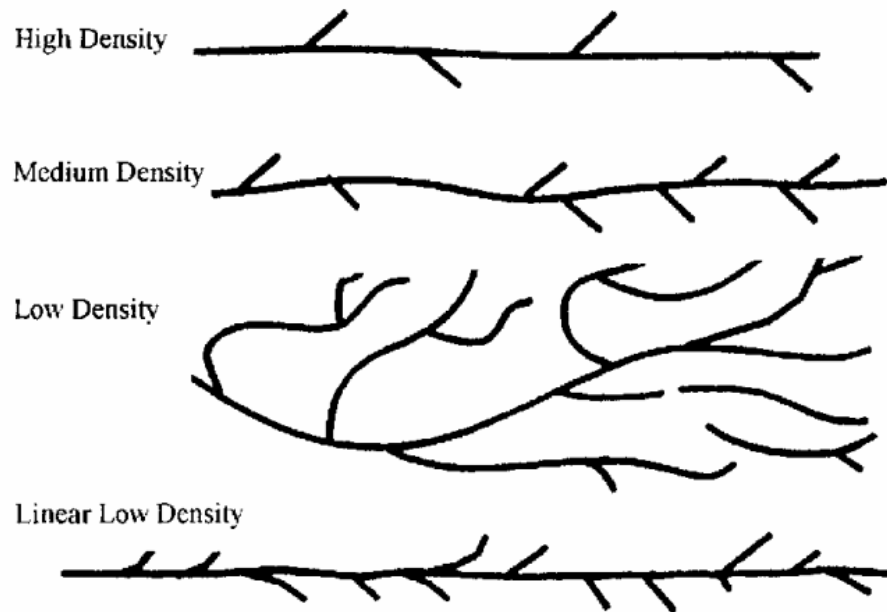
Figure 2-2: Structure of polyethylene [4].

In reality, chains in PE are not 'straight' as in Figure 2-2 above. The polymer has high tendency to coil or in other words, has a random configuration which is influenced by the branching. These entanglements will contribute to some resistance to movement when the chains are pulled apart. Hence, the entanglements influence the mechanical properties of the polymer. The ability of the polymer chain to coil as well as tendency to align themselves relative to each other, make PE grouped into the semicrystalline polymer. The chain portions that are aligned is called 'crystalline' and the chain portions that coil are described as 'amorphous' as illustrated in Figure 2-3.
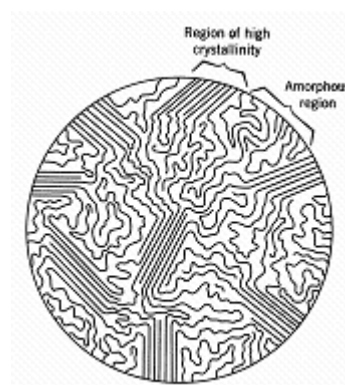
Figure 2-3: Crystalline and amorphous regions [10].

The crystalline regions give PE many good properties for cable insulation, such as toughness, high modulus and moisture and gas permeation resistance. The 'tighter' chain packing in the aligned portions also increases the density of the polymer. Hence, increased crystallinity also depicts higher density. On the other hand, amorphous regions increase the flexibility, ductility and facilitate processing.

High Density Polyethylene (HDPE) for instance, has a density range of greater or equal to 0.941 g/cm^3. With low degree of branching, HDPE has a stronger intermolecular forces and tensile strength. It is used in products and packaging such as containers, folding chairs, storage sheds and water pipes. Medium Density Polyethylene (MDPE) with a density of 0.926-0.940 g/cm^3 is normally used in gas pipes and fittings, sacks, shrink film, packaging film, carrier bags and screw closures [11]. Due to their stiffness which makes them difficult to handle, HDPE and MDPE are not suitable for cable insulation.

Low Density Polyethylene (LDPE) is one of the favourite materials used for insulation. LDPE has a density range of 0.910 - 0.925 g/cm³ and is generally 50-60% crystalline [12]. Compared to HDPE, LDPE has more branching and thus, it has weaker intermolecular forces, lower tensile strength and higher ductility. Its excellent properties such as low dielectric loss, high dielectric strength, chemical inertness, low moisture up-take and ease of extrusion, make it easy to use in many kinds of telecom and power applications.

Table 2-1: General properties of LDPE [13].

Properties	Values
Molecular Weight	28.0 g/mol
Dielectric constant at 1MHz	2.2-2.35
Dielectric strength	27 kV mm^{-1}
Coefficient of thermal expansion	$(100-200)\times10^{-6}$ K^{-1}
Thermal conductivity at 23°C	0.33 W m^{-1} K^{-1}

Table 2-1 shows some general properties of LDPE. The discrepancy between LDPE and Linear Low Density Polyethylene (LLDPE) is the absence of long chain branches in

LLDPE due to different manufacturing process in both LDPE and LLDPE. Although LLDPE has higher tensile strength and puncture resistance than LDPE, LLDPE is more difficult to process compared to LDPE. One disadvantage of LDPE is its low melting point which makes it unsuitable for high voltage cable insulation. However, with research developments, a polymer that has almost the same electrical properties as LDPE and can withstand higher temperature was produced.

2.2   The Crosslinking Polyethylene

Crosslinking process is a process of joining different polyethylene chain together by chemical reaction. The crosslinking of LDPE with Dicumyl Peroxide (DCP) to form XLPE was first accomplished by Gilbert and Precopio in 1955. XLPE can be considered to a branched PE with the end of the branches are connected to a different PE chain. Figure 2-4 shows the fundamental crosslinking process in polymer.
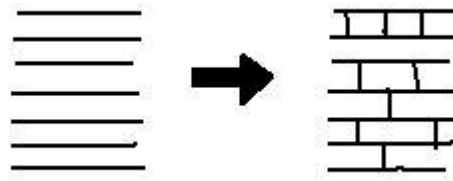
Figure 2-4: Simplified description of crosslink network [4].

Crosslinking process retains the electrical properties of LDPE and at the same time improves certain properties of PE. Such properties are resistance to deformation and stress-cracking as well as improve tensile strength and modulus. Usually, antioxidant is added in the crosslinking process to prevent oxidative degradation to happen. If the oxidative degradation is significant, it may be harmful as it can lead to chemical changes within the insulation that could introduce more polar material which in turn, may change the electrical properties that prone to failure during ageing [4]. There are a few crosslinking mechanisms that are used in manufacture which are the high energy radiation-induced crosslinking, silane-induced crosslinking, and peroxide-induced crosslinking.

2.2.1 *High Energy Radiation-Induced Crosslinking*

A beam of electrons emanating from special equipment can interact with the polymer chains and form free radicals. These reactive radicals interact with other chains and hence induce crosslinking. In this radiation crosslinking process, the high energy electrons interact with the polymer chain and cleave the C-H or C-C bond. When C-H bond is broken, one hydrogen atom is released and ~C· radical tries to stabilize itself by combining with other radicals hence provides the crosslinking. The hydrogen atom combines with another hydrogen atom to form hydrogen gas. The radiation process is performed at room temperature which means polymer structure is in both crystalline and amorphous state [4]. Radiation-induced crosslinking is employed primarily for low voltage cable where the speed of crosslinking is a key issue. One weakness found in radiation-induced crosslinking is the non-uniformity of energy absorbed by thick specimen. The total energy absorbed is depending upon the electron beam energy. Therefore the degree of crosslinking by electron beam technology is not uniform within the component thickness and depends on the geometry. However, radiation-induced crosslinking do not produce any byproduct that stay in the polyethylene.

2.2.2 *Silane-Induced Crosslinking*
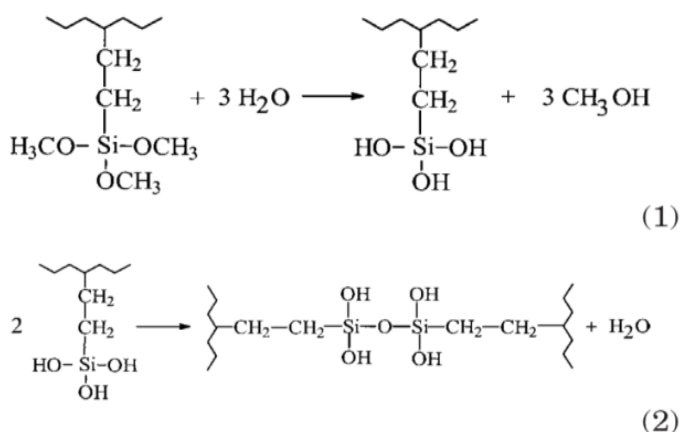
Figure 2-5: Silane-induced crosslinking process [14]. (1) The crosslinking reactions of silane-grafted polyethylene through the hydrolysis of silyl trimethoxy groups with water. (2) Condensation of the formed silanol groups.

Silane-induced crosslinking is a method that employs "moisture curing". This type of crosslinking utilises the grafting of silane onto the PE and followed by the condensation reaction of silane graft by moisture [15]. The most common silane used in the manufacture is vinyl trimethoxysilane. The silane is commenced into PE by melt grafting using peroxide. Silane and peroxide are mixed together, compounded in an extruder at high temperature and immersed into water. Water induces chemical reaction leading to crosslinking [4,14]. The process is explained in Figure 2-5.

Silane-induced crosslinking has various advantages, such as easy processing, low cost and capital investment, and favourable properties in the processed materials. It also has less homocharge when stressed, lower conduction current, as well as has higher ac breakdown strength than peroxide crosslinked polyethylene [16]. However, this technique has been commonly employed for low voltage cables, as thicker cable insulation will take longer time for it to be crosslinked.

2.2.3 *Peroxide-induced Crosslinking*

The most common way in crosslinking polyethylene is through the use of peroxide agent. This organic peroxide agent is stable in room temperature but decompose at elevated temperature. For example, Dicumyl peroxide (DCP), which is well used peroxide for medium and high voltage cable [17], decomposed at 120°C [18]. The crosslinking agent is normally incorporated into PE pallets by the material supplier. After extrusion process (conversion of pallets into cable insulation), the PE is now surrounding the conductor and placed into a long curing tube where high temperature and pressure are applied. The PE is then melted and peroxide decomposes and induces the crosslinking process.

When DCP decomposes during curing process, the peroxide splits into active oxygen containing components and attract hydrogen atom from the polymer. As a result, it forms a free radical that is unstable. Polymer chain becomes active and unstable. Thus two such chains naturally combine to crosslink to stabilize the system and forms the XLPE [4]. During this process, several byproducts are formed from the peroxide and the major ones are methane, cumyl alcohol (dimethyl benzyl alcohol), acetophenone and α-methylstyrene.
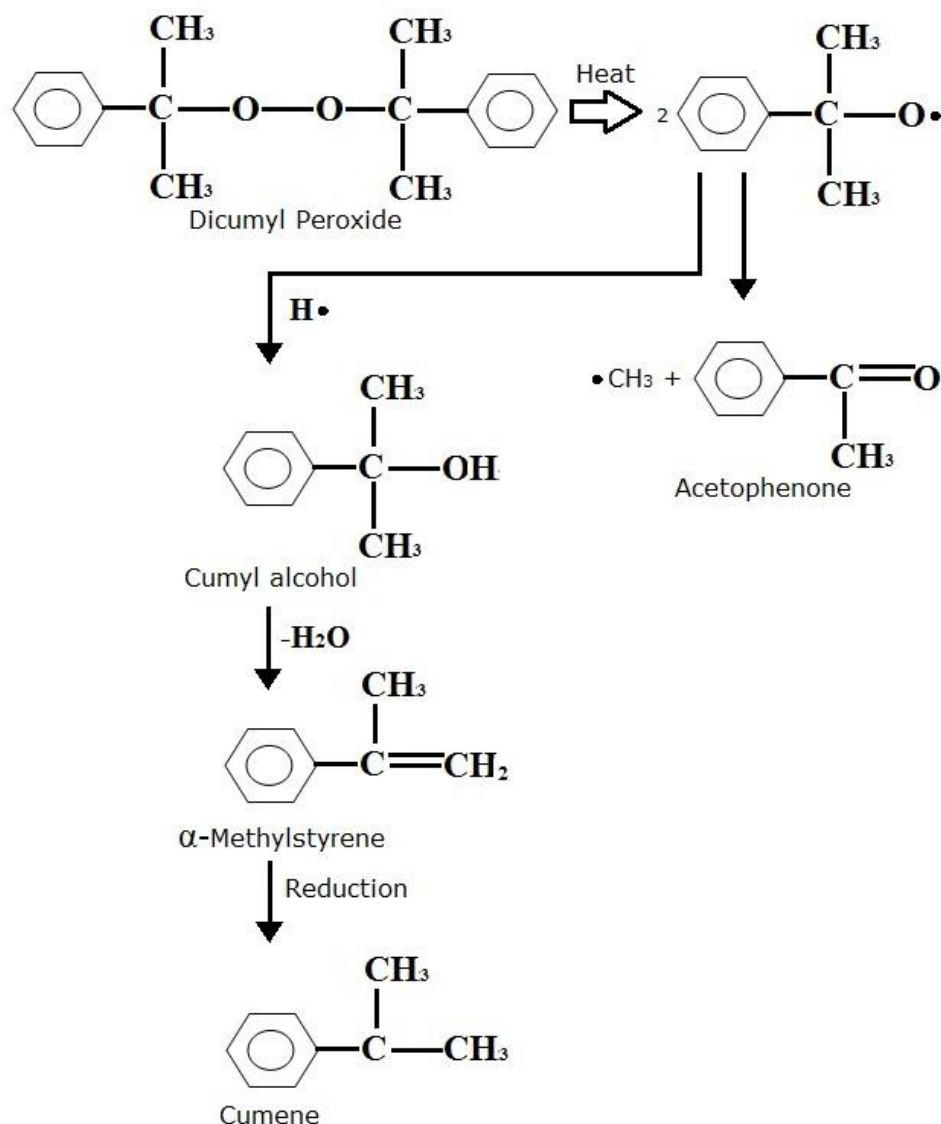
Figure 2-6 : Decomposition of DCP in crosslinking process producing byproducts.

When the free radical is generated, it will undergo 2 types of reaction to reach stabilisation. These 'roots' can be observed in the Figure 2-6. Firstly, the radical could rearrange itself and doffs a methyl radical to form acetophenone. The reactive methyl radical may also pick off a hydrogen atom from the polymer and forming methane gas. Secondly, the radical could also 'grab' the hydrogen atom from the PE chain and composes the relatively stable cumyl alcohol. Water may also form if the dicumyloxy radical expels a hydroxyl and hydrogen radical, to form water. As water is formed, the dicumyloxy radical converted to α-methylstyrene.

Cumyl Alcohol, acetophenone and methane are always found in greatest quantities in XLPE. Acetophenone is a liquid at ambient temperature due to its low melting point (approximately 20º C). It has somewhat sweet odour and not soluble in water and extent depending on the temperature. The methane gas must be allowed to readily protrude out of the freshly manufactured XLPE cable. α-methylstyrene could be found in smaller concentration. And sometimes, from further reaction of α-methylstyrene, another byproduct called cumene could be produced.

To ensure that the peroxide is uniformly dispersed which then means the cable is uniformly crosslinked, the temperature and pressure need to be properly controlled throughout the curing tube. This crosslinking process must happen in amorphous region, since the crystalline region cannot hold the peroxide preceding to the extrusion process. As the curing tube is heated, the whole polymer is amorphous and peroxide is considered uniformly dispersed. As the cable is cooled down, recrystallisation takes place and the byproducts are 'forced' into the new amorphous region.

2.2.4   *Tree Retarded Crosslinked Polyethylene (TR-XLPE)*

Numerous researches have been done to develop a better insulator. XLPE has been improved to be water treeing resistant. The earliest TR-XLPE cable made available in the early 1980s. A few approaches are proposed to achieve this property.

1. Replacing the polyethylene homo-polymer with a more polar copolymer.
2. Using an additive or placing additives into the homo-polymer (or co-polymer)
3. Using both of the options above

It was reported that there are high possibility for several additives present in the polymer. This additive serves as the agent to bind water molecules and provides the resistance to water tree. Acetophenone and dodecyl alcohol were found to facilitate resistance to treeing. Fillers may also trap water. Silane groups as we discussed before react with water. The overall aim here is to stop water from damaging the insulation by holding or trapping the water.

One issue appears in regarding TR-XLPE, on the definition of TR-XLPE or the degree of water tree retardancy. Although in this material, water tree growth has been removed along with the increment of AC breakdown strength compared to XLPE, one unclear issue is to what extend does the material has be improved in order to be considered 'tree-retardant' material. Table 2-2 compares the components that presence in XLPE and TR-XLPE

Table 2-2: Comparison between XLPE and TR-XLPE Insulated Cable

Components	XLPE	TR-XLPE
Tree Retardant Additives	No	Yes
Residual of DCP	Yes	Yes
Crosslinking byproducts		
Acetophenone	Yes	Yes
Cumyl alcohol	Yes	Yes
α-methylstyrene	Yes	Yes
Antioxidant + antioxidant byproducts	Yes	Yes

2.2.5 *Antioxidant*

During manufacturing process, it is usual for the insulation cable to undergo oxidative degradation. This process happens as the insulation temperature increases up to the level in which oxidation happens. If this happens, the molecular structure may change due to chemical reaction in the insulator hence introducing more polar molecules in the insulator. Antioxidant also changes the morphology of the polymer as it appears to have acted as a nucleating agent [19].
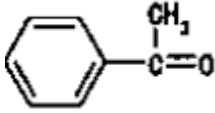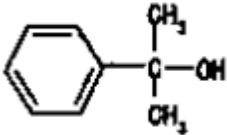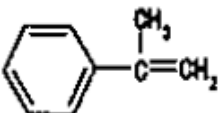
Antioxidant is incorporated into the polymer pallets to prevent the degradation mechanism process from happening. Antioxidant will naturally decompose in the extruder due to high thermal environment. At the beginning of curing process, the antioxidant will reside in the amorphous region. As the temperature increases, the crystalline melted and the antioxidant can migrate over the whole part of the molten polymer. During cooling process, the remaining un-reacted antioxidant as well as the non-volatile antioxidant degradation byproducts will inhabit in the amorphous region.

Many researches have been reported on the influence of antioxidant on electrical properties of XLPE. Goshowaki et. al in [20] reported that antioxidant containing sulphur has a great influence on the conductivity of XLPE. This measurement however was conducted on XLPE in which the conductivity value may be affected by the byproducts remaining in the XLPE. This hypothesis is in agreement with Sekii et. al in [21] who observed the formation of heterocharge in XLPE containing sulphur-base antioxidant. It is presumed that the heterocharge is created in the combine effect of the antioxidant and acetophenone. However reports in [22,23] stated that LDPE with antioxidant may generate deep traps or increase the deep trap density.

2.2.6 *Peroxide Crosslinking Byproducts*

Several properties of acetophenone, cumyl alcohol and α-methylstyrene are presented in Table 2-3.

Table 2-3: The physical properties of the chemical byproducts.

Chemical Byproducts	Acetophenone	Cumyl Alcohol	α-methylstyrene
Chemical Structure			
%wt in cable [3]	0.6%	1.2%	0.02%
Melting point	19 - 20 °C	32-34 °C	-24°C
Boiling Point	198 - 204 °C	88-90°C	164-168 °C
Dielectric constant	17	9.7	3.8
Conductivity	2.4×10^{-4} S/m	1.4×10^{-7} S/m	3.6×10^{-9} S/m
Appearance	-clear to light yellow liquid -slightly soluble in water -Sweet odour	-Clear slightly yellow liquid -Insoluble in water	-Colourless clear liquid

A lot of researches have been done to investigate the properties of the byproducts in the performance of XLPE cable. There were various papers reporting on the contribution of crosslinking byproducts on the performance of XLPE and quite a number of them detailed the research on each of the byproducts. And these researches relate the decomposition of DCP with various electrical properties. For instance, Aida et al compared how each of the byproducts influence tan δ value [24]. At low electrical stress, tan δ value does not alter by adding the additives. However, this value is increased at high electrical stress region [25]. Limited sources have discussed on the effect of these byproducts on the breakdown. As in [3,26,27] the authors showed that short term AC breakdown strength of XLPE is improved with the presence of these chemicals. However, there are also some authors reported no significant effect of AC breakdown strength due to their existence in polymer [28].

Nevertheless, the effects of crosslinking byproducts on the accumulation of space charge were the most reported of all. Heterocharges were said to be observed in the bulk of the untreated XLPE [29-32]. The accumulation of heterocharges is explained by the mechanism of ion-pair separation from the byproducts [30]. However, the space charge accumulation was also associated with the production of water in the decomposition of cumyl alcohol [3,33]. The hole injection gets enhanced due to the increase of water content. This is considered to be the presence of water ions (H_3O^+) [34]. However, the main cause for heterocharges formation is the crosslinking byproducts in the XLPE.

T. Ohara et. al in [35] that focuses on the acetophenone suggested that this byproduct increases the conductivity of the soaked LDPE. By using the coated sample, they proved that holes are moving towards the uncoated side. Acetophenone changes the σ/ϵ value which causing charge accumulation at the interface of soaked and un-soaked sample. Same result was observed by Y. Ohki et. al, and from calculation, acetophenone soaked LDPE was said to have higher conductivity than α-methylstyrene soaked LDPE which are 10^{13} and 10^6 times of un-soaked sample, respectively [5]. And due to the difference in (σ/ε) at the interface of soaked and un-soaked sample, charges are generated at the interface. In the same paper, the authors concluded that positive charge migration in the LDPE soaked in α-methylstyrene is faster than the one soaked in acetophenone due to the permeation velocity in LDPE.

In most of the reports, acetophenone and α-methylstyrene give no effect on the space charge formation. It was said that the chemicals accelerate the charges transportation in LDPE thus leave no charge in LDPE [7,36,37]. It was also said that acetophenone reduces the injection barriers and enhance the charge injection [38]. However, heterocharges were observed when water molecule and acetophenone present in LDPE. Hirai et. al in [36] reported that the conduction current for acetophenone or α-methylstyrene decreases with time, unlike the conduction current for cumyl alcohol that initially increases, and then decreases with time. However, despite of its high conduction current, cumyl alcohol was observed to cause deep traps in soaked LDPE sample. This observation is also reported in other papers. The formation of homocharge can be observed as deep traps from cumyl alcohol trap the charges injected from the electrodes [39].

2.3 Chapter Summary

In this chapter the fundamental theory of polymer particularly PE is presented. PE is graded based on its' density with each density of PE is useful for different usage. Later, when crosslinking process is introduced, XLPE has become an alternative to the oil impregnated paper for cable insulation for higher voltage cable. Table 2-4 presents the comparison between the types of crosslinking available.

Table 2-4: Comparison of the crosslinking technique.

Criteria	Crosslinking type		
	High Energy Radiation	Silane	Peroxide
Operating temperature	Room temperature	Room temperature	>120°C
Byproducts	-	-	Acetophenone, methane, α-methylstyrene, cumyl alcohol, cumene
Advantages	-No byproduct	-does not need	-uniform crosslinked

	-crystalline region remain the same	curing tube or radiation equipment - no byproduct	structure across thickness -suitable for high voltage cable (thicker insulation)
Disadvantages	-Degree of crosslinking is not uniform across thickness -degradation process occur during crosslinking -only suitable for low voltage cable (small cable)	-Complex process -crosslinking period is too long (at room temperature) Crosslinking process may occur after the cable is manufactured -only suitable for low voltage cable (small cable)	-Formation of byproducts -require curing tube -must take place at amorphous region

Peroxide induced crosslinking has been the most popular crosslinking technique despite the formation of byproducts in the crosslinked structure. Peroxide induced crosslinking could offer a uniform crosslinking process in thicker sample which suitable for high voltage operation. In chapter 6, this type of crosslinking will be performed to produce XLPE sample for space charge measurement.

Chapter 3   Space Charge in Polymer

3.1   Introduction

From the context of dielectric material, the term 'space charge' corresponds to the carriers (electrons, holes and ions) that move around in the dielectric material by the applied field and become trapped in the material. Low charge carrier mobility and charge trapping within the polymer give rise to the space charge, leading to localised electric stress enhancement. The formation of space charge may distort the electrical field and distribution throughout the cable insulation thickness which may lead to the premature failure of the cable insulation at stresses below the anticipated value [30,32]. This condition becomes more severe during dc application. The strong correlation between the space charge and breakdown in cable insulation is reported in [40] where the evidence linking space charge build up, tree growth and breakdown in XLPE is presented. The presence of space charge is also linked to aging acceleration mediated by lowering of degradation process activation energy [41,42].

There are a few mechanisms of space charge formation in the polymer. Basically, space charge may result from;

i)   Charge injection and extraction from electrodes;
ii) Electric field assisted ionisation of impurities in the polymeric material or from an inhomogeneous polarization;
iii) Application of a mechanical/thermal stress.

For the purpose of this research, we will only focus on the effect of impurities in the polymer as the other variables such as type of electrodes, and mechanical/thermal stress will remain constant. Homocharges and heterocharges are terms that are often used to describe the polarities of the space charges. Homocharges refer to the charges with the same polarity to the adjacent electrode while heterocharges refer to the opposite polarity. When voltage is applied across the polymer, small molecules may become ionised and drift towards the electrode with opposite polarity which eventually produce heterocharges. This type of space charges will increase the stress at the electrode interface but reduce the electric stress in the bulk. Meanwhile, homocharges are usually formed from the charge injection or charge extraction near the electrode. Homocharges reduce the stress in the vicinity of the electrode interface but enhance the bulk stress [43].

3.2   Trapping and Detrapping

As voltage is applied across the polymer, all carriers experience the same force but they move with different velocities. These are what we called as fast and slow moving charges. The charge movement depends on the 'roots' at which it takes towards the electrode.

This phenomenon is possible with the existence of traps in the dielectric bulk. Localised states that results from assorted physical attributes such as broken bonds within the crystalline structure, chain branches, polarised states, dislocations foreign particles, crosslinking impurities and additives will act as traps to the charge carriers at energy states below the conduction band of the polymer. These traps for electrons are known as the acceptor and the traps for holes are known as donors. However, there are also traps that act as the recombination centres by trapping both electrons and holes [44,45].

The best way to describe traps is by the energy level diagram of polymer, which consists of a conductive band which is separated from the valence band by a huge forbidden gap (more than 7eV) [46] . It can be pictured as a potential well that exists in the energy diagram where it effectively acts as a potential barrier that obstructs the carrier movement in the conduction or valance band [47]. Generally, traps are divided into two types; deep

traps and shallow traps, depending on their depth. The former energetically located 0.8 to 1.4 eV below the conduction band and the latter is at 0.1 to 0.3 eV below the conduction band. Trapped charges normally reside longer in the deep traps and inevitably introduce space charge. Under the influence of the electric field the trapped charges may begin to detrap and move. Figure 3-1 shows the representation of the traps in electron energy diagram.
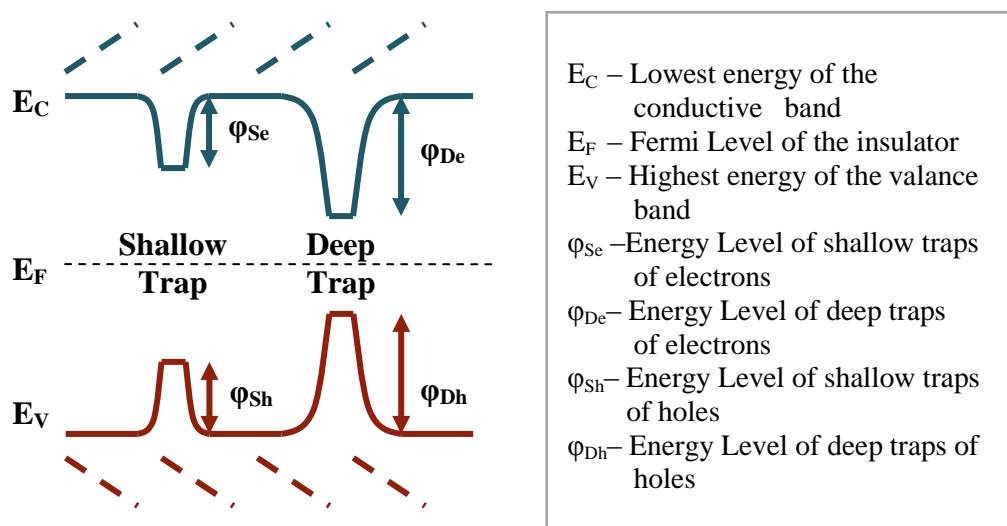
Figure 3-1: Schematic representation of shallow and deep traps in energy band diagram.

Basically, the slow moving charges are the charges which are trapped into the deep traps, while the fast moving charges are the free moving charges or charges that are trapped in the shallow traps.

When discussing about the charge transportation in insulating polymer, there are two parts need to be considered; the charge injection from the electrode and the high field conduction process in the bulk.
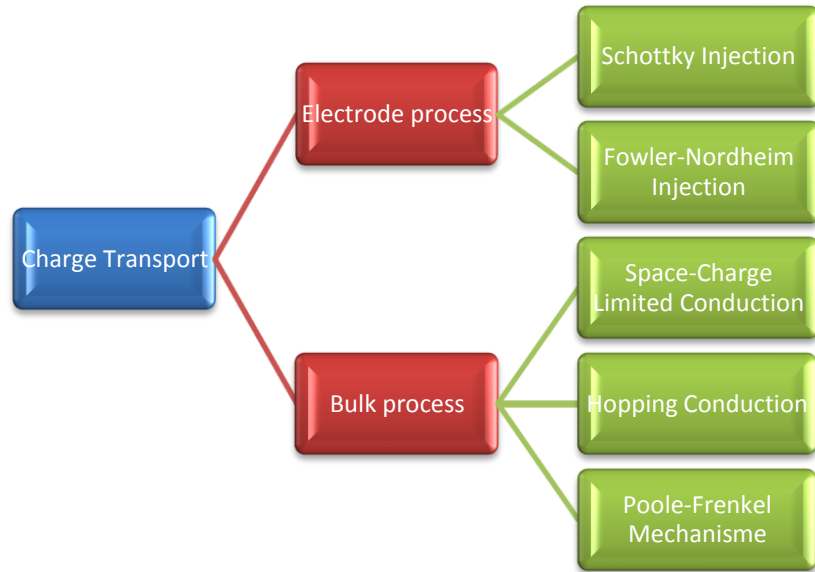
Figure 3-2: Charge transport mechanisms of electrode interface and in bulk process.

3.3 Electrode Process

3.3.1 *Schottky Injection*

Injection due to Schottky theory is based on the potential barrier height of the metal-insulator interface. This value depends on the type of interface, In the case of metal-vacuum boundary, barrier height equal to the work function of the metal. However for metal-dielectric interface, the barrier height depends on the metal-dielectric work function difference as well as the local condition of the electric polarisation. [43].

In the simple band structure, the barrier between metal and insulation is assumed to be precipitous as shown in Figure 3-3 (a). However in Schottky injection theory, the barrier height is reduced by the electrostatic attraction between the electron and metal. In this case, the metal is positively charge as it loss an electron to the dielectric. As a result, the barrier height is constantly changed due to the potential energy of the electron.
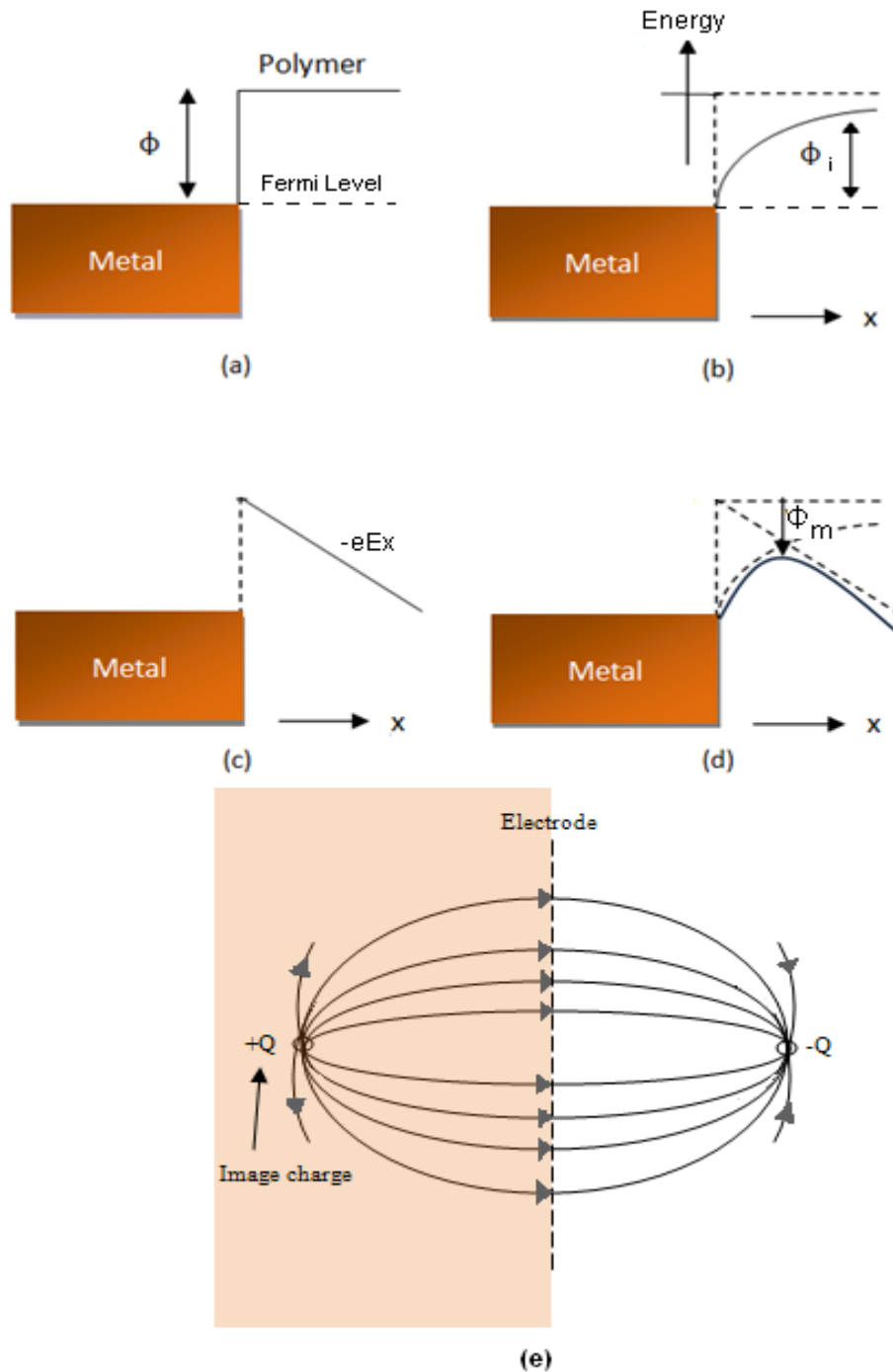
Figure 3-3: Modification of the potential barrier between metal and polymer by an applied field. (a) total barrier height, (b) shape of barrier including effect of coulombic image force, (c)potential energy due to the applied field, and (d) total barrier shape and (e)illustration of the classic law of image.

To calculate the attraction between the metal and electron, consider the electrode to be replaced by an equal and opposite polarity charged point at equal distance from behind the

electrode surface. This is known as image charge theorem which is illustrated in Figure 3-3(e). If electron is in x-distance from the interface, then the distance separating electron and image is $2x$, and the force of attraction due to Coulomb's Law is:

$$F_i = \frac{e^2}{4\pi\varepsilon_0\varepsilon_r(2x)^2} = \frac{e^2}{16\pi\varepsilon_0\varepsilon_r x^2} \qquad \text{Equation 3-1}$$

Also the potential barrier due to the image field (Figure 3-3(b)) is given by:

$$\Phi_i = \int_x^\infty F_i(x)dx = \frac{e^2}{16\pi\varepsilon_0\varepsilon_r x} \qquad \text{Equation 3-2}$$

Potential due to applied field, Φ_a is represented in a straight declining line illustrated in Figure 3-3(c) given by

$$\Phi_a = -e(Ex) \qquad \text{Equation 3-3}$$

Hence, the total resulting potential, given by $\Phi(x)= \Phi_i+\Phi_a$ is

$$\Phi(x) = \frac{e^2}{16\pi\varepsilon_0\varepsilon_r x} - e(Ex) \qquad \text{Equation 3-4}$$

The maximum potential is given by

$$\frac{d\Phi}{dx} = -\frac{e^2}{16\pi\varepsilon_0\varepsilon_r x^2} - eE = 0 \qquad , x = x_m \qquad \text{Equation 3-5}$$

Considering magnitude of electric field E= |E|, we could obtain maximum stationary point ,x_m

$$x_m = \sqrt{\frac{e}{16\pi\varepsilon_0\varepsilon_r E}} \qquad \text{Equation 3-6}$$

And the barrier height is now reduced by Φ_m (Figure 3-3(d)) ;

$$\Phi_{\mathrm{m}} = -eV = \sqrt{\frac{e^3 E}{4\pi\varepsilon_0\varepsilon_r}} \qquad\qquad \text{Equation 3-7}$$

So that the effective barrier height is

$$\Phi_{eff} = \Phi - \sqrt{\frac{eE}{4\pi\varepsilon_0\varepsilon_r}} \qquad\qquad \text{Equation 3-8}$$

Employing Richardson-Dushman equation, $J_T = AT^2 \exp(-\frac{\Phi}{kT})$, to Schottky injection effect ;

$$J(E) = AT^2 \exp(-\frac{\Phi_{eff}}{kT}) \qquad\qquad \text{Equation 3-9}$$

$$J(E) = AT^2 exp\left(-\frac{\Phi}{kT}\right) exp\left(\frac{1}{kT}\sqrt{\frac{e^3 E}{4\pi\varepsilon_0\varepsilon_r}}\right) \qquad\qquad \text{Equation 3-10}$$

where A is the Richardson-Dushman constant and T is the absolute temperature. Giving the current density:

$$J(E) = J_T exp\left(\frac{1}{2kT}\sqrt{\frac{e^3 E}{\pi\varepsilon_0\varepsilon_r}}\right) \qquad\qquad \text{Equation 3-11}$$

3.3.2   *Fowler-Nordheim Injection*

Fowler-Nordheim effect is also known as the tunnelling effect from bulk metal to other bulk crystalline solids. It is found that electron may tunnel through a potential barrier although it has less energy to overcome the barrier's height. This is due to the particle-wave duality characteristic of electron as shown in Figure 3-4(a). As the electron wave travel through the barrier, the wave will attenuate reducing its' amplitude but leaving the energy unchanged.

Figure 3-4 (b) shows the schematic diagram of tunnelling injection through a barrier. If very high field is applied, the height and width of the potential barrier will be reduced.

This tunnelling process is width dependent and in fact, in this charge injection theory, the width of the potential barrier is much more important than the barrier height. The probability of tunnelling decreases for taller and wider barriers. This emission process will occur at which the potential barrier is the thinnest, marked as x_0 in Figure 3-4 (b).
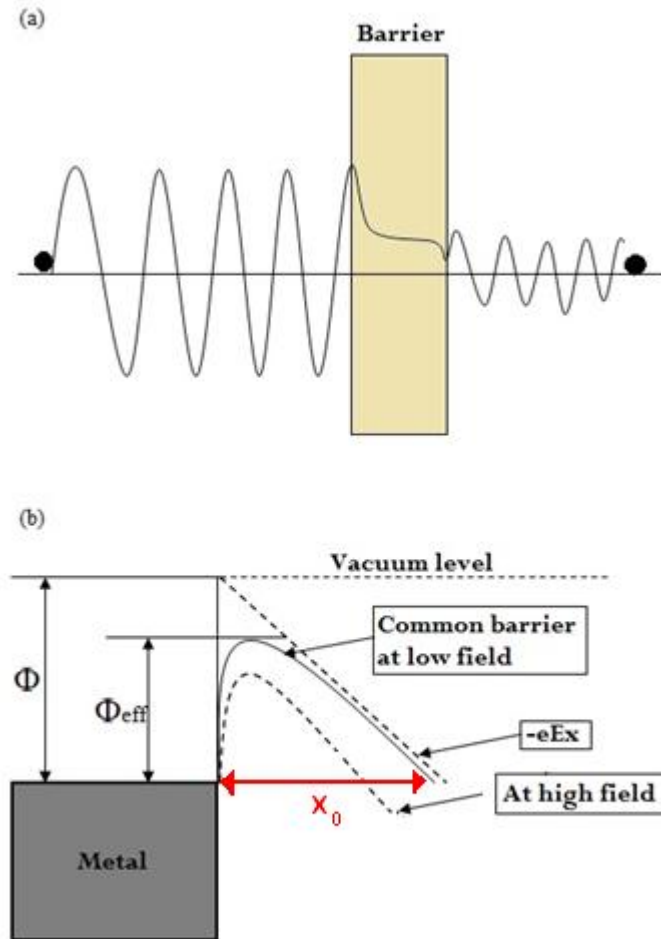
Figure 3-4: Illustration of Fowler Northeim tunnelling injection; a) electron wave travel through the barrier, and b) potential barrier reduction due to applied field.

The conduction current from Fowler-Northeim injection can be described as;

$$J = \frac{e^3 E^2}{8\pi h \Phi_{\text{eff}}} \exp(-\frac{8\pi\sqrt{2m}}{3ehE} \Phi_{\text{eff}}^{\frac{3}{2}})$$

Equation 3-12

Here e is the electron charge, h is the Plank constant, m is the mass, Φ_{eff} as the effective potential barrier height and E the electric field. The hole transport, which only happen via electron vacancies, requires inter-chain hole transfer, a reverse resonant tunnelling process of electron [48] and therefore, hole transfer normally happen in crystal region. The tunnelling process only happens at very high field where the barrier width is very thin.

3.4   Bulk Process

3.4.1   *Space-Charge Limited Conduction*

Space-charge limited current is found to be incredibly dependent on the thickness in which the current is the result from the movement of charges that injected into the polymer. Polymer with high dielectric constant will lead to high charge built up in the material.

(a)   Trap-free SCLC

In this model, an ideal dielectric is considered, which has [43];

- No trap
- No thermally generated charge, all charges come from injected charge
- Good injection due to Ohmic contact
- Negative-charged carrier only (i.e. electrons)

The dielectric with d thickness is placed in between two parallel electrodes. The x-direction is perpendicular to the electrodes, straight through the dielectric. The conduction current which have three components; drift, diffusion and displacement current is given by:

$$J = ne\mu E - eD_n \frac{dn}{dx} + \varepsilon_0 \varepsilon_r \frac{dE}{dt} \qquad \text{Equation 3-13}$$

where D_n is the Fick's diffusion coefficient. Two assumptions are made here which are; steady state condition, dE/dt=0, and space charge concentration is constant throughout the dielectric (although in real life space charge build up near electrodes will experience the greatest diffusion). In the latter, the diffusion term will be neglected. From Poisson equation;

$$\frac{dE}{dx} = \frac{ne}{\varepsilon_0 \varepsilon_r}$$

Equation 3-14

So that:

$$J \simeq \varepsilon_0 \varepsilon_r \mu E \frac{dE}{dx}$$

Equation 3-15

By rearranging this equation and integrating both sides gives;

$$E = \sqrt{\frac{2J}{\varepsilon_0 \varepsilon_r \mu} (x + x_0)}$$

Equation 3-16

where x_0 is a constant of integration. Integrate once again from x=0 to x=d with V(0)=V and V(d) = 0, it gives

$$V = \int_0^d E \, dx$$

$$= \int_0^d \sqrt{\frac{2J}{\varepsilon_0 \varepsilon_r \mu} (x + x_0)} \, dx$$

$$= \frac{2}{3} \sqrt{\frac{2J}{\varepsilon_0 \varepsilon_r \mu}} \left((d + x_0)^{\frac{3}{2}} - x_0^{\frac{3}{2}} \right)$$

Equation 3-17

Assuming $x_0 \ll d$ so that the current density is given by:

$$J = \frac{9\varepsilon_0 \varepsilon_r \mu V^2}{8d^3}$$

Equation 3-18

This is also known as Mott & Gurney square law in which the current is proportional to square of the voltage. By rearranging equation 3-18, mobility could be obtained from;

$$\mu = \frac{8Jd^3}{9V^2 \varepsilon_0 \varepsilon_r}$$

Equation 3-19

(b) Trap-limited SCLC

Unlike the trap-free dielectric with all carriers in conduction band, dielectric with traps will have some carriers being trapped in the material. Although the injected charges contribute to the space charge, but only a portion of it contribute to the current. Hence, a fraction of $\theta=(n_c/n_t)$, where n_c and n_t attribute to the number density of conduction band electrons and that of occupied trap states respectively, is necessary to be added into the current equation ;

$$J = \theta \frac{9\varepsilon_0 \varepsilon_r \mu V^2}{8s^3}$$

Equation 3-20
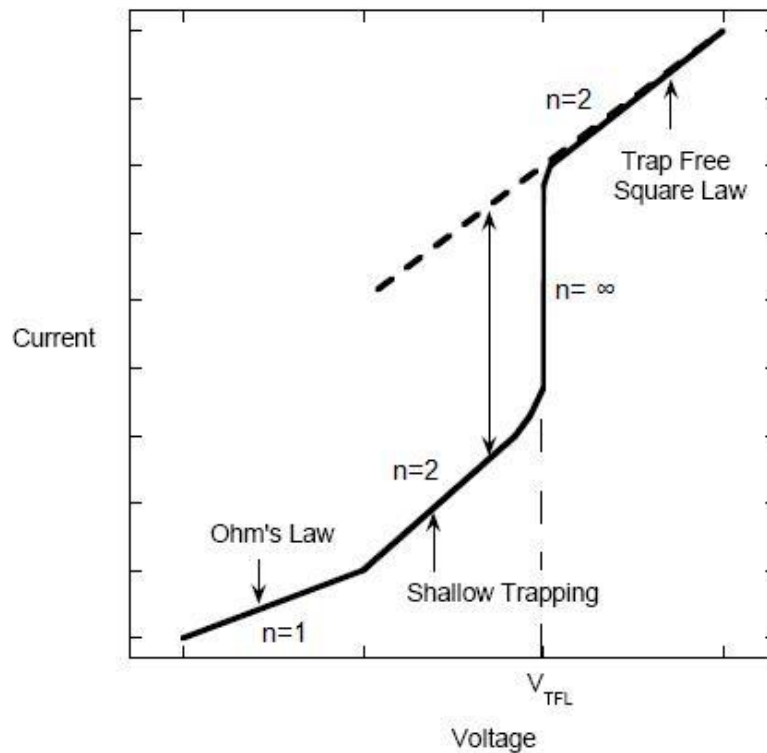
Figure 3-5: Log-log plot of current-voltage characteristics for one carrier, SCLC injection into an insulator.

SCLC current-voltage characteristic is commonly illustrated in log-log plot due to their power law relationship. This characteristic is demonstrated in figure 3-5. At low voltage, SCLC effect is not noticeable thus Ohmic conduction dominates the current-voltage

33

characteristic. As the voltage becomes higher, the SCLC effect starts to appear as it entering the shallow trapping region. As the voltage increases further, more electrons injected and ultimately fill in all the traps giving the current rises vertically at V_{TFL} (Trap-Filled- Limit). This steep increase the current-voltage characteristic will follow the trap-free SCLC relationship having similar slope with that in the trapping region. The concentration of the trapping state could be found by knowing V_{TFL}[49] .

3.4.2 *Hopping Conduction*
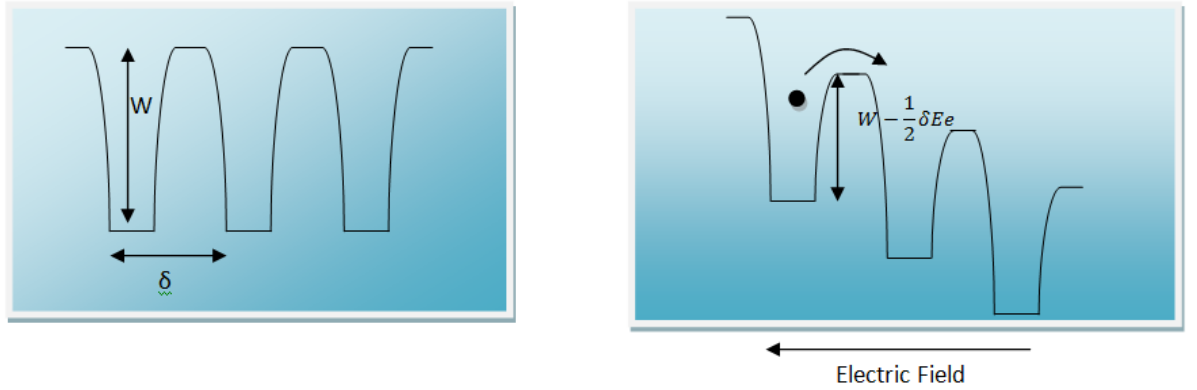
Figure 3-6: Hopping conduction mechanism; before and after electric field application.

When no electric field applied to the polymer, electron may move in any direction. The probability of this electron to move in any direction is 1/6 given by the positive and negative direction of three coordinates that perpendicular to each other [50]. With electric stress application, the barrier height is reduced and this reduction will help promote charge tunnelling effect. With higher electric fields, the potential barrier in the forward direction will continue to reduce and make conduction easier.

During the application of electric field, the barrier height will be changed. The new barriers' height along or against the direction of electric field become $W + \frac{1}{2}\delta Ee$ and $W - \frac{1}{2}\delta Ee$ respectively. Thus, the probability of electron hopping in these two directions is;

$$P(+E) = v \exp\left[-\left(W + \frac{1}{2}\delta Ee\right)/kT\right]$$ Equation 3-21

$$P(-E) = v \exp\left[-\left(W - \frac{1}{2}\delta Ee\right)/kT\right]$$ Equation 3-22

where v is the escape frequency of electrons.

3.4.3 *Poole-Frenkel Effect*

Poole and Frankel mechanism is the bulk limited version of the Schottky effect at electrode interface. In contrast to the Schottky effect, Poole and Frankel mechanism reduce the trap barrier localising the carries in the dielectric itself. For this mechanism to occur, the dielectric must have a wide band gap with donor or acceptor resides in it. With the presence of electric field across the dielectric material, reduction on the potential barrier will occur and the schematic diagram of this effect can be seen in Figure 3-7.
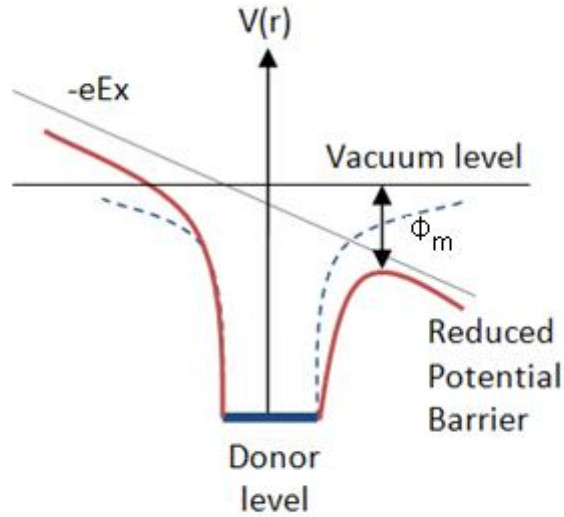
Figure 3-7: Schematic diagram of the Poole-Frenkel effect.

The potential energy, V(r) related to the Coulombic interaction between the electron and ionised donor is given by:

$$V(r) = -\frac{e}{4\varepsilon_0\varepsilon_r r}$$ Equation 3-23

where r is the distance of separation. With the application of electric field of E, the potential energy becomes:

$$V(r) = -\frac{e}{4\varepsilon_0\varepsilon_r r} - Er$$

Equation 3-24

Applying the procedure in 3.3.1, the position of the maximum potential surface, r_m is given by

$$r_m = \sqrt{\frac{e}{4\pi\varepsilon_0\varepsilon_r E}}$$

Equation 3-25

And thus giving Φ_m:

$$\Phi_m = \sqrt{\frac{e^3 E}{\pi\varepsilon_0\varepsilon_r}}$$

Equation 3-26

By reducing the new potential barrier into the equation of Schottky injection, the current density obtained is:

$$J(E) = J_T exp\left(\frac{1}{kT}\sqrt{\frac{e^3 E}{\pi\varepsilon_0\varepsilon_r}}\right)$$

Equation 3-27

Equation 3-27 could be rewrite as :

$$\ln J(E) = \frac{1}{kT}\sqrt{\frac{e^3}{\pi\varepsilon_0\varepsilon_r}}\sqrt{E} + \ln J_T$$

Equation 3-28

Which clearly illustrate a straight line with slope $\frac{1}{kT}\sqrt{\frac{e^3}{\pi\varepsilon_0\varepsilon_r}}$ when $\ln J(E)$ is plotted against $\sqrt{E}$.

3.5 Charge Transfer and Polymer Morphology
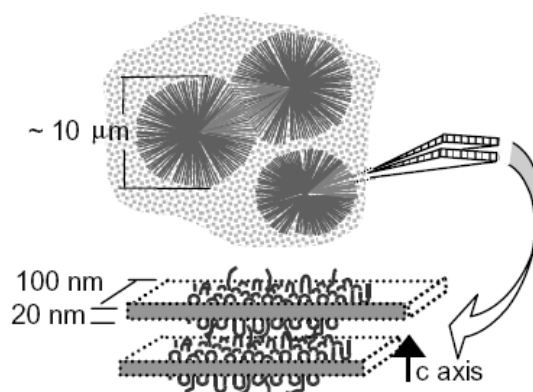
Figure 3-8: Morphology of semi-crystalline PE showing spherulites array of lamella crystallite.[48]

Polymer chains in PE always arrange itself to form crystalline lamella ribbons. The lamellas normally grow from a nucleating site to form spherulites which may have diameter of more than 10μm. This array of lamella crystal is separated by less dense amorphous polymer. Figure 3-8 illustrates the spherulites in PE. J.P. Jones et al. in his work [48] , mentioned about the effects of polymer morphology to charge transfer.
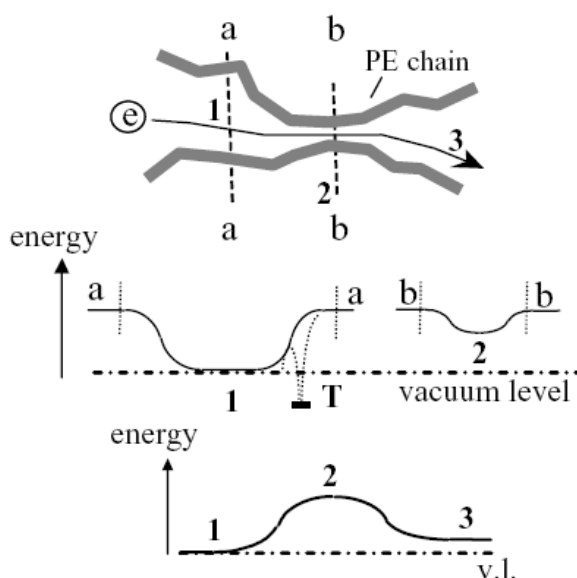
Figure 3-9: Change of energy level in electron transfer due to the polymer morphology. [48]

Electron for example, will move in inter-lamellar-phase particularly in chains that align with the applied electric field, to avoid PE chains in which has higher energy barrier. Localised polaronic energy state, such as at T in Figure 3-9 is found due to the neighbouring electrons, acts as the restricting barrier to electron transport. Therefore, electron transport depends on;

1. Local polarisation
2. Chain conformation

In the same figure, as electron travels from region 1 to 3, higher energy required to overcome the barrier at region 2. The closer the electron path to the polymer chain, the higher energy is required to attain them. Thus, this path is less preferred. The numerous hills of electron affinity are due to the chain configuration in PE and region with lowered density tends to become macro (deep) traps. Hence, the polymer creates an energy landscape in which the electron travels.
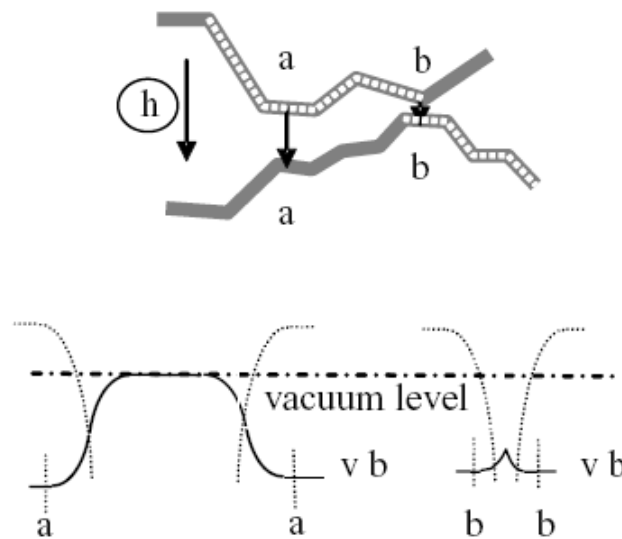
Figure 3-10: Positive hole transfer between two chain via valance band of polymer chain and inter-chain tunnelling which is difficult at a-a and easy at b-b. [48]

Holes on the other hand, only travel via electron vacancies in polymer chains. For a hole to transfer in a long range, it will depend on two transfer mechanisms;

1. Inter-chain hole transfer, and

2. Reverse resonant tunnelling process of electron between chains that are close to each other.

Thus, in amorphous region, holes transfer becomes more difficult due to the morphology of the region which encouraging the hole trapping.

3.6 Chapter Summary

This chapter is important as later in this thesis we will discuss on the charge build up in the tested samples and the influence of crosslinking byproducts on charge injection at electrodes, charge movement in the bulk as well as changing the trapping landscape of the dielectric. Thus it is important to grab the idea of deep and shallow traps from the beginning so that the result obtained from the tests could easily be analysed. The effect of hopping will also be seen in the tested sample during the charge decay process in space charge measurement. No voltage is applied across the sample and charge in the tested sample decay gradually depending on the type of sample.

The theories on conduction process that presented in this chapter will also be useful as we discuss the effect of byproducts on dc conductivity. Some of the conduction models will be referred to calculate the mobility of the charges in samples. Last but not least, the effect of dielectric morphology on charge conduction demonstrates the importance of local condition as well as the polarisation effect of the neighbouring molecules towards the trapping properties of the dielectric.

Chapter 4   Space Charge

Measurement Techniques

Since the term space charge is introduced, there have been a few devices developed to enable the space charge in polymer to be determined. Three main non-destructive techniques have been adopted which are the thermal step or pulse method, laser-induced pressure pulse (LIPP) method and also last but not least the pulse electroacoustic (PEA) technique [51]. These methods use space charge displacement technique in order to measure the charges that exist in the specimen. The difference among them is the technique used to introduce the small displacement to the charges and this matter will be discussed in here.

4.1   Thermal Step Method

Collins, in mid-1970s, was the first person who introduced diffusion of heat pulses in the sample to measure space charge. Later, in 1988 the thermal step method (TSM) was proposed by Toureille which measures the external current in response to the thermal expansion in the sample [52].
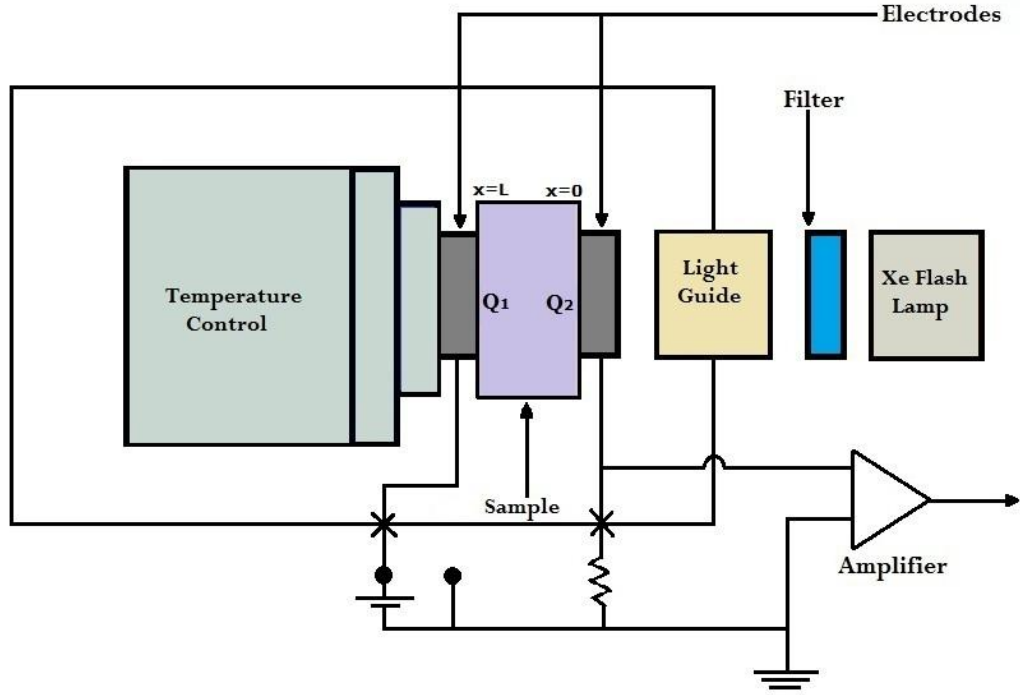
Figure 4-1: Diagram of thermal step principle.

To have a better understanding on the principle of the thermal step method, let's consider a dielectric slab with a thickness L, that contains Q charges at a distance x. Before the experiment, the sample is at low temperature. The sample is placed in between two electrodes and at t=0, the hot source is placed at one electrode at position x=0, meanwhile the cold sink is at x=L. The thermal expansion can be created by a flash light or illumination of a laser. During short circuit, the electrodes are connected to the ground resulting to no potential difference. When the thermal step is introduced to the system, the material layers shifted resulting to the charges Q in the sample to be displaced. Consequently, the induced image charges Q_1 and Q_2 at the electrodes are also modified to fulfil the electrostatic equilibrium:

$$Q_i + Q_1 + Q_2 = 0 \hspace{3cm} \text{Equation 4-1}$$

As a result, small current is produced in the external circuit and it is given by [53,54] :

$$I(t) = -AC \int_0^L E(x) \frac{\partial \Delta T(x,t)}{\partial t} \, dx \hspace{2cm} \text{Equation 4-2}$$

where A is the parameter related to the variation in thickness and permittivity with temperature, C is the material capacitance and $-AC = \delta C/\delta T$ the variation of C with temperature and E(x) is the local electric field in the sample.

Application of a suitable deconvolution procedure using Fourier analysis allows extraction of the space charge distribution from the current flow data. However, this technique is particularly suitable for thicker samples, between 2 and 20mm since there is essentially an unlimited amount of heat available and useful data can be collected until the temperature distribution across the sample has equilibrated. Due to this low resolution, some other new methods have been introduced so that the space charge in thinner sample could be measured.

4.2   Laser-Induced Pressure Pulse
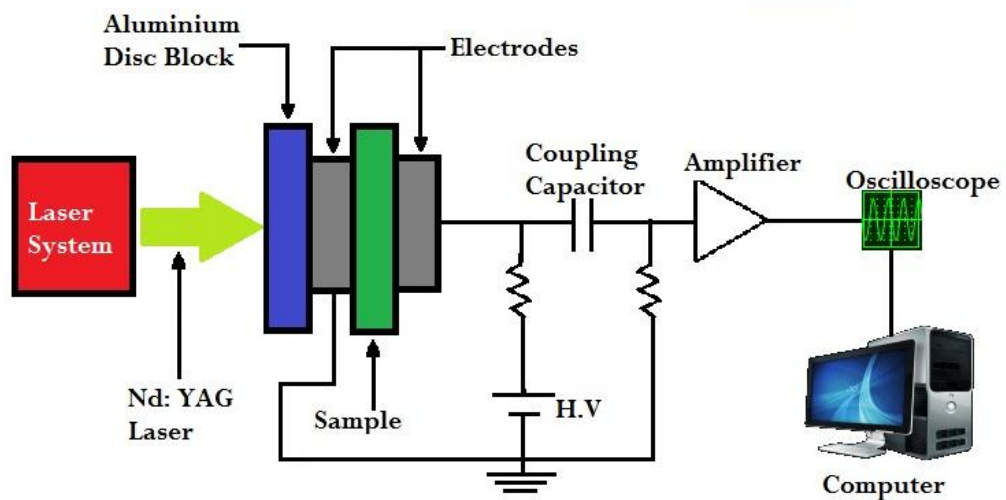
Figure 4-2: Illustration of a laser induced pressure Pulse (LIPP) system

Laser Induced Pressure Pulse (LIPP) initiates the charge displacement from the pressure wave that is produced when the laser beam hits the target. LIPP system is illustrated in figure 4-2. In this case, the target used is a semiconductor electrode which has the same acoustic impedance with the dielectric material. As the pressure wave travels through the sample thickness, it induces an external signal (current or voltage) which tells the electric field profile of the sample. In the case of external current, the induced signal is given by [55,56];

$$i(t) = A \int_0^d E(x) \frac{\partial P(x,t)}{\partial t} dx \qquad\qquad \text{Equation 4-3}$$

where *A* is a constant that depends on the sample properties (permittivity, compressibility and electrical capacity), *d* is its thickness, *E(x)* the local field resulting from both the applied voltage and from space charge, and *P(x, t)* the pressure pulse. By deconvolution technique, the charge distribution of the sample could be obtained. Compared to TSM, LIPP allows any space charge measurement to be conducted on thin samples by controlling the laser intensity to obtain a high signal-to-noise ratio in order to have a good data. However, there are a few technical problems encountered when applying this method [55].

During the formation of the pressure pulse, the optical energy is converted into mechanical energy. Consequently, some of the high optical energy may be converted into heat which increases the local temperature and change the target surface into gas. This gas could be ionised and forms 'plasma' which radiates electromagnetic energy that can disturb the signal and increase the noise in the system. The formation of plasma can be observed in Figure 4-3. In addition, due to the heating effect, thermal step diffusion may occur in the measured sample. If this happens, the induced signal may result from both thermal and mechanical stresses and the signal cannot be treated.

The impact of laser beam to the target is more severe when it burns away the target electrode with each laser pulse. With the damaged target surface, the induced signal becomes out of phase. From equation 4-3, the current produced is dependent to the internal field distribution E(x) and its pressure shape P(x, t). The pressure shape is related to the laser beam energy which normally have 5% variation (for commercial laser beam). This non-uniform laser beam energy may lead to variation of i(t) signal which consequently affects the charge profile. Due to these limitations, the use of piezoelectric is more preferable compared to a laser in generating the pressure pulse. This brings us to the final method, which uses a better technique to measure space charge.
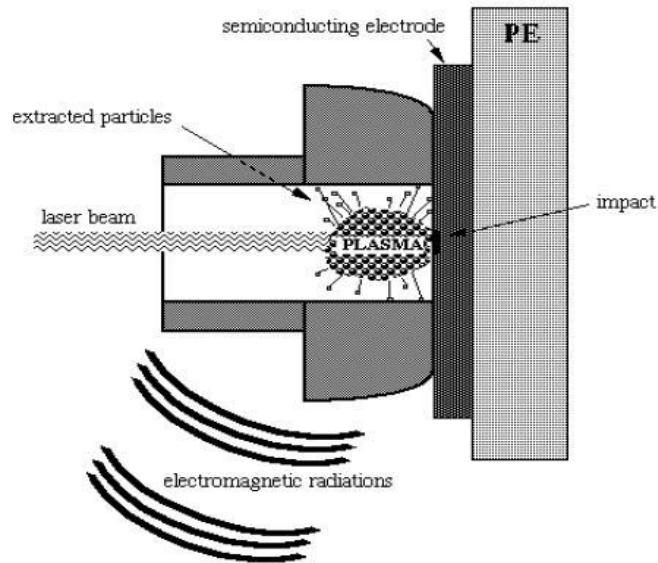
Figure 4-3: Laser-Induced Pressure Pulse and the formation of plasma [55].

4.3 Pulsed Electroacoustic Technique
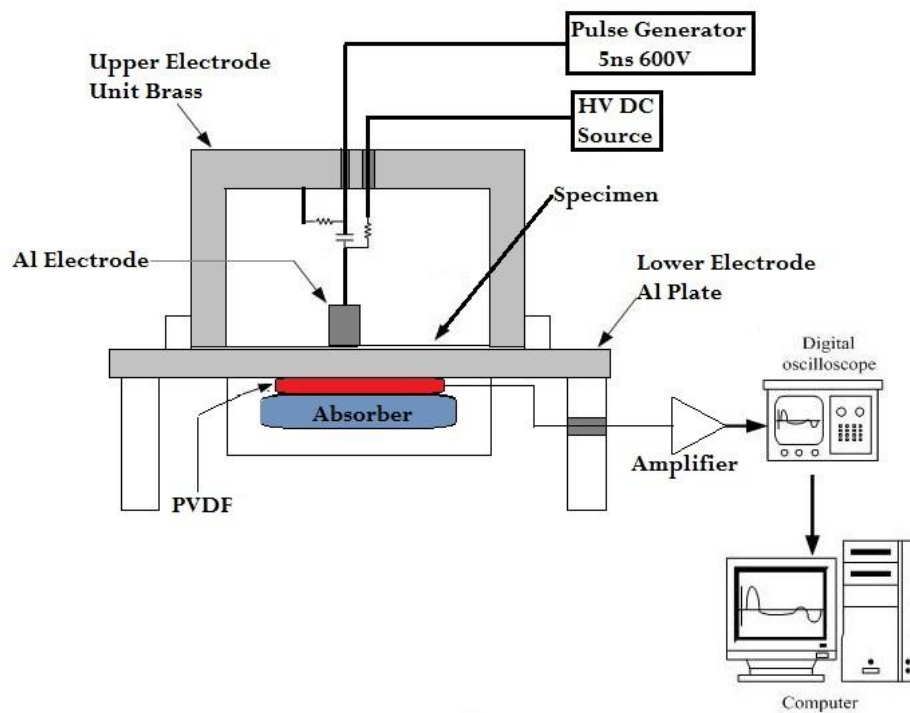
Figure 4-4 : High resolution PEA system

Due to simplicity, low cost, non destructive and ease of implementation, PEA method is now more commonly used, rather than the other two. Figure 4-4 shows the experimental setup of the pulse electroacoustic (PEA) technique. It consists of two aluminium electrodes

with semiconductor attached to the top electrode to match with the acoustic impedance of the dielectric sample. PEA introduces the charge displacement by applying short voltage pulse $e_p(t)$ with duration ΔT across the sample. Any charges $\rho(x)$ in the sample will experience perturbation force that causes the charge displacement. This displacement launches an acoustic wave which travels through the sample and bottom electrode, towards the transducer. The generated acoustic wave has amplitude proportional to the local charge density in the sample. Piezoelectric transducer will then transform the acoustic wave into electric signal.

Piezoelectric transducer which is made of Polyvinylidene Difluoride (PVDF) is connected to oscilloscope via amplifier to enlarge the voltage signal. The oscilloscope will then record the signal as a function of time [51,57,58]. The spatial resolution for acoustic technique depends on the product of the pressure pulse duration and the speed of sound in the sample. In the PEA method, pressure pulse duration is equivalent to the voltage pulse duration. However, the thickness of the piezoelectric transducer must also be considered since the practical resolution improves as the transducer thickness decreases. The thickness of the device is normally 4 to 110µm. An absorber is attached to the transducer to delay and restrain the reflection of the acoustic wave from going back to the transducer. Other than acting as the bottom electrode, aluminium also plays an important role of delaying the arrival of the acoustic pulse until the instability due to the pulse source disappears before allowing the acoustic wave to reach the transducer. A full description on the acoustic method in measuring electric charge distribution is reported in [59].
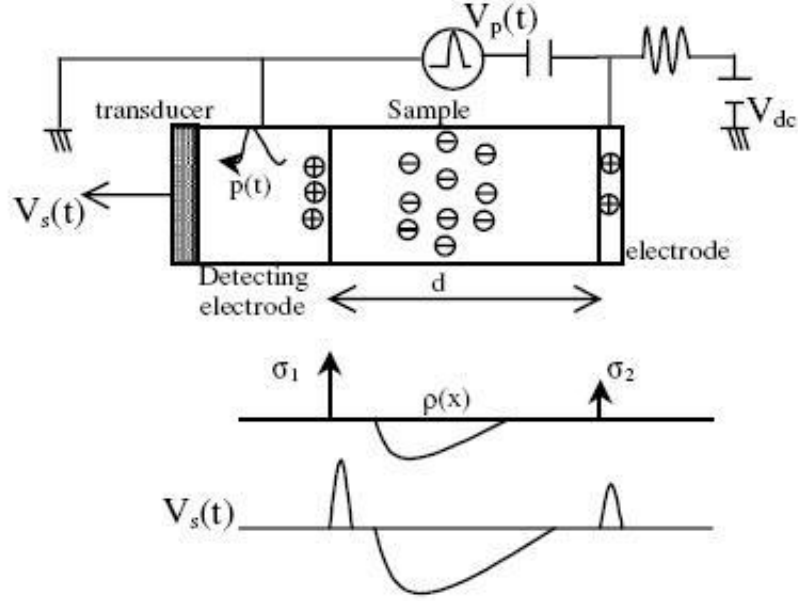
Figure 4-5: Schematic diagram of the PEA system

Figure 4-5 illustrates the schematic diagram of the PEA system. As shown in the figure, σ_1 and σ_2 appears at the electrode, as the surface image charges. These values are dependent on the electric field E_{dc} as well as the magnitude and distribution of the total charge density $\rho(x)$. The magnitude of σ_1 (at x=0) and σ_2 (at x=d) are described by equations 4-4 and 4-5 respectively [60].

$$\sigma_1 = -\varepsilon E_{dc} - \int_0^d \frac{d-x}{d}\rho(x)dx \qquad \text{Equation 4-4}$$

$$\sigma_2 = \varepsilon E_{dc} - \int_0^d \frac{x}{d}\rho(x)dx \qquad \text{Equation 4-5}$$

where $\varepsilon = \varepsilon_0\varepsilon_r$ and d is the sample thickness. The electric field will generate surface charges equal in magnitude but opposite sign, meanwhile the total charge in the bulk will generate surface charges in different magnitude but the same sign. Equation 4-6 shows the corresponding voltage proportional to the space charge density $\rho(x)$ [60]:

$$V_s(t) = G_0\left[\begin{array}{c} K_1\sigma_1\delta\left(t - \frac{B}{v_{Al}}\right) + K_2K_3\sigma_2\delta\left(t - \frac{B}{v_{Al}} - \frac{d}{v_{sa}}\right) \\ +0.5\,K_3v_{sa}\rho(x = v_{sa}t) \end{array}\right]e_p\Delta T$$

Equation 4-6

Vs is the electric signal obtained in the time domain which represents the charge distribution, where σ_1 and σ_2 are the surface charges at the electrodes at time t. B and d are the electrode and sample thickness respectively. v_{Al} and v_{sa} are the sound velocity through the aluminium electrode and sample thickness respectively. ΔT is the width of the pulse, ρ is the bulk charge and e_p is the amplitude of the pulse voltage. G_0 is a constant meanwhile K_1, K_2 and K_3 are the transmission coefficients associated to the impedance of the materials, and are given by equation 4-7 to 4-9;

$$K_1 = \frac{Z_{Al}}{Z_{Al}+Z_{sa}}$$

Equation 4-7

$$K_2 = \frac{Z_{sa}}{Z_{Al}+Z_{sa}}$$

Equation 4-8

$$K_3 = \frac{2Z_{Al}}{Z_{Al}+Z_{sa}}$$

Equation 4-9

where Z_{Al} and Z_{sa} are the acoustic impedances of the aluminium electrode and sample respectively. In equation 4-6, the constant G_0 needs to be determined and this is typically done by applying a small voltage across the sample to generate a known charge density on the two surfaces at the electrodes. If there is no bulk charge in the material, the third term in equation 4-6 will become zero and thus,

$$V_{\sigma 1}(t) = G_0 K_1 \sigma_1 e_p \delta \left(t - \frac{B}{v_{Al}} \right) \Delta T$$

Equation 4-10

$$V_{\sigma 2}(t) = G_0 K_2 K_3 \sigma_2 e_p \, \delta \left(t - \frac{B}{v_{Al}} - \frac{d}{v_{sa}} \right) \Delta T$$

Equation 4-11

Where $K_1 = 0.5\ K_3$ (from equation 4-7 and 4-9) and $V_{\sigma 1}(t)$ and $V_{\sigma 2}(t)$ are the output voltage associated to the surface charges σ_1 and σ_2. In practice, Equation 4-10 is used since the bottom electrode is nearer to the transducer and thus less loss due to attenuation and dispersion of the signal. The propagated signal will gradually decrease in amplitude and broaden its shape due to scattering, absorption and dissipation of energy [61]. By integrating equation 4-10 within ΔT region, as well as applying equation $\sigma_1 = -\varepsilon E_{dc}$, we obtain [60];

$$\int_0^{\Delta T} v_{\sigma 1}(t)dt = G_0 K_1 \sigma_1 e_p \Delta T \qquad \text{Equation 4-12}$$

$$G_0 K_1 = \left[\frac{1}{\sigma_1 e_p \Delta T}\right] \int_0^{\Delta T} v_{\sigma 1}(t)dt \qquad \text{Equation 4-13}$$

Substituting equation 4-13 to the third term of equation 4-6, the space charge density profile $\rho(x)$ which is proportional to the output voltage $v_s(t)$ is obtained;

$$V_s(t) = (G_0 K_1 v_{sa} \Delta T)\rho(x = v_{sa}t)e_p \qquad \text{Equation 4-14}$$

In the PEA software, V_s value is calculated from electric field and charge density of the sample. This value will match the applied voltage across the tested sample from the volts on measurement signal. In some cases, the output signal can sometimes be misinterpreted as space charge, where it actually is a result from the frequency response of the transducer and amplifier. The transducer with a high capacitance (typically 0.1-5nF) as well as low noise and high frequency amplifiers (500 MHz) which often have low input impedance (50Ω), acts as a high pass-filter. If $G(f)$ is the transfer function of the system, the output signal in frequency domain, $V(f)$ can be described as;

$$V(f) = G(f)\rho(f) \qquad \text{Equation 4-15}$$

where $\rho(f)$ is the impulse response of the system, including the sensor and amplifier in the frequency domain. If $G(f)$ can be found, the actual space charge distribution can be computed using Fast Fourier Transform (FFT), division, software filtering and Inverse Fast Fourier Transform (IFFT). The full mathematical principle behind deconvolution is well documented in [62].

4.3.1 Calibration of Pulsed Electroacoustic Signal

Ideally in a clean sample, no bulk charge can be found. However, due to the system respond and noise subsequent to the applied pulse voltage, the signal from PEA at bulk of sample is not always zero. The surface charge σ_1 and σ_2 are produced by the applied pulse voltage and the actual pulse voltage on sample is related to the capacitance ratio of

decoupling capacitor and sample. Therefore, the calibration of the PEA signal is a must to eliminate the effect.

By applying a dc voltage in the opposite direction to the pulse voltage, these induced charge at the top and bottom electrodes cancel each other. Due to the equivalent applied voltage to the output signal from the pulse voltage, it is possible to cancel the effect of the latter. The relationship between the pulse voltage and its equivalent dc voltage can be used to improve the charge analysis. For example, 600V pulse voltage can be used to calibrate sample stressed at 2kV. Due to the noise from surrounding and from pulse generator, signal from pulse voltage only could have low signal-to-noise ratio (SNR). Thus, calibration process requires additional voltage to perform a better calibration. It is also important to confirm that no bulk charge is produced by the applied dc voltage. From previous studies [63,64], in a 200μm LDPE sample, homocharge is initiated when a 3kV dc is applied. At the same time, the applied voltage must be high enough to yield a signal of acceptable SNR.

Hence, a suitable signal of calibration is the signal measured at 2kV. This value however will vary with the thickness. A higher voltage could be used for a thicker sample. For sample with a trapped charge, the same batch of samples without charge is used for calibration purpose. The measurement is carried out on the sample without involving sample loading and unloading in the PEA system to avoid the slightest difference in the sample assembling which will result in a variation in the output signal [63]. It should also be noted here that calibration process must be conducted on every sample before any further measurement is done on the sample.

In Tony Davies High Voltage Laboratory in University Of Southampton, this technique has been used for many years due to its advantages as stated above. PEA measurement for cable insulation is also available to measure the space charge accumulation in plaque or coaxial-cables. Improvement has been made on the conventional cable PEA system by Fu and Chen [65], to allow measurement on the cable at the same radius. A flat electrode system was introduced and employed in the system and the measuring assembly is illustrated in Figure 4-6 below:
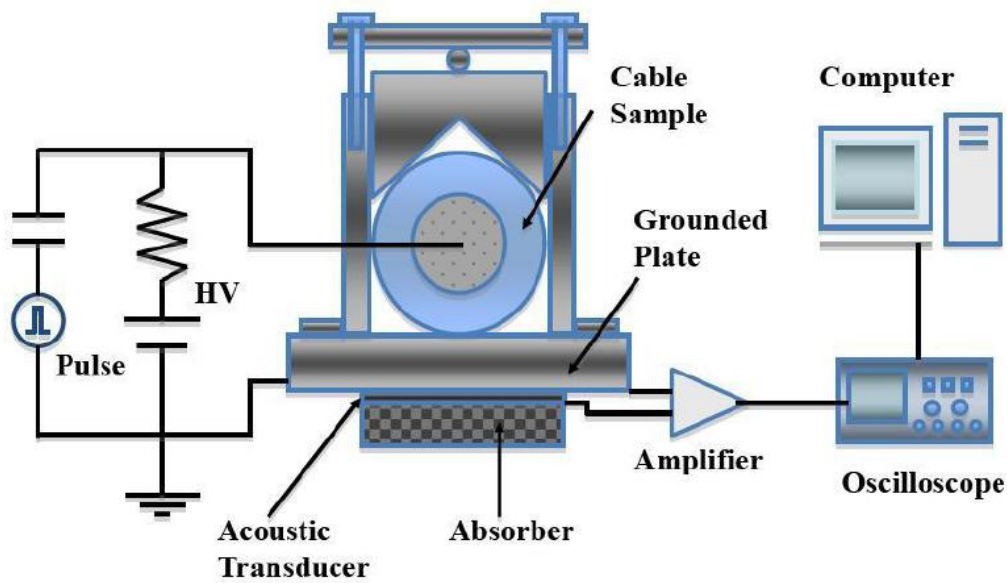
Figure 4-6: Illustration of a modified pulsed electro-acoustic (PEA) system for cable [65].

By using this equipment, the space charge profile in XLPE cable with temperature gradient was successfully measured [66].

4.3.2 *Pulsed Electroacoustic Technique In AC Condition*

The accumulation of space charge under ac condition has not been fully investigated due to a few factors. Firstly it may due to less interest on this study because of smaller space charge accumulation in ac condition making it less problematic than that at dc. Secondly, ac space charge measurement needs to have faster data acquisition and good synchronisation with the ac supply to measure the phase related charge [67]. Previously, authors like Wang et. al and Chong et. al have used the point on wave technique to measure the ac space charge profile [64,68]. This method is shown in Figures 4-7 and 4-8.
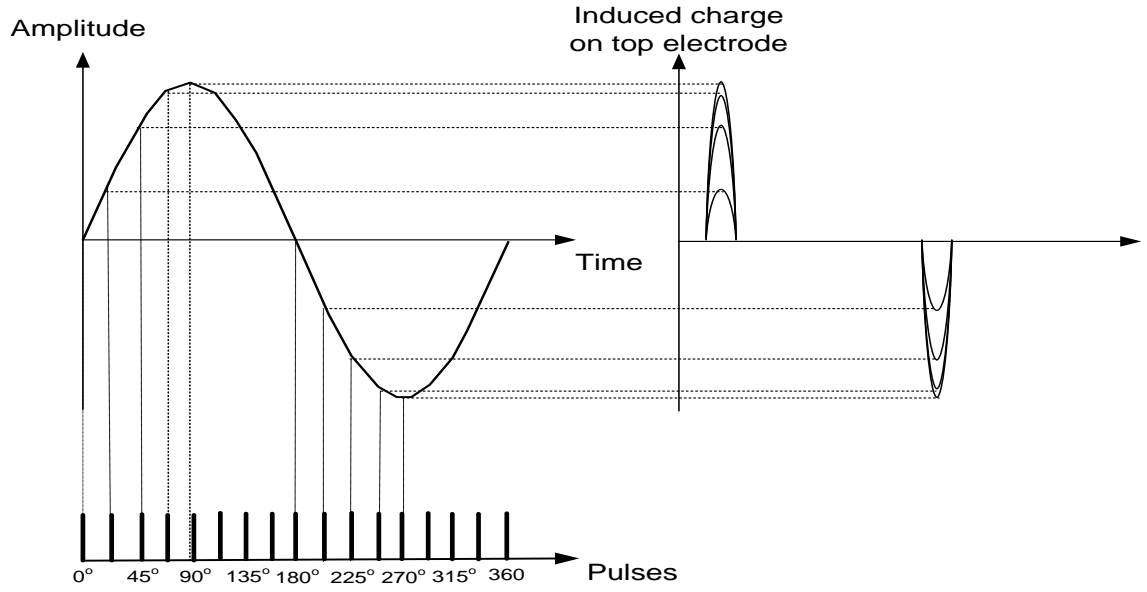
Figure 4-7: Illustration of point on wave method[69]
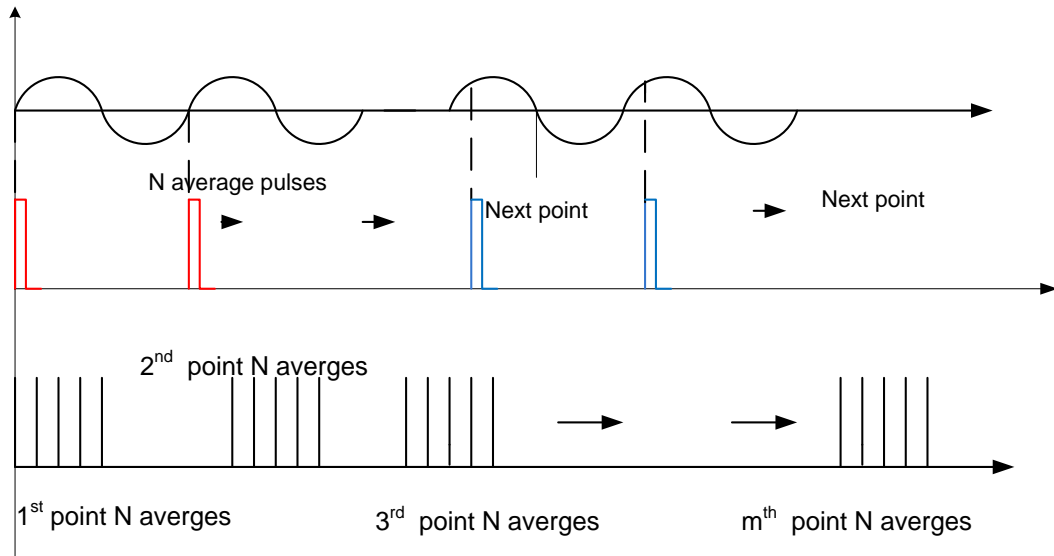
Figure 4-8:Demonstration of pulse train and applied voltage in point on wave method [69]

Due to low switching frequency of the pulse generator as well as the slow data transferring between the oscilloscope and GPIB card, only one set of data could be recoded per cycle. 'm' in figure 4-8 is defined as the number of point to be measured in one cycle meanwhile 'N' is the average number of pulses required on each point to obtain a good signal to noise ratio. The number of m is limited by the frequency of the pulse generator such that $f_{pulse} <$ m.f_{ac}. If a sine waveform of 50Hz applied with the 500Hz pulse generator, maximum

52

number of m will be 10. To have 500 pulses for averaging on these 10 data points, the required time for this process is 20ms x 10 x 500 = 100s. This long measurement time may cause inaccurate result as the charges profile especially at high voltage may change during this period.

To overcome these problems, a new system has been introduced [70,71]. In Tony Davies High Voltage Laboratory, this modification and improvement was done by Xu [72]. A specially built pulse generator that could produce 4kV narrow pulse of at most 5ns width as well as Eclipse signal averager console are used to give high sampling rate, high speed pulse and high speed data acquisition. Synchronisation of the pulse and ac waveform is provided by the function generator which sends trigger signal to both pulse generator and HV trek amplifier. Figure 4-9 shows the system set up that was used for ac measurement.
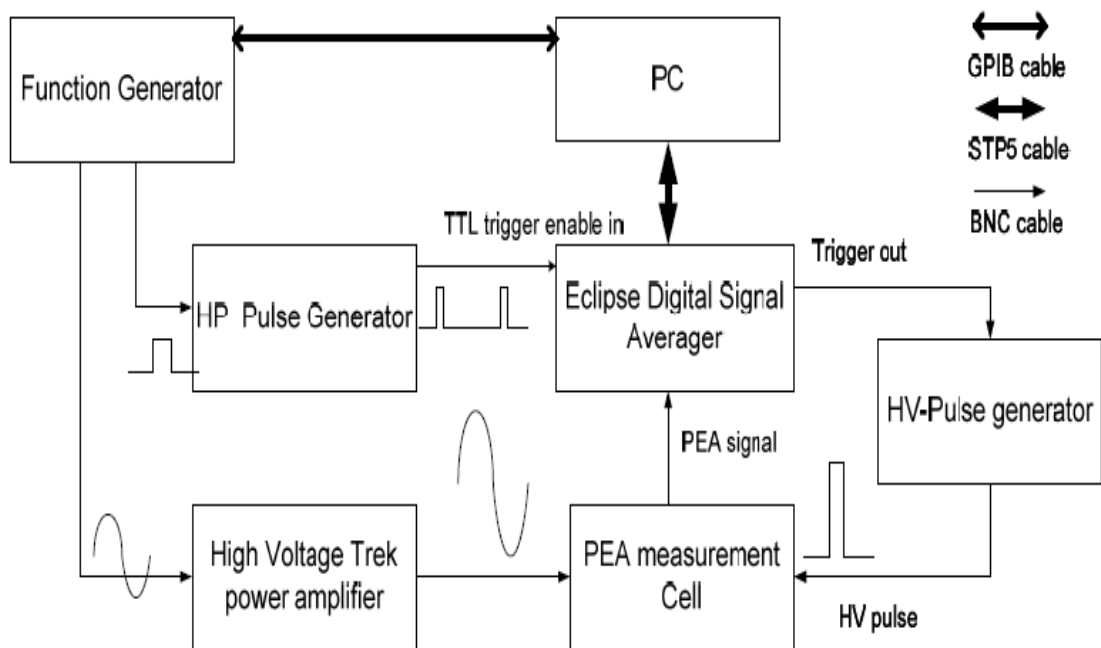
Figure 4-9: The Eclipse PEA system setup for AC measurement [70].
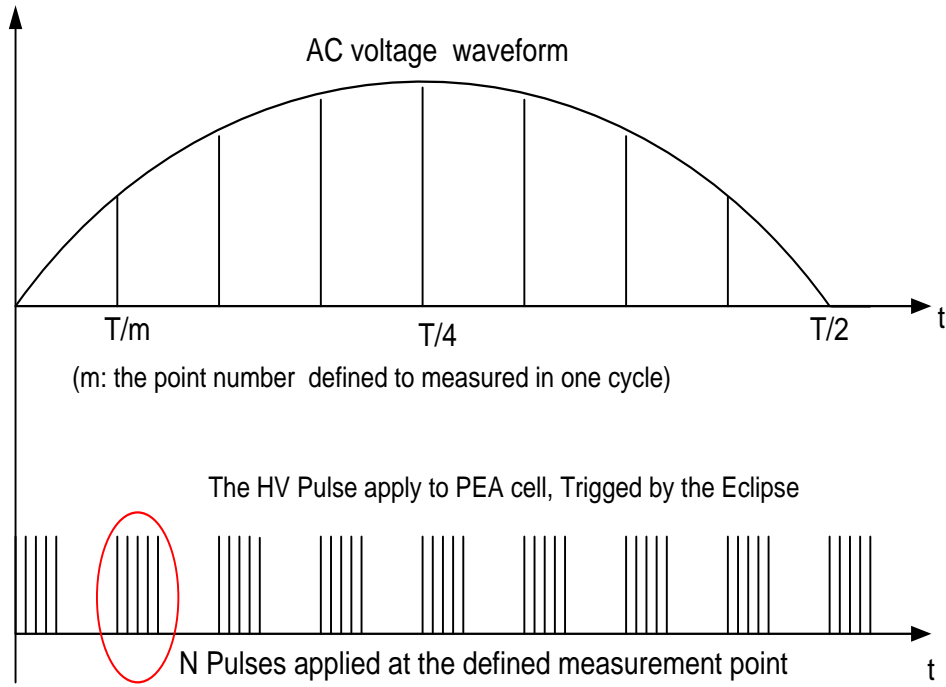
Figure 4-10: The average set of pulses in one cycle for the new PEA system.

In the new system, the relation between the pulse generator frequency and ac signal frequency is described as $f_{pulse} = N \times m \times f_{ac}$. With sampling interval of 0.5, 1 or 2ns, the system could record up to 262,000 data points. The eclipse system has its owned interlacing requirements for example 0.5ns interval and 10 records could give 40 averages. For an applied sine wave of 10 Hz and 2 kHz HV pulse, if 20 points are defined, 10 averages can be accomplished. To obtain 200 averages, 20 cycles is required and the system only take 2s to finish the measurement compared to the old system that took 400s (200x0.1x20=400s) for similar measurement [70].

4.4 Chapter Summary

In Tony Davies High Voltage Laboratory, space charge measurements used to be conducted using LIPP. However, due to its' complex operation, this technique has no longer been employed. Some issues related to this equipment includes high frequency noise during ac stress, offset on the point on wave voltage, effect on the semicon thickness to measurement resolution, degradation of the target material as well as complicated signal

correction that performed after the measurement [73]. Since then, LIPP has been replaced by PEA technique due to simplicity, low cost, non destructive and ease of implementation. This technique has shown its reliability to produce good data for space charge measurement.

Chapter 5   Sample preparation

5.1   Preparation of XLPE film

The polyethylene in pallet form, containing almost 5% of DCP was heated at 150°C in a pre-shaped mould as shown in Figure 5-1. Mould release liquid was applied on the mould surface to ease the removal process of the sample after it has been crosslinked. When the pallet melt, a pressure of 2 ton (equivalent to 0.2 Mpa) was applied for 30 seconds to push any bubbles out of the mould. The sample was then left to crosslinked at 200°C for 5 minutes. After that the mould was quenched cooled using tap water. The fresh XLPE was peeled out from the mould and cut into circular sample with a diameter of ≈19mm. The thickness of the samples made from this mould varies from 180μm to 210μm.

material pellets   Metal plate
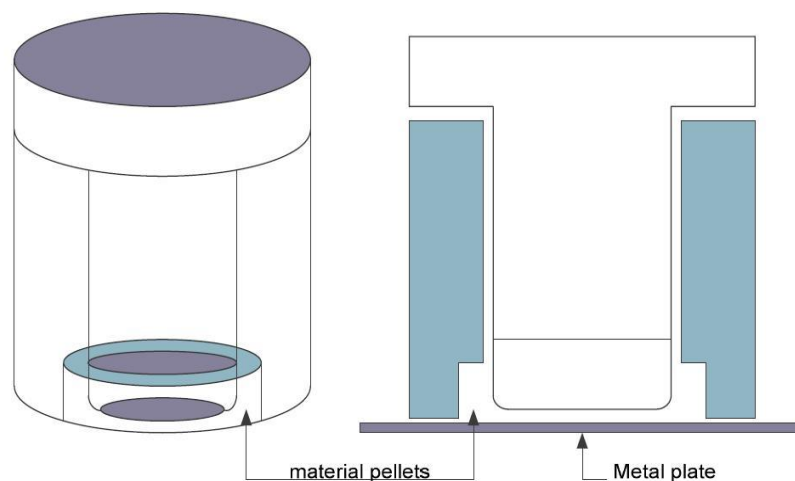
Figure 5-1: Mould tool [74]

To investigate the effect of byproducts in XLPE, the fresh XLPE was degassed in the vacuum oven at 80°C for 4 days. It was reported in [75] that degassing process may change the quality of the crystal forming more perfects crystals depending on the temperature, degassing period as well as the sample thickness. However, the amount of byproducts is more significant compared to the change of morphology in term of space charge formation since it was found that samples with comparable amount of byproducts but different morphology structure have almost similar charge profile. In order to confirm the existence of any byproduct in the fresh and degassed XLPE samples, the Fourier transform infrared (FTIR) spectrum has been used and this spectrum will be discussed later in this chapter.

Gulmine et. al reported that LDPE pallets with 1.5% of DCP that crosslinked at 170°C for 15 minutes produce 84% of gel content[76]. Thus, with the XLPE sample produced here, one can estimate that the gel content in the sample is as high as 80-90%.

5.2   Preparation Of Soaked LDPE Sample

All samples that were used in this part are supplied by GoodFellow [77] (supplier), with the density of $0.92 gcm^{-3}$. The samples with a thickness of 180μm were cut into circular films. The diameter of the circular films varies depending on the electrode size of the measurement equipment. In this research, LDPE was chosen over XLPE to eliminate any possibility of having more than one byproduct in the sample. In addition, the possibility of having byproduct-free XLPE via degassing cannot be guaranteed [39]. Thus, LDPE is chosen over XLPE.

In the soaking process, the LDPE film acts like a sponge which means the byproducts will be absorbed by the film and settle in the space in between the crystalline structure as well as in the amorphous region. This condition is similar to the real XLPE cable where during the crystallisation process, the byproducts are displaced into the amorphous region. Hence, the tests could be conducted in a condition similar to the real cable.

5.2.1 *The Soaking Process*

All samples were soaked at room temperature except for those soaked into cumyl alcohol which were treated at 80ºC since the melting temperature for cumyl alcohol is 23ºC. The soaking process of the samples took 2 hours. To obtain optimum absorption, a small weight was used to keep the sample immersed in the chemicals. The absorption rate can be observed from the percentage weight increase and these values are plotted in the graph of Figure 5-2. The percentage weight increases rapidly during the first 20 minutes before it becomes steadier until the soaking process finish. After one hour, the percentage of α-methylstyrene is about 4 times larger than acetophenone due to low permeation velocity of the latter into LDPE. By having almost similar amount of acetophenone and α-methylstyrene in soaked sample, we could check if any difference on electrical properties of test sample is due to the different amount of byproducts in the sample. This result shows that by soaking LDPE sample into the chemicals for 2 hours, the amount of them in the sample is sufficient enough for electrical test to be conducted on it. These values are similar to the values that are reported in [37].

It is also worth to address here that this percentage weight of byproducts per sample film is not relative to the actual percentage of the byproducts in commercial XLPE which is much lower. These samples were soaked so that the distribution of byproducts was uniform across the sample thickness. The small increment of the byproducts in the samples after 20 minutes of soaking indicates that the byproducts were uniformly distributed in the sample. Hence, the big amount of byproduct is inevitable. In the soaked samples, the amount of acetophenone, cumyl alcohol and α-methylstyrene are 3, 8 and 500 times larger that in practice, respectively. This discrepancy should not a big problem in the research since the focus here is to identify the individual effects of the byproducts towards the electrical performance of LDPE. However, extra consideration on the percentage weight differences must be taken when the quantitative value from the measurement is to be used in real cable. Later in chapter 8, the percentage weights of the byproducts are considered in calculation of the conductivity increment by the byproducts.

It is also important to see the decay of the chemicals in the soaked sample so that we could see how long the chemicals could reside in the sample due to its volatility. The decay of

these chemicals in soaked LDPE can be observed in Figure 5-3. From the result, we learnt that the test should be conducted within one hour after the 2 hours of soaking to guarantee sufficient amount of chemicals in the tested sample so that the objective to see effect of the chemicals on the electrical properties of LDPE could be fully achieved. However, the chemicals could retain longer in the sample if it is in a closed environment. As in PEA method, the sample is placed in between 2 electrodes where there are only small room for the chemicals to evaporate. As in the graph below, it can be considered that the amount of chemicals is constant throughout the measurement.
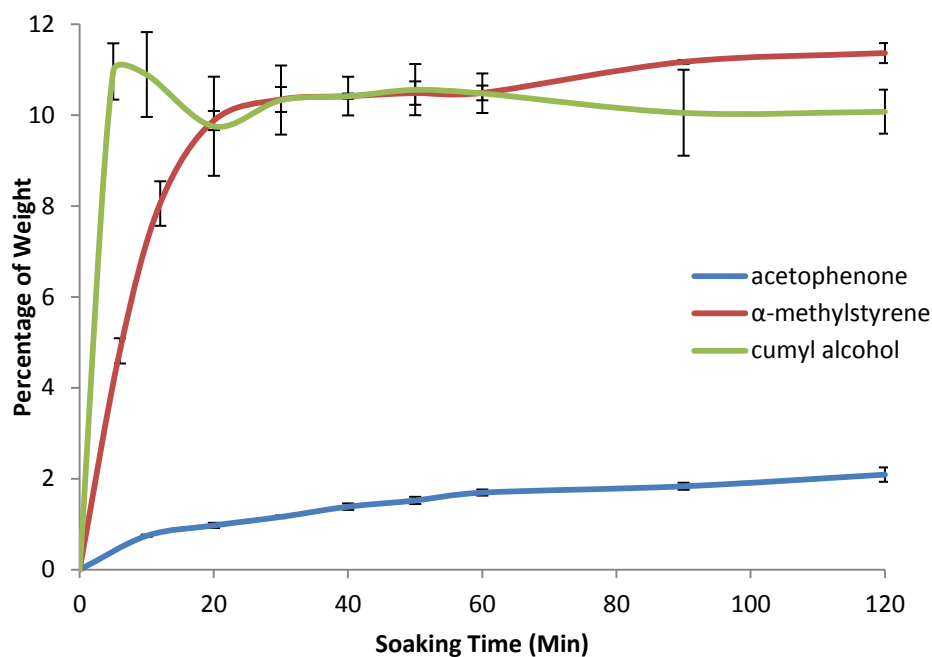
Figure 5-2: The Soaking rate of acetophenone, α-methylstyrene and cumyl alcohol in LDPE.
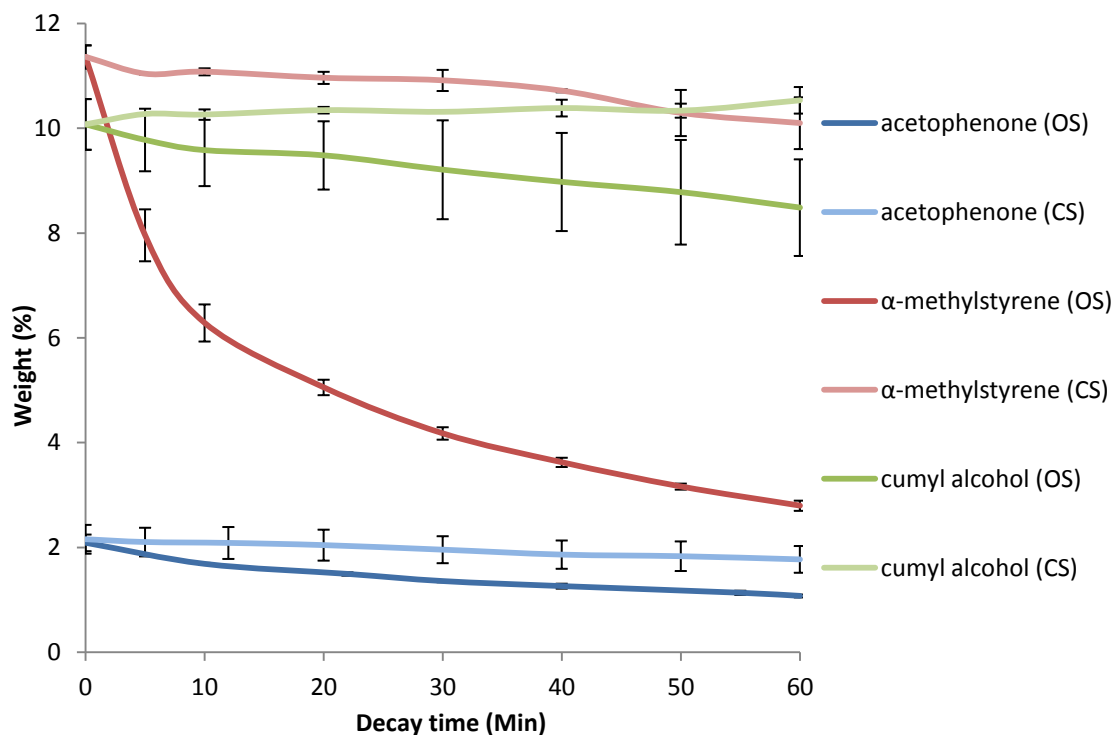
Figure 5-3: The decay of chemicals in soaked LDPE in open system (OS) and closed system (CS).

In dielectric spectroscopy and conductivity measurement, all samples were coated with gold to obtain good contact between the electrode and insulator. It is also observed in these measurements that gold coated samples produce better result (high signal-to-noise ratio) compared to the uncoated samples. The coating process was carried out before soaking to prevent any removal of the byproducts from samples due to the employment of vacuum during the gold coating process. The percentage weight of the byproducts in each samples are almost similar and these values are presented in Table 5-1. The specifications of samples used in each measurement are also presented in Table 5-2.

Table 5-1: Comparison of percentage weight of byproducts in coated and uncoated samples.

Byproducts	Acetophenone	α-methylstyrene	Cumyl alcohol
Uncoated LDPE	2.09%	10.07%	11.36%
Coated LDPE	2.26%	9.33%	10.09%

Table 5-2: Samples specification for each measurement.

Test/Measurement	Sample Thickness	Sample diameter	Gold coated
Space charge measurement	180 µm	36mm	No
Dielectric Spectroscopy measurement	180 µm	25mm	Yes
DC Conductivity test	50 µm (Clean LDPE) 180 µm (soaked samples)	50mm	Yes
AC Breakdown Test	50 µm	-	No

5.3   Fourier Transform Infrared

In this research, FTIR was also used to study the byproducts in the sample. The infrared spectrum was obtained by applying the infrared radiation through the sample. Some of the radiation will be absorbed by the sample and some of it is transmitted. Depending on the responses from the vibrational spectroscopy, the molecule structure could be determined. Some vibration modes of the molecules are symmetrical stretching, anti-symmetrical stretching, scissoring, rocking and twisting. Figure 5-4 illustrates the vibration mode of CH_2 group. The resulting spectrum represents a fingerprint of a sample with absorption peak corresponding to the frequencies of vibration between the bonds constructing the material.
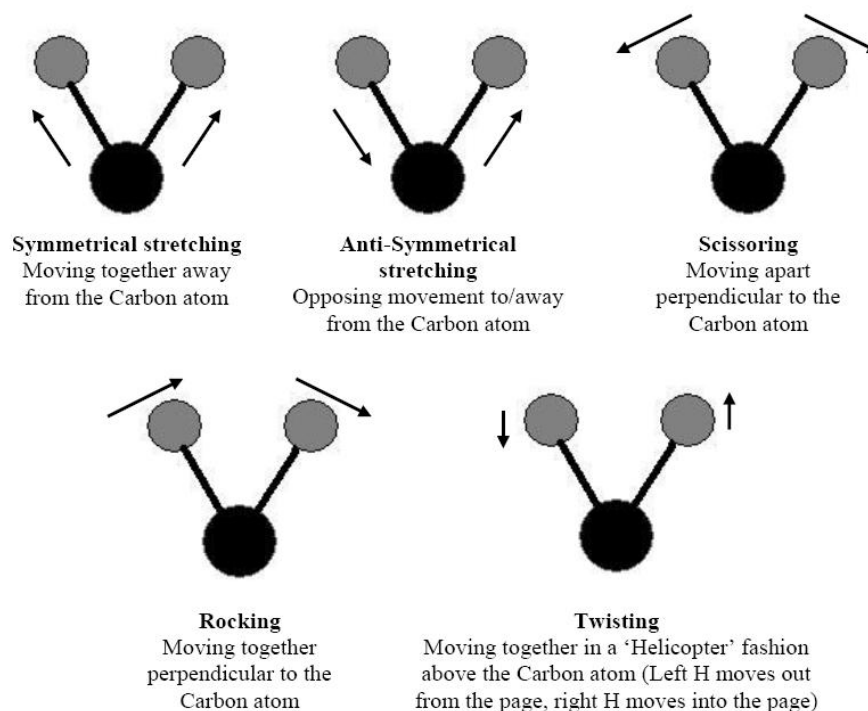
Figure 5-4: Some example of vibration modes of CH$_2$ group

Figure 5-5 illustrates the principle of FTIR. FTIR consists of two mirrors located at a right angle to each other, oriented perpendicularly to a beam splitter at a 45° angle relative to the two mirrors. Radiation incident on the beam splitter is then divided into two parts, each of which propagates down one of the two arms and is reflected off one of the mirrors. The two beams are then recombined and transmitted out to the detector. When the position of one mirror is continuously varied along the axis of the corresponding arm, an interference pattern is swept out as the two phase-shifted beams interfere with each other [78].
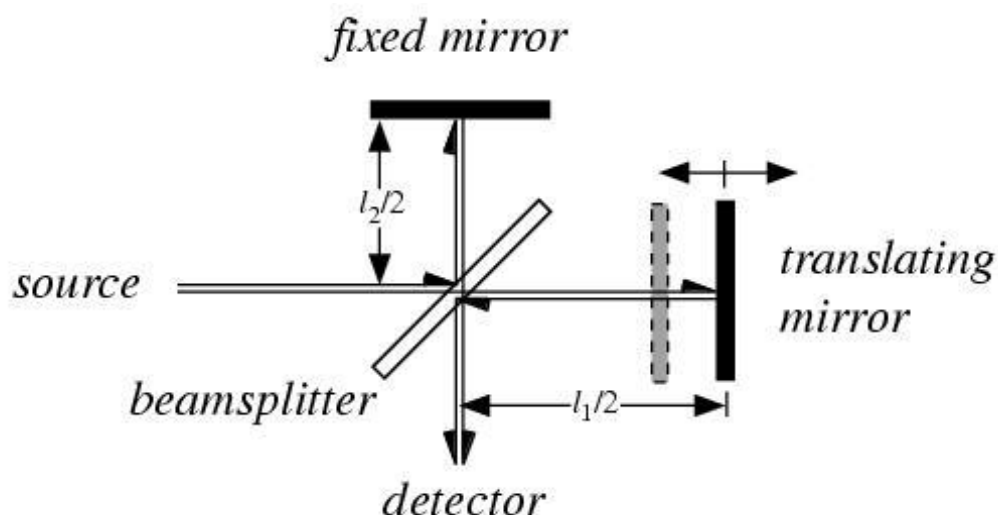
Figure 5-5: The principle of Fourier Transform Infrared

According to quantum mechanics, these frequencies correspond to the difference in the energy between the ground state (E_0, lowest frequency) and several excited states (E_n, higher frequencies). The transition between these two states will involve the absorption of the light energy (determined by the wavelength) equal to the difference in energy between the two states [79]. FTIR is usually used to identify unknown materials, determine the quality or consistency of a sample, as well as determining the amount of components in a mixture. This technique has successfully adapted before [80].

FTIR spectrum can be used to detect the existence of the crosslinking byproducts in the sample. For instance, C=O for acetophenone, O-H or C-O for cumyl alcohol and C=C for α-methylstyrene. To represent the main peaks and associated interactions for the entire wavenumber range, Table 5-3 has been formed.

Table 5-3: Wavenumbers and related vibrations compiled from [81], [82]* and [83]**

Functional group	Description of Vibration	Wave number (cm^{-1})
O-H	stretch, H-bonded	3200-3600
O-H	stretch, free	3500-3700
C-H	stretch	2850-3000
C=O	stretch	1670-1820
C=C	stretch	1400-1600
-C-H	bending	1350-1480
C=C	-	1375, 1263**
C-O	stretch	1050-1150
C-H	bending	936*
C=CH$_2$	twisting	578*

Figure 5-6 illustrates the FTIR absorbance spectrum of the fresh and degassed XLPE in comparison to LDPE spectrum. The spectrum confirms that 4 days of degassing at 80°C could not remove the whole byproducts as shown in the red line in the figure. Other than FTIR, the effect of degassing could also be observed by weight reduction through out the degassing period such as reported in [9]. However this technique will not divulge the exact byproducts left in the sample. More importantly, there is no accurate measure to tell that the sample is free from any byproducts. The small peak seen in the degassed XPLE spectrum from 2800-3000 cm^{-1} may due to the C-H peak that was detected during the background scanning. This peak is considered as the measurement error.

The amount of byproducts in the sample could also be quantified by using the absorbance spectrum. Figure 5-7 shows the relation of the absorbance intensity with the soaking time. Absorbance level depends on the absorptivity of the species at that particular wavenumber, the path length as well as the concentration of the species. The absorbance level that presented in Figure 5-7 is the height of the peak corresponding to the molecular bond that exist in the byproduct. For acetophenone, peak of C=O was observed at 1694cm^{-1} and peak of C=C in α-methylstyrene is observed at 1630cm^{-1}. Meanwhile the peak of O-H in cumyl alcohol appears to be at 3370cm^{-1}.The level of acetophenone and cumyl alcohol are

almost similar to what have been reported in [5] and [36]. However the absorbance level of α-methylstyrene shows some deviation.
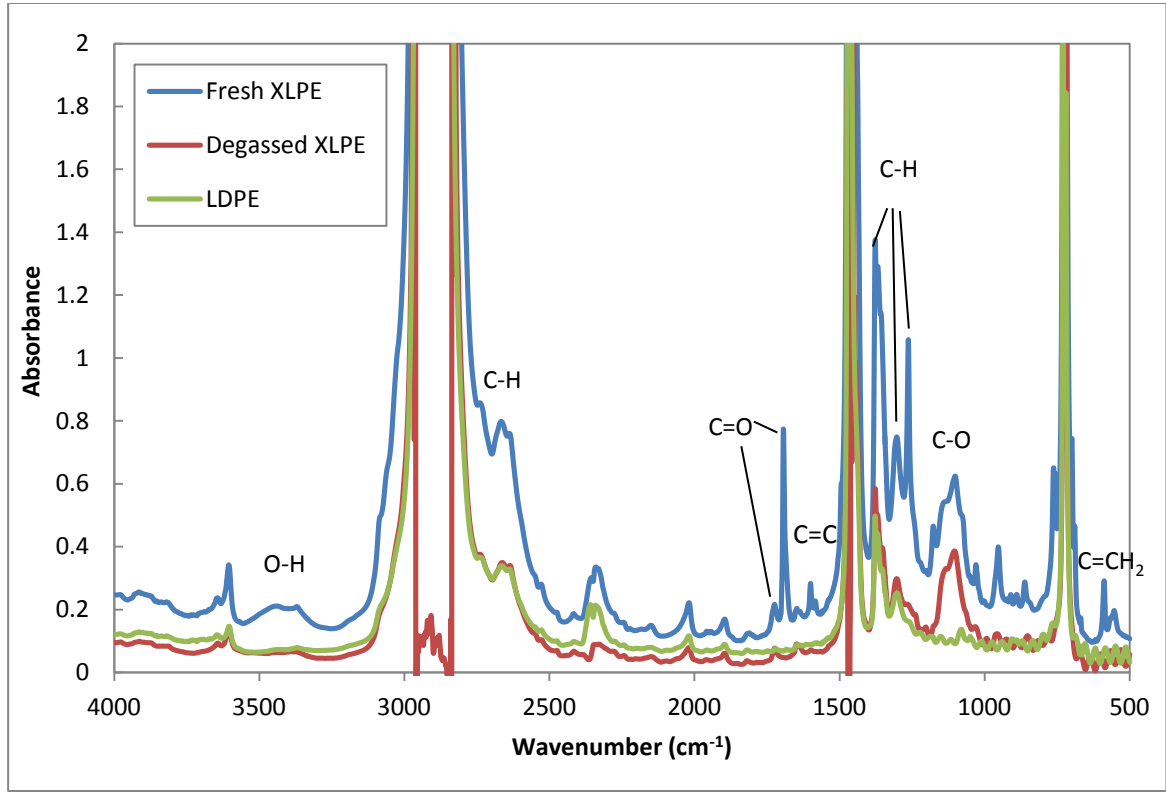
Figure 5-6: FTIR absorbance spectrum of fresh XLPE, degassed XLPE, and LDPE sample.
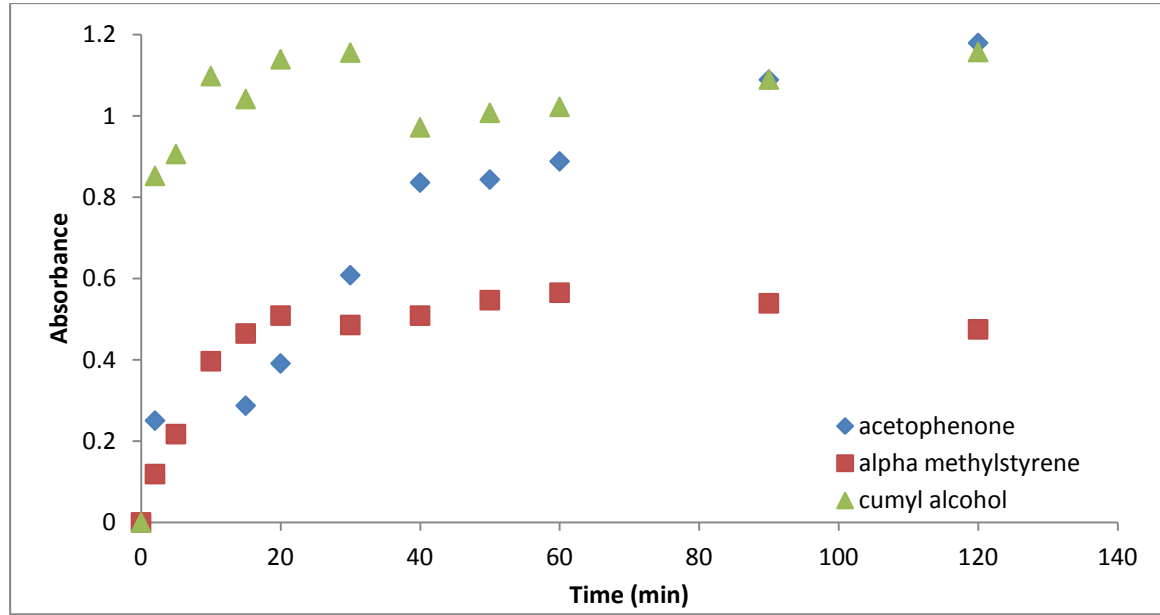
Figure 5-7: The Absorption level of the crosslinking byproducts in the samples during soaking process.

5.4   Chapter Summary

The importance to ensure only one byproduct exist in each sample is emphasised here. Therefore LDPE is chosen as the base material over XLPE film. The soaking process took 2 hours and the amount of the byproducts in each sample is measured using percentage weight as well as the FTIR absorbance level.

The percentage weight of byproducts in the test samples is higher than in practice. This limitation is unavoidable in order to obtain uniform byproduct distribution across the sample thickness. However, since the focus of this research is to gain knowledge on the influence of these byproducts on electrical properties, this big amount of byproducts will not affect the research aim. Furthermore, some calculation could be made to estimate the quantitative increment or decrement of the measured value by each percent of the byproducts.

Chapter 6   Space charge Measurement

6.1   The Measurement Procedures.

In the space charge measurement, a pulse voltage of 600 V with a duration of 5 ns was applied to the sample to generate an acoustic signal wave. Two types of base materials were used in this measurement; XLPE and LDPE. For the former material, fresh and degassed XLPE (degassed for 4 days at 80°C) were stressed at 8kV for 2 hours followed by an hour of decay.

For LDPE based sample, all samples were soaked into the chemicals for 2 hours and subsequently applied to 3 different positive dc voltages which were 5kV, 8kV and 10kV. For space charge measurement, PEA technique was employed. Readings were taken using the *easy data* software in Lab View environment for every 10 minutes.   In this measurement, semiconductor (top electrode, anode) and aluminium (bottom electrode, cathode) were applied directly to the specimens.

Before the sample was stressed at the specified voltage, 2kV dc voltage was applied across the sample for calibration purpose which has been discussed in Chapter 3 before. The charge density pattern at 2kV was then used in the PEA software as the reference signal in software written in Lab View TM environment.

During charging process, two measurements were conducted which is volts on and volts off measurements. For volt on, the measurement was taken while the power was still 'on', whiles for volt off measurement, the reading was taken 10 seconds after the dc voltage was removed (short circuit condition). As soon as the reading was taken, the sample was recharged again until the next reading time, for 1 hour of total charging period. Consequently, the power supply was permanently removed and the sample is discharged. This time, the decay of the accumulated charge in specimen was measured for another hour. For a better understanding on the volt on and volt off measurement procedure, Figure 6-1 could be referred.
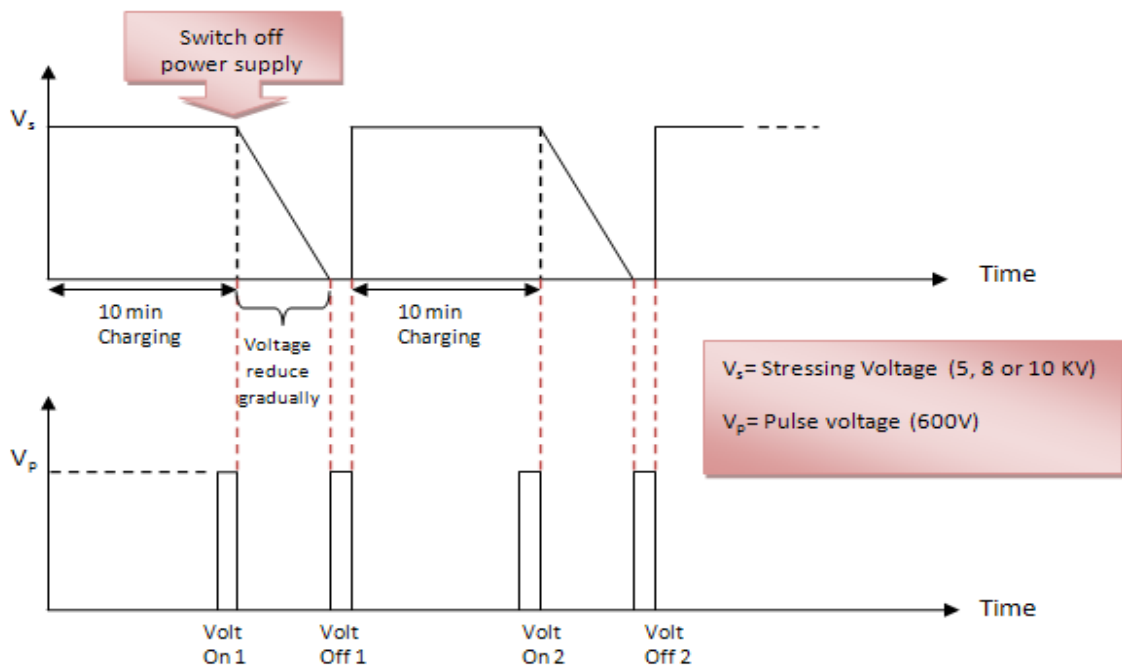
Figure 6-1: The volt on and volt off measurement

6.2   Measurements With And Without Voltage Applied

Volt on measurement will include both fast and slow moving carriers. Meanwhile, for volt off measurement, the results will only show the slow moving carries. These fast and slow moving carries signify the path in which the carriers will take towards the opposite polarity electrode. The fast moving carriers are the carriers that are free from trap or those which

escape from the traps very shortly after the dc voltage is removed. On the other hand, the slow moving carriers are the carriers that are trapped in the deep traps and thus their movement are very limited depending on the energy that is required to overcome the barrier. As the power supply is disconnected, the carriers with energy less than the barrier will stay in the traps.

6.2.1 *Fresh XLPE*
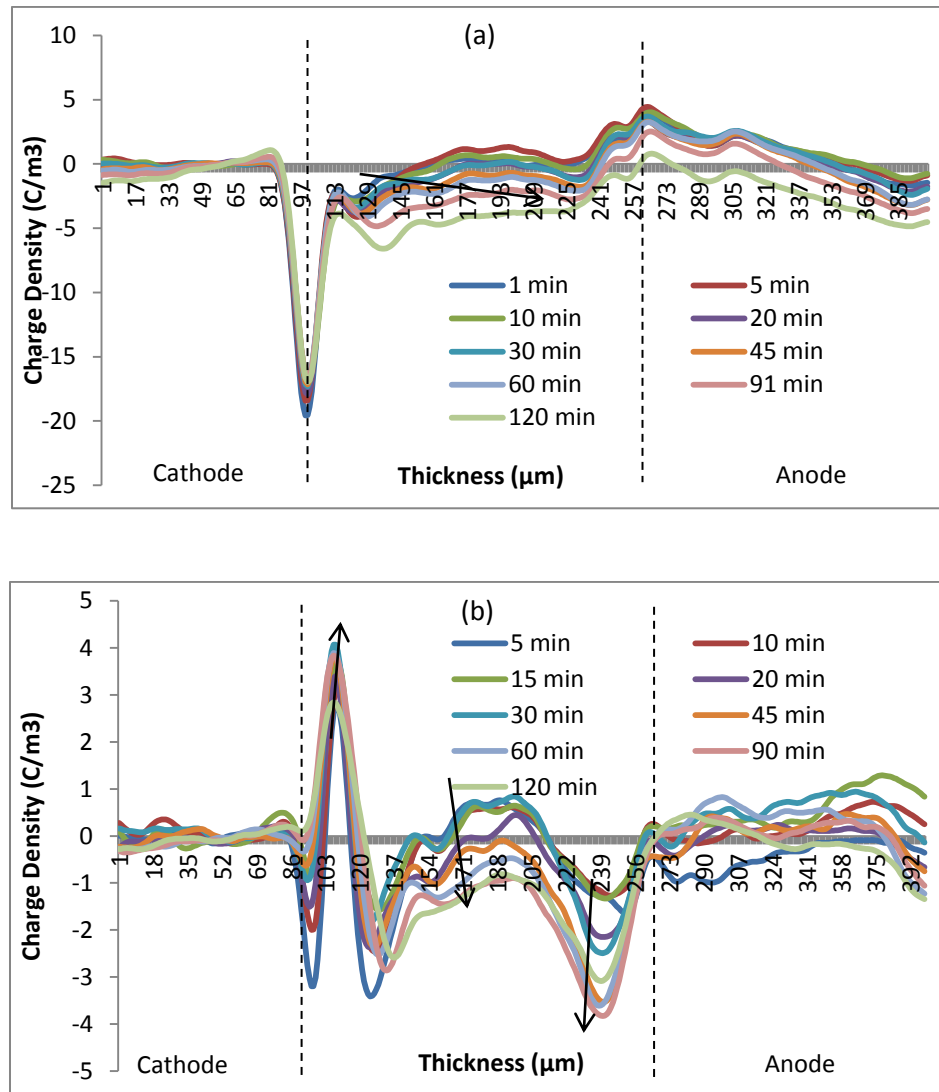
Figure 6-2: The space charge profile of fresh XLPE during a) volt on and b) volt off.

The volt on result for fresh XLPE sample shows that the formation of homocharge in the vicinity of the electrodes. As the sample is stressed for longer time, more negative charges

are seen penetrated into the sample bulk. When the voltage is removed from the sample, it is observed that heterocharges are accumulated very near to the electrodes. The heterocharge peaks are increasing with the stressing time and becomes constant after 45 minutes. In term of the bulk charge, electrons or negative charge carrier dominate this region. The charge profile of the fresh sample is presented in Figure 6-2.
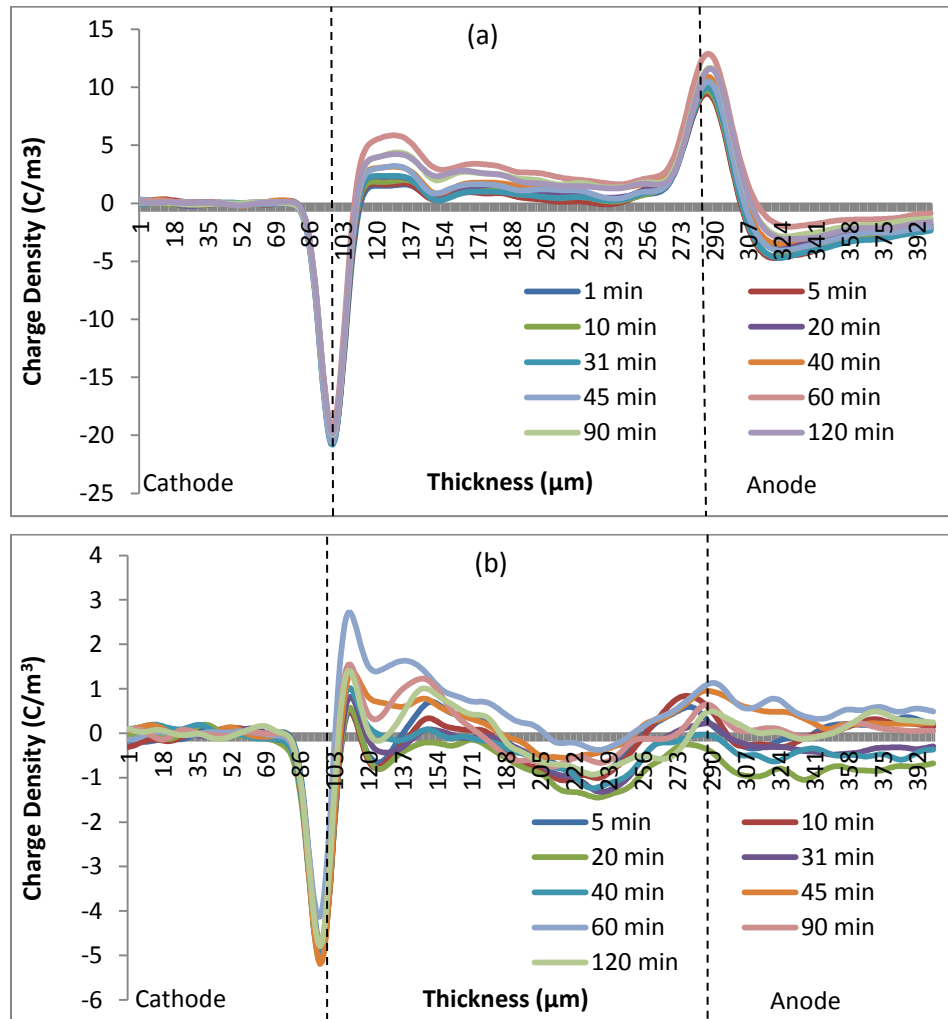
Figure 6-3: The space charge profile of degassed XLPE during a) volt on and b) volt off.

The volt on charge profile for the degassed XLPE sample (Figure 6-3(a)) shows the formation of positive heterocharge near the cathode. The positive peak near electrode, as well as the spread of positive charge in the sample bulk increase by time. Volt off result in Figure 6-3 (b) reveals that there is a small amount of negative heterocharge accumulated near the anode. However these negative hetero charges get smaller by time. From both

results, it is seen that the XLPE samples causes the formation of heterocharge in the sample. The fresh XLPE sample has more charge injection in the sample hence out numbering the heterocharge that actually accumulated near the electrodes. The amount of heterocharge is also less in the degassed sample due to less byproduct left in the sample. These charges may be due to the remaining byproducts that still reside in the XLPE sample. Equivalent results were reported in [84]. After degassing XLPE sample for 3 days at 90°C, Fu et. al also observed charges in degassed sample although instead of heterocharges, homocharges was observed near electrode.
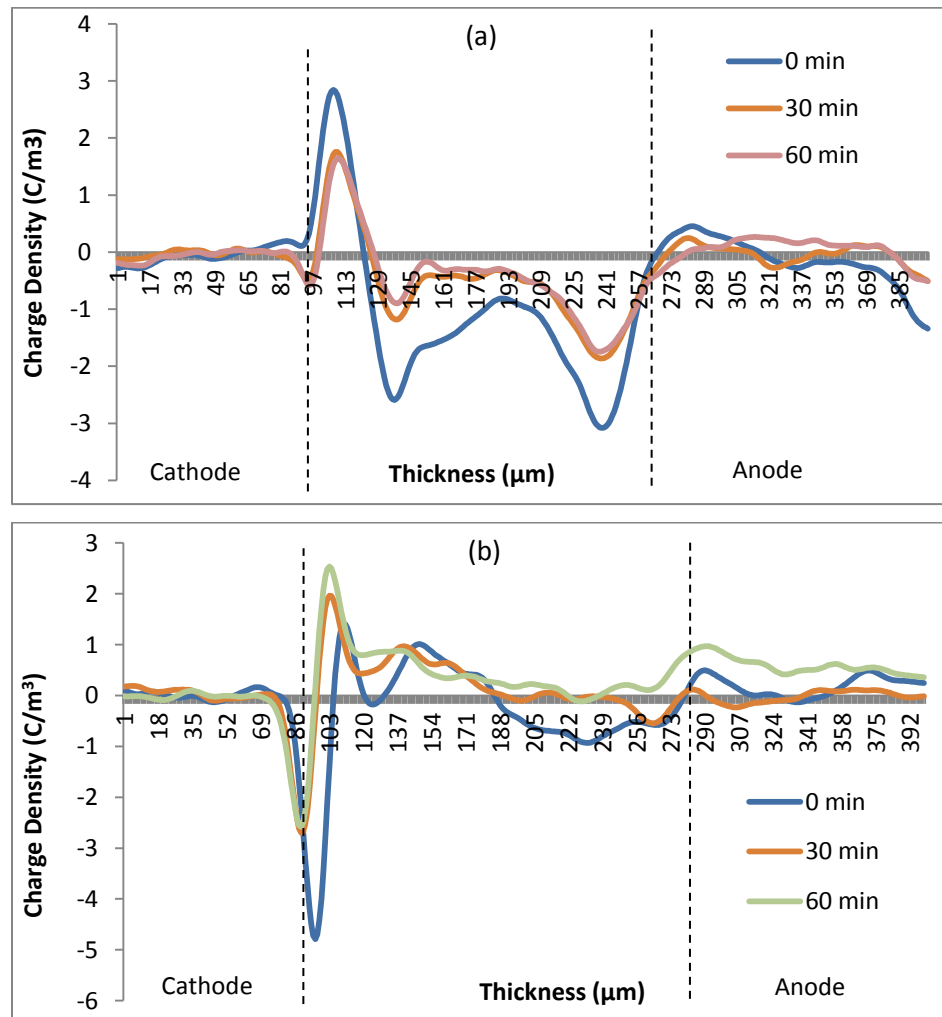
Figure 6-4: The decay charge profile of a) fresh XLPE and b) degassed XLPE.

The charge decay in fresh XLPE is seen to be very fast in the first 30 minutes and become slower after that. The charge profile after decaying for 60 minutes is very similar to that of 30 minutes. The charge decay characteristic of the degassed sample is not straight forward.

The negative charge near the cathode may be drifted into the electrode revealing the positive charges that reside in the region. As a result, the positive peak appears in the vicinity of the cathode. The space charge profile of fresh and degassed XLPE do not give much understanding on the characteristics of the byproducts in term of space charge accumulation. Hence, separate investigation on each byproduct is crucial.

6.2.2 *Clean LDPE*

Before we could analyse the accumulation of space charge in the soaked sample, it is important to study the charge behaviours in the clean LDPE so that the analysis of the space charge accumulation will not be deluded. The results of clean untreated LDPE will be used as the reference to the results obtained for soaked samples. The charge build up in the clean LDPE can be seen in Figure 6-5.
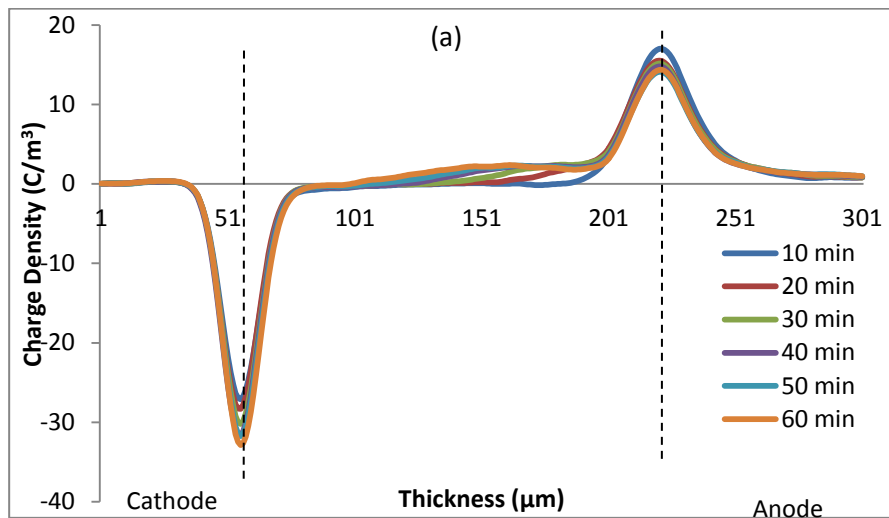
a) Clean LDPE stressed at 5kV,
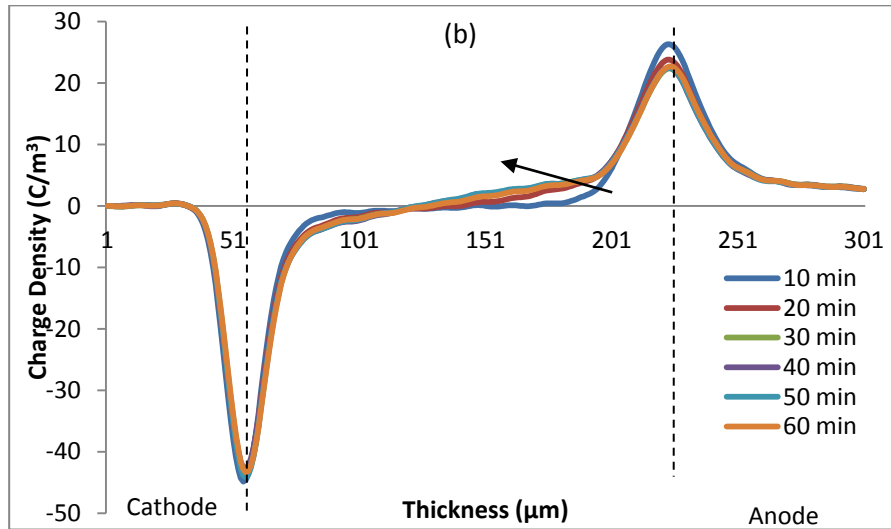
b) Clean LDPE stressed at 8kV,
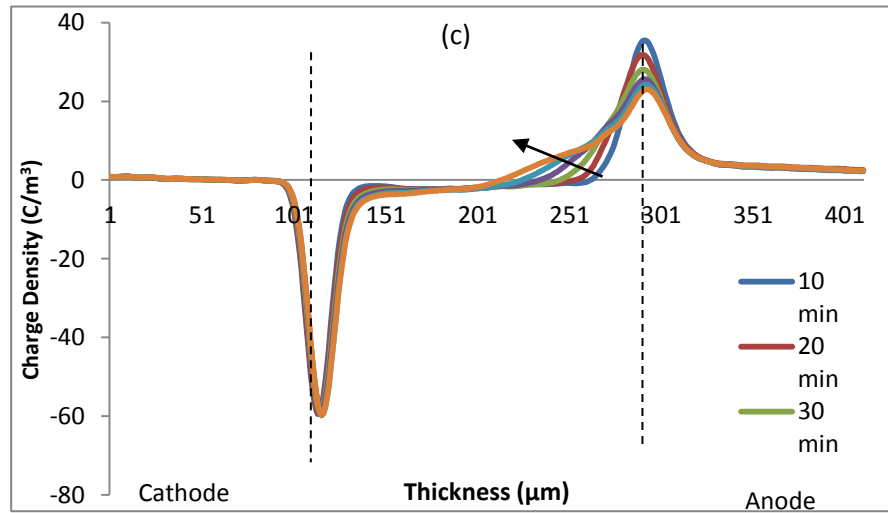
c) Clean LDPE stressed at 10kV,

Figure 6-5: Charge Density of 180µm clean LDPE; a) stressed at 5kV, b) stressed at 8kV, c) stressed at 10kV, during Volt ON condition

This observation is consistent in the volt off measurement results and in fact, the charge build up could be seen even clearer. These results are presented in Figure 6-6. For the sample stressed at 5 kV, the increasing stress time results in the charges of both polarities gradually increasing in the sample. Negative charges are trapped in the region near to the cathode which stops them to move towards the anode. It is also observed that the injected positive charges tend to move towards the cathode due to different polarity attraction. At 8kV and 10kV, a greater volume of negative charges injected from the cathode and slowly

Figure 6-6: Charge Density of 180µm clean LDPE; a) stressed at 5kV, b) stressed at 8kV, c) stressed at 10kV, during Volt OFF condition.

the charges drifted in the sample bulk. It is clear that the meeting point of positive and negative charges moves towards the middle of the sample with increasing applied voltage. The gradual increase of positive and negative charges is similar to the result in [30].

6.2.3   *Acetophenone Soaked LDPE*

For acetophenone soaked LDPE sample, the volt off results at the three voltages are illustrated in Figure 6-7. This time, the domination of negative charges is obvious. In the vicinity of the positive electrode, the amount of positive charge decreases with time indicating either the positive charges migrated towards the nearby electrode, or the amount of negative charges is greater than that of positive charges at that specific area. It is observed that the amount of negative charges that move into the bulk of the sample, towards to anode, is proportional to the stressing time. This observation can be seen at all three stressing voltages and more noticeable at higher voltage. As the positive charges from the anode are suppressed, one observes distinguishable differences in the charge profile of LDPE soaked in acetophenone compared to an untreated sample.

a) Acetophenone soaked LDPE stressed at 5kV,
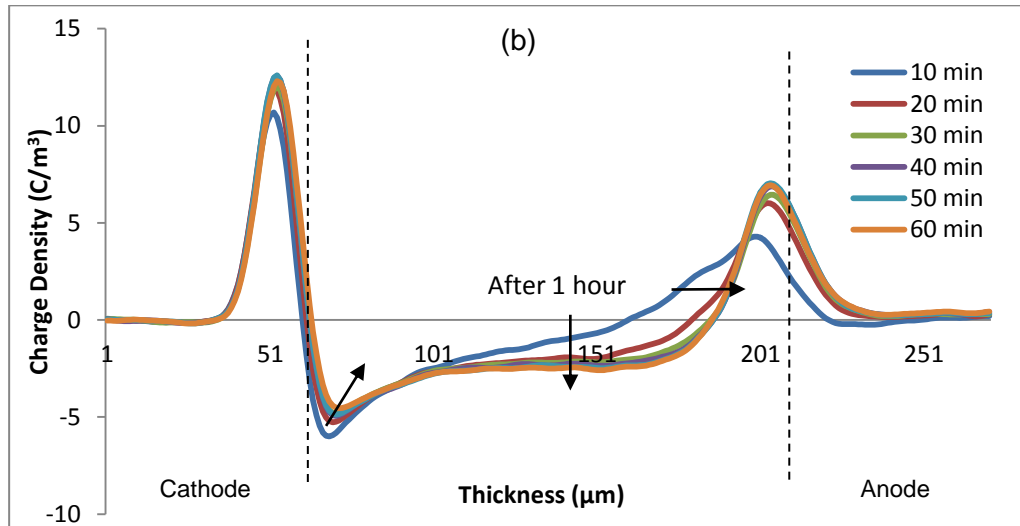
b) Acetophenone soaked LDPE stressed at 8kV,
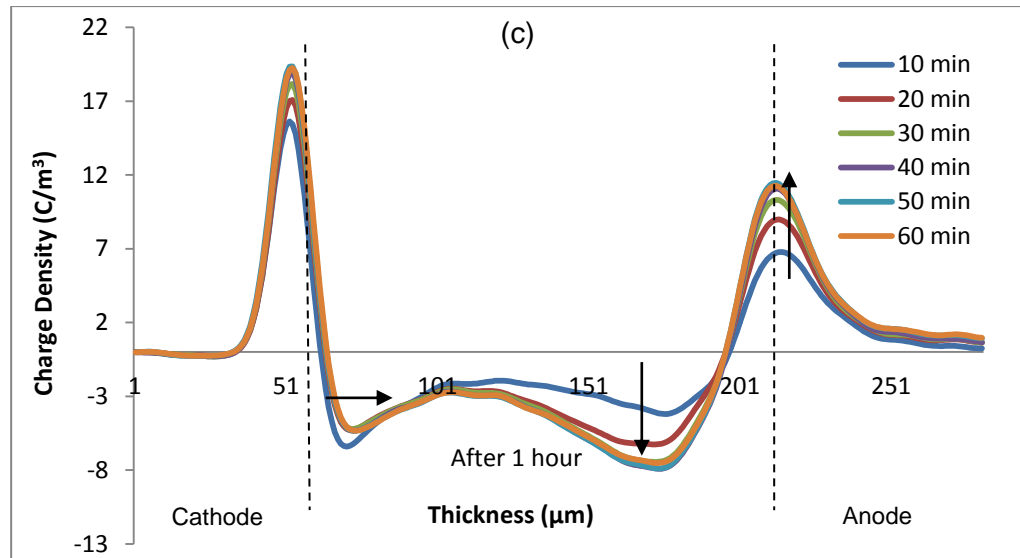
c) Acetophenone soaked LDPE stressed at 10kV,

Figure 6-7: Charge Density of 180µm acetophenone soaked LDPE; a) stressed at 5kV, b) stressed at 8kV, c) stressed at 10kV, during Volt OFF condition.

The negative charge build up is also seen in the volt on measurement result at 8 kV and 10 kV. This result is presented in Figure 6-8. In sample stressed at 5kV, any charge build up could hardly been seen.
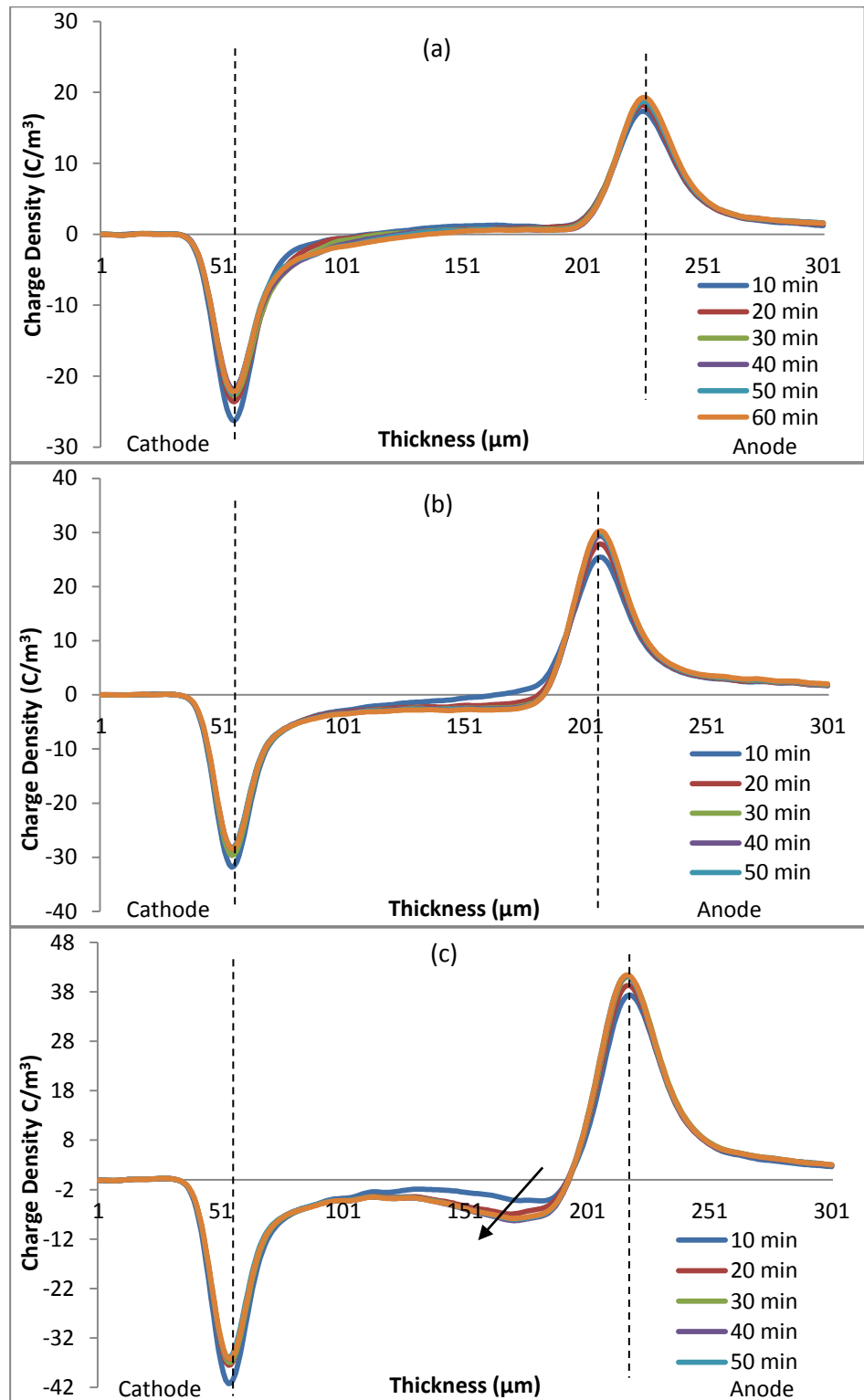
Figure 6-8: Charge Density of 180µm acetophenone soaked LDPE; a) stressed at 5kV, b) stressed at 8kV, c) stressed at 10kV, during Volt ON condition.

6.2.4 *α-methylstyrene Soaked LDPE*

Volt on measurement results for α-methylstyrene soaked LDPE is presented in Figure 6-9 meanwhile charge density during volt off, is illustrated in Figure 6-10. The charge profiles for α-methylstyrene soaked LDPE and untreated clean sample are almost similar except that the positive charges in clean untreated LDPE increases gradually compared to the easy domination of positive charge in the α-methylstyrene soaked sample. Due to that, we could say that α-methylstyrene assists the movement of positive charges into the sample bulk.
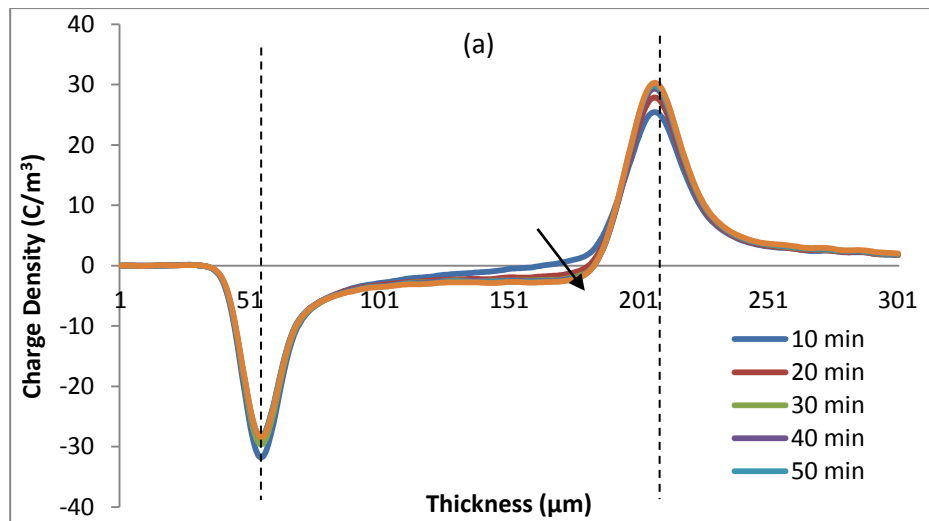
α-methylstyrene soaked LDPE at 5kV
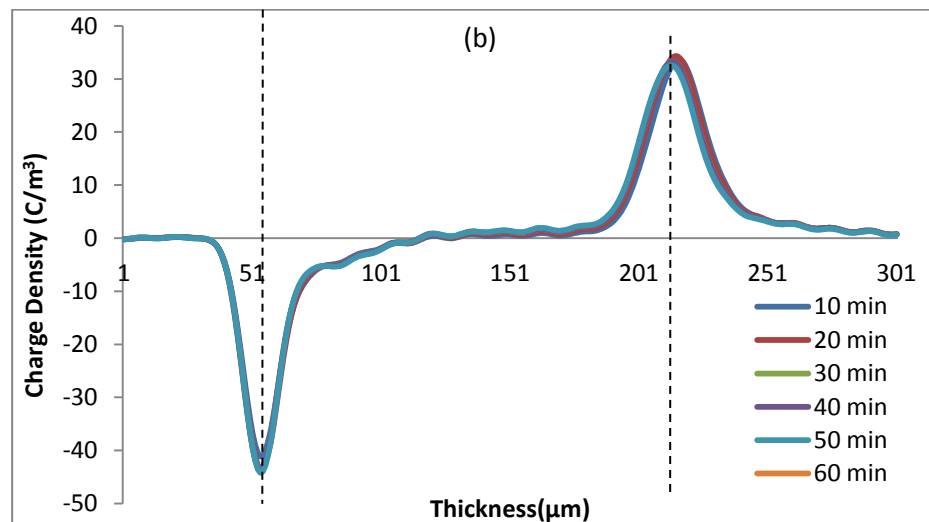
b) α-methylstyrene soaked LDPE at 8kV
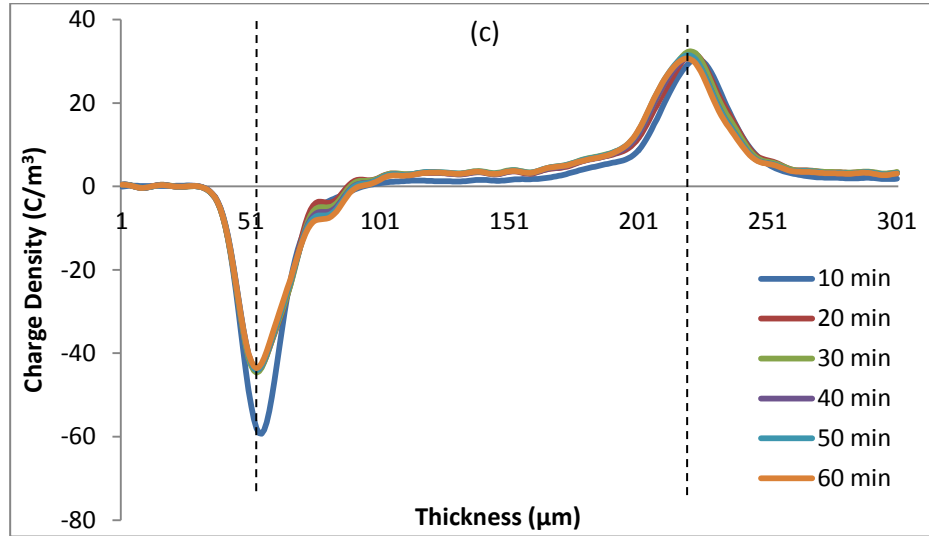
c) α-methylstyrene soaked LDPE at 10kV

Figure 6-9: Charge Density of 180µm α-methylstyrene soaked LDPE; a) stressed at 5kV, b) stressed at 8kV, c) stressed at 10kV, during Volt ON condition.

In term of magnitude, samples stressed at 5kV and 8kV shows almost the same amount of charge accumulation in sample. At 10kV (Figure 6-10(c)) positive charges have already accumulated in the bulk of the sample as early as the first 10 minutes of stressing. Similarly to Figure 6-10, authors have reported [5] a rapid migration of positive charges in a α-methylstyrene soaked sample, it is concluded that α-methylstyrene has a greater effect on the positive charge migration than acetophenone as it can permeate faster into the polymer structure.
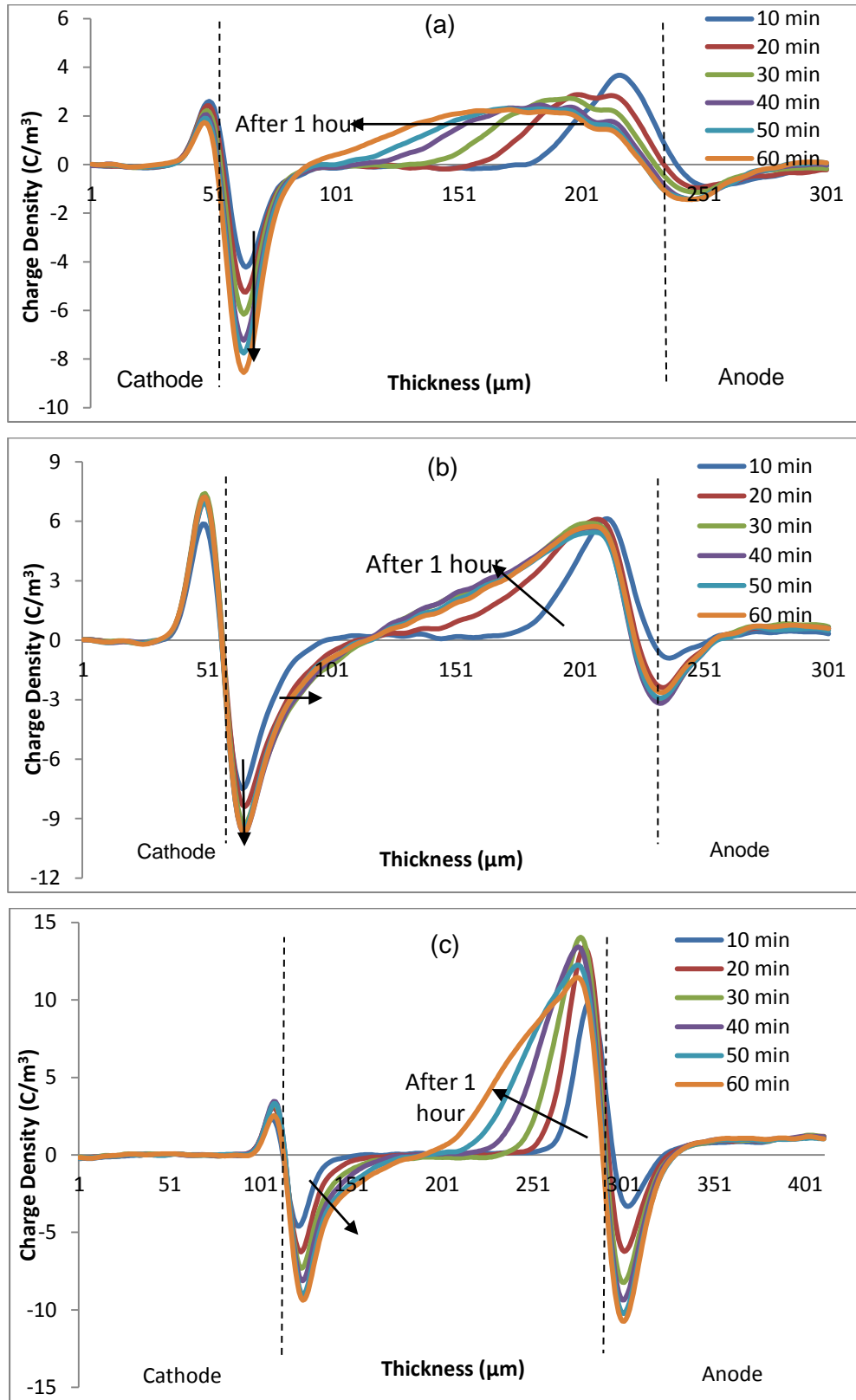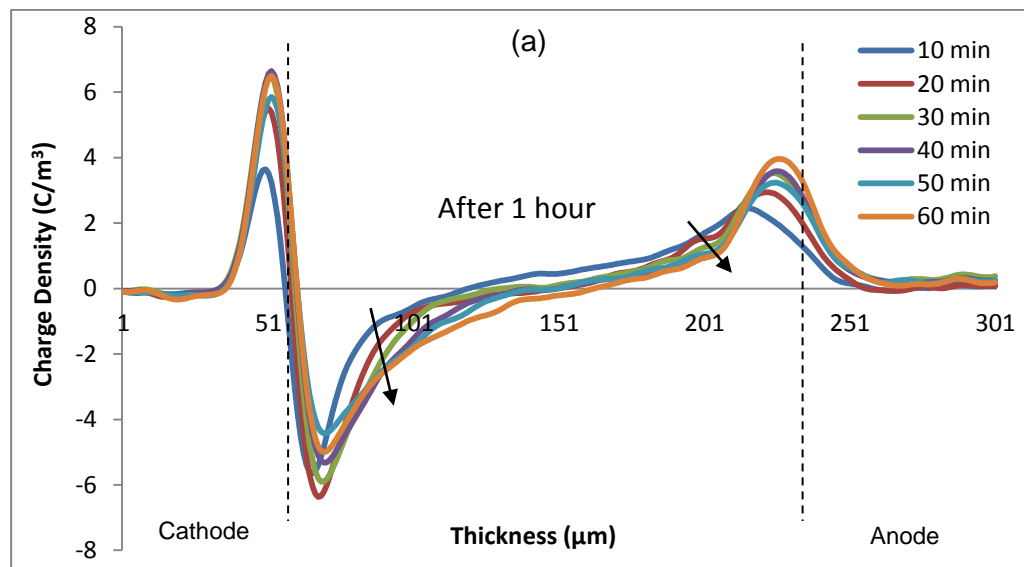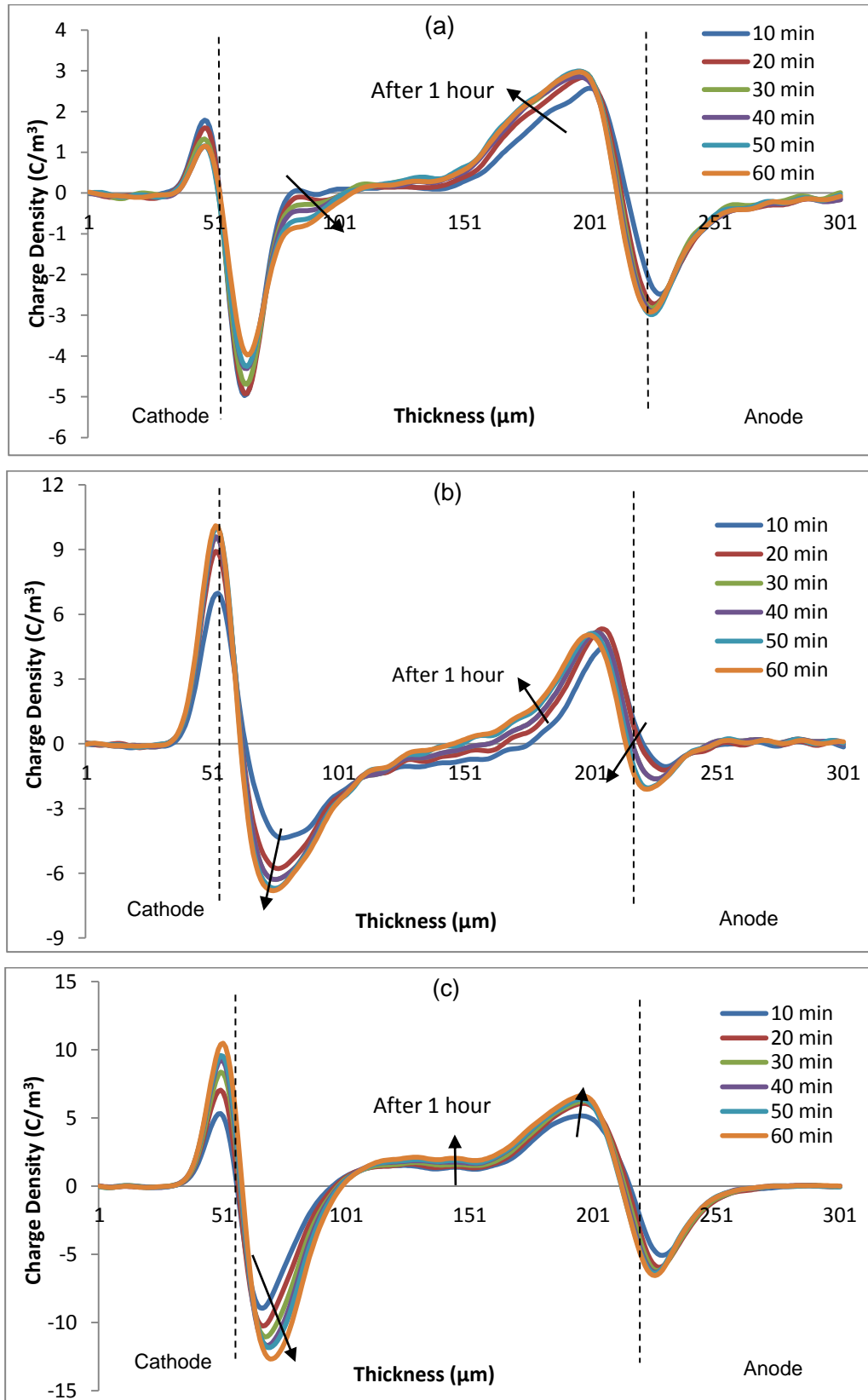
Figure 6-10: Charge Density of 180μm α-methylstyrene soaked LDPE; a) stressed at 5kV, b) stressed at 8kV, c) stressed at 10kV, during Volt OFF condition.

6.2.5 *Cumyl Alcohol Soaked LDPE*

The space charge characteristic of cumyl alcohol soaked LDPE is different from the two former chemicals discussed. The charge density of the sample during volt on and volt off are shown in Figure 6-11 and Figure 6-12 respectively.

Cumyl alcohol causes charge accumulation of both charge polarities with heterocharges appeared when the sample is stressed at 5kV and 8kV. Cumyl alcohol introduces more charge injection into the sample compared to the other byproducts. Both positive and negative charges were introduced into the sample. In Figure 6-11 (a) and (b), after 10 minutes charging, the negative charges migrated into the bulk, reducing the height of the positive peak near cathode. After 20 minutes, the positive peak is totally disappears and negative charges are now accumulated in the bulk of sample. Similar observation is seen for the negative peak near the anode. However, as the voltage is increased, heterocharges begin to diminish gradually due to charge injection from the electrodes. This phenomenon is reported in [85]. Heterocharges are also observed in cumyl alcohol soaked sample that reported in [86] but not discussed.
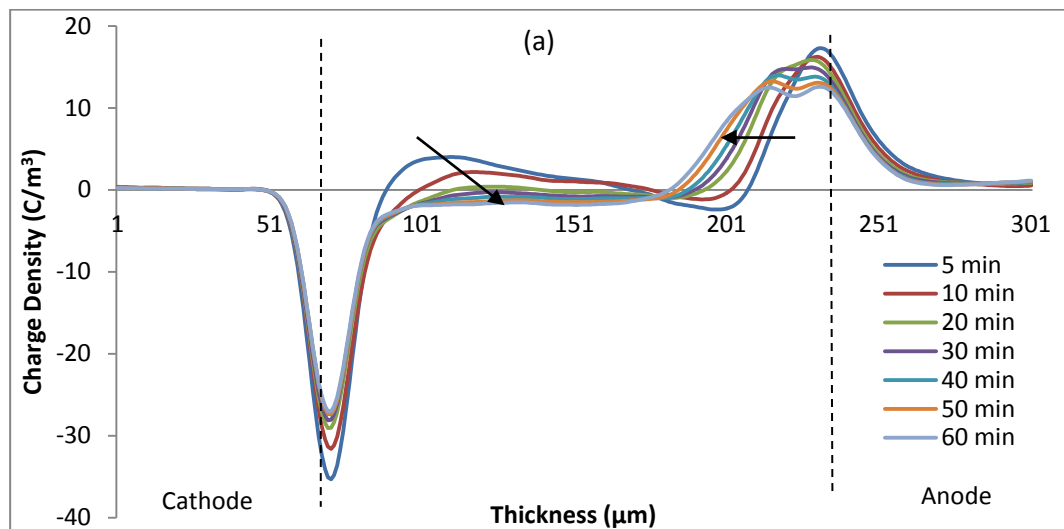
a) cumyl alcohol soaked LDPE stressed at 5kV
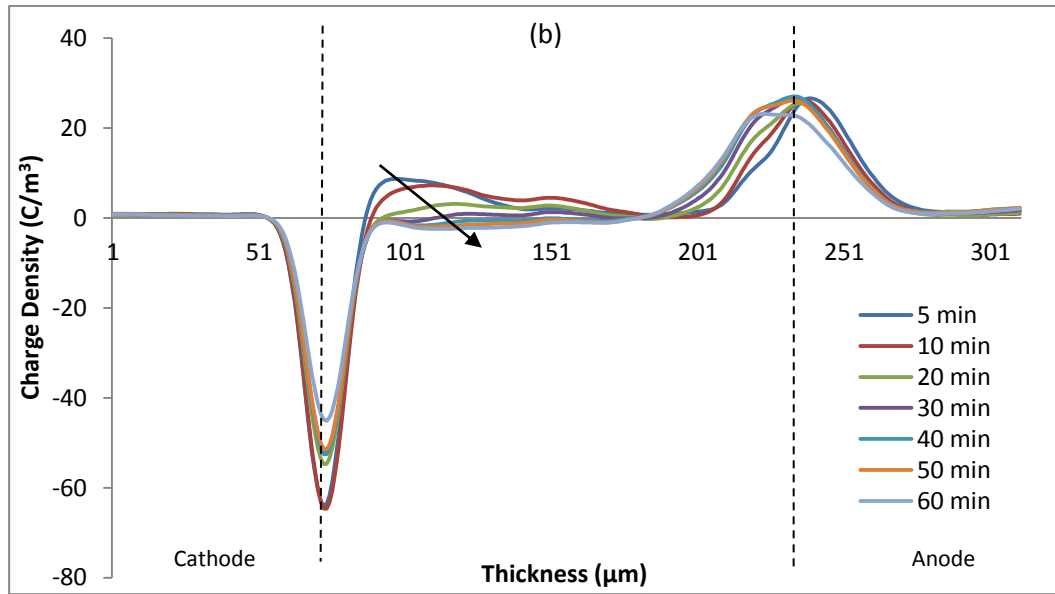
b) cumyl alcohol soaked LDPE stressed at 8kV
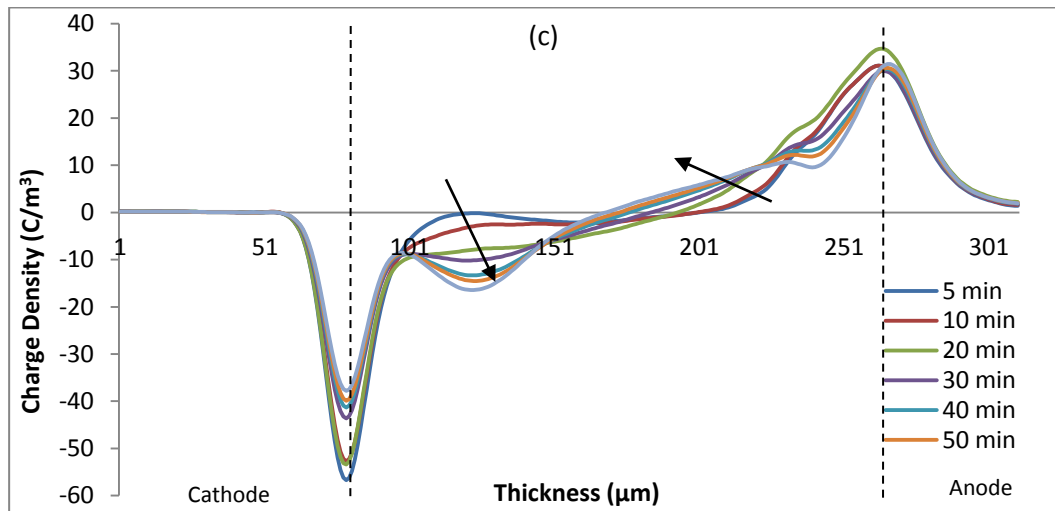
c) cumyl alcohol soaked LDPE stressed at 10kV

Figure 6-11: Charge Density of 180µm cumyl alcohol soaked LDPE; a) stressed at 5kV, b) stressed at 8kV, c) stressed at 10kV, during Volt ON condition.
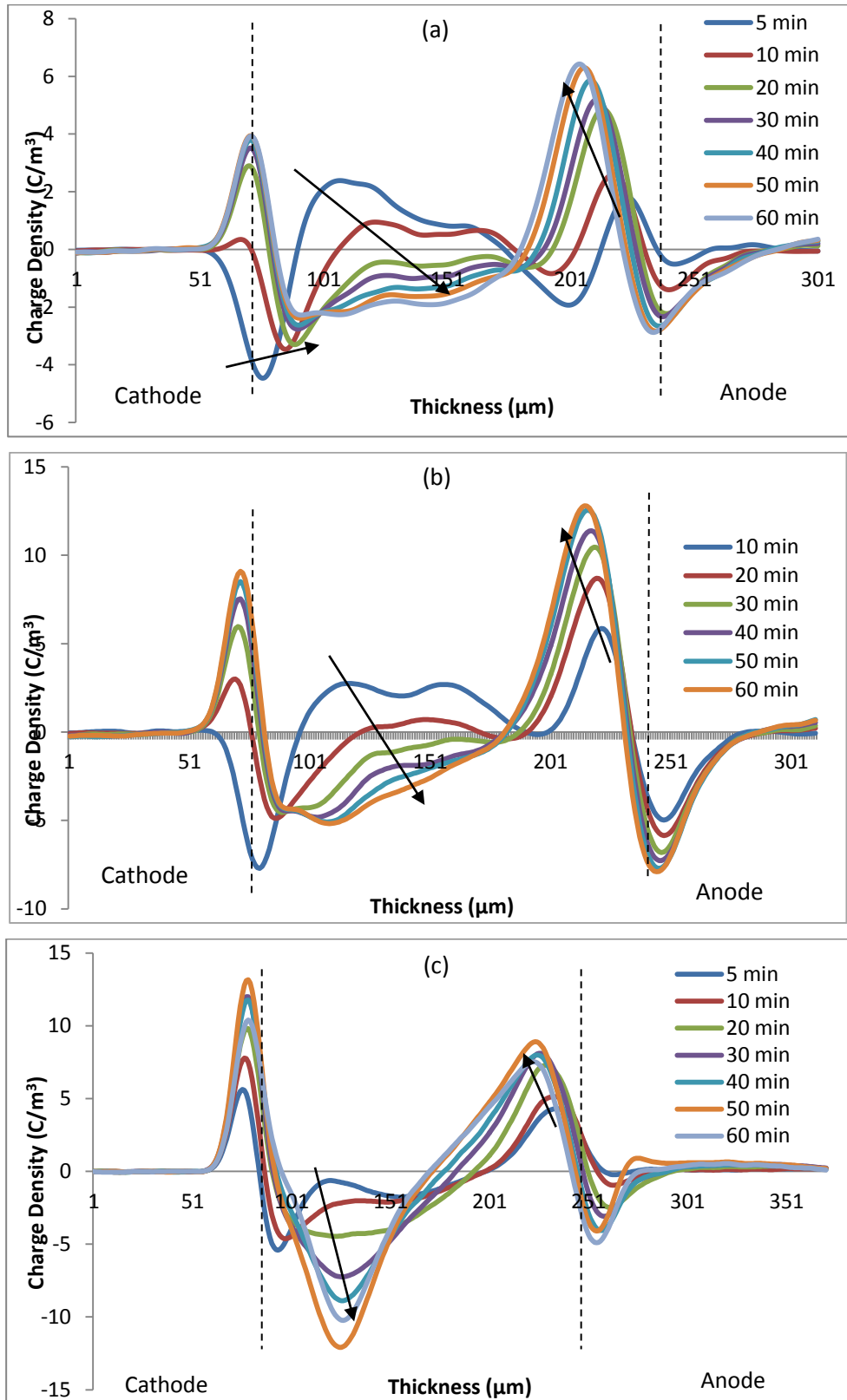
Figure 6-12: Charge Density of 180µm cumyl alcohol soaked LDPE; a) stressed at 5kV, b) stressed at 8kV, c) stressed at 10kV, during Volt OFF condition.

6.3 Charge Decay Results

6.3.1 *Clean LDPE*

By monitoring charge decay after the applied voltage is removed, one can see the influence of these byproduct chemicals on the charge transportation in the insulator. Figure 6-13 shows the changes in charge profiles in clean LDPE after the removal of the applied voltage.
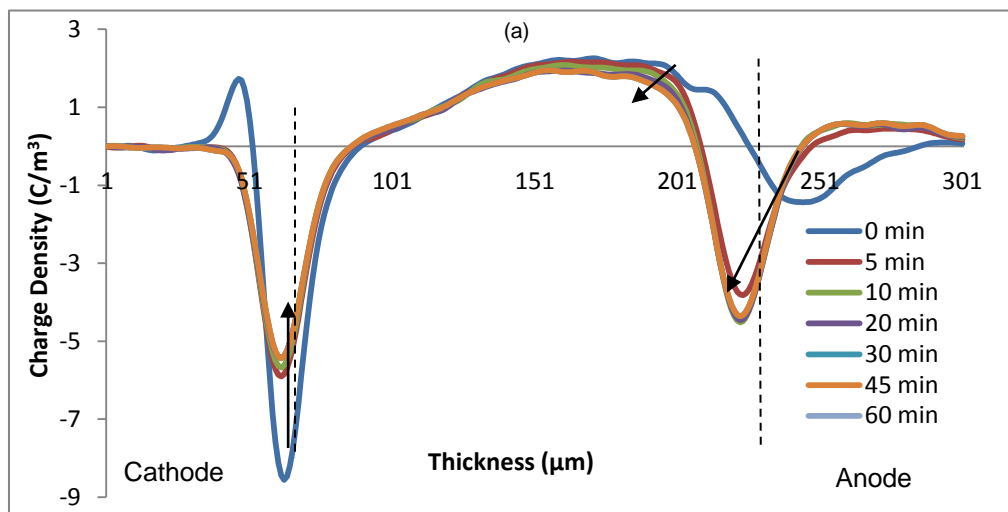
Charge decay in clean LDPE after stressed at 5kV,
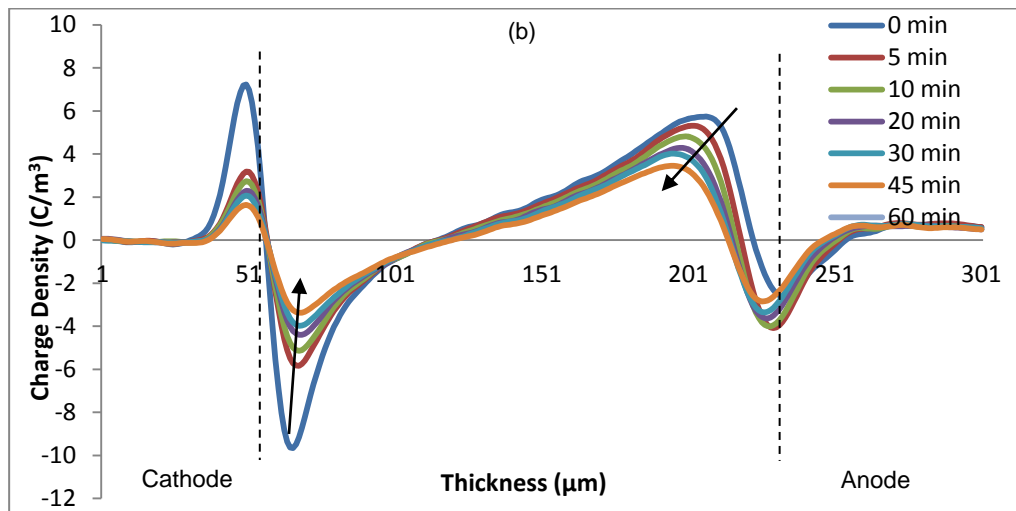
b) Charge decay in clean LDPE after stressed at 8kV
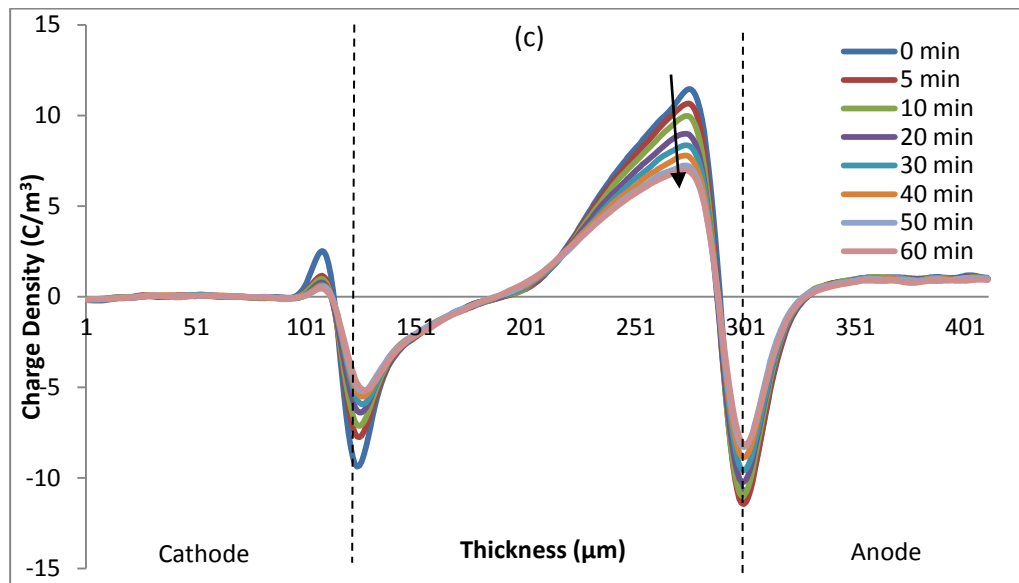
c) Charge decay in clean LDPE after stressed at 10kV

Figure 6-13: Charge Decay in 180um clean LDPE after; a) stressed at 5kV, b) stressed at 8kV, c) stressed at 10kV , for 1 hour

The clean LDPE shows a very slow charge decay rate as more charges are left in the bulk of sample even after 60 minutes. The negative charges near the top electrode shows an increment in density as more positive charges possibly leak into the anode, leaving the negative charges in the vicinity of electrode.

6.3.2 *Byproducts Soaked LDPE*

Figure 6-14 to Figure 6-16 show the changes in charge profiles in the soaked LDPE samples after the removal of the applied voltage started by acetophenone followed by α-methylstyrene and cumyl alcohol soaked LDPE.
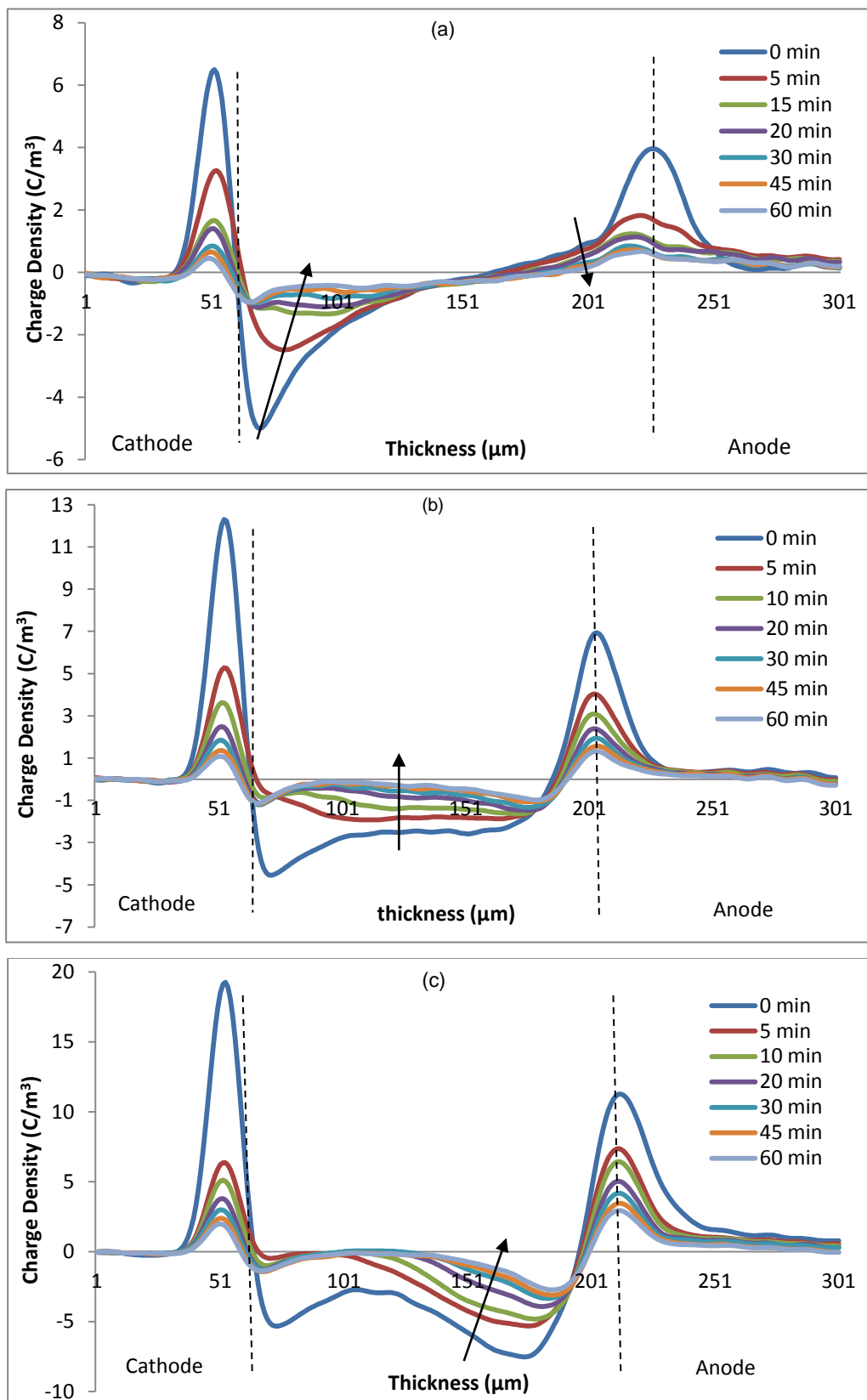
Figure 6-14: Charge Decay in 180μm acetophenone soaked LDPE after; a) stressed at 5kV, b) stressed at 8kV, c) stressed at 10kV , for 1 hour
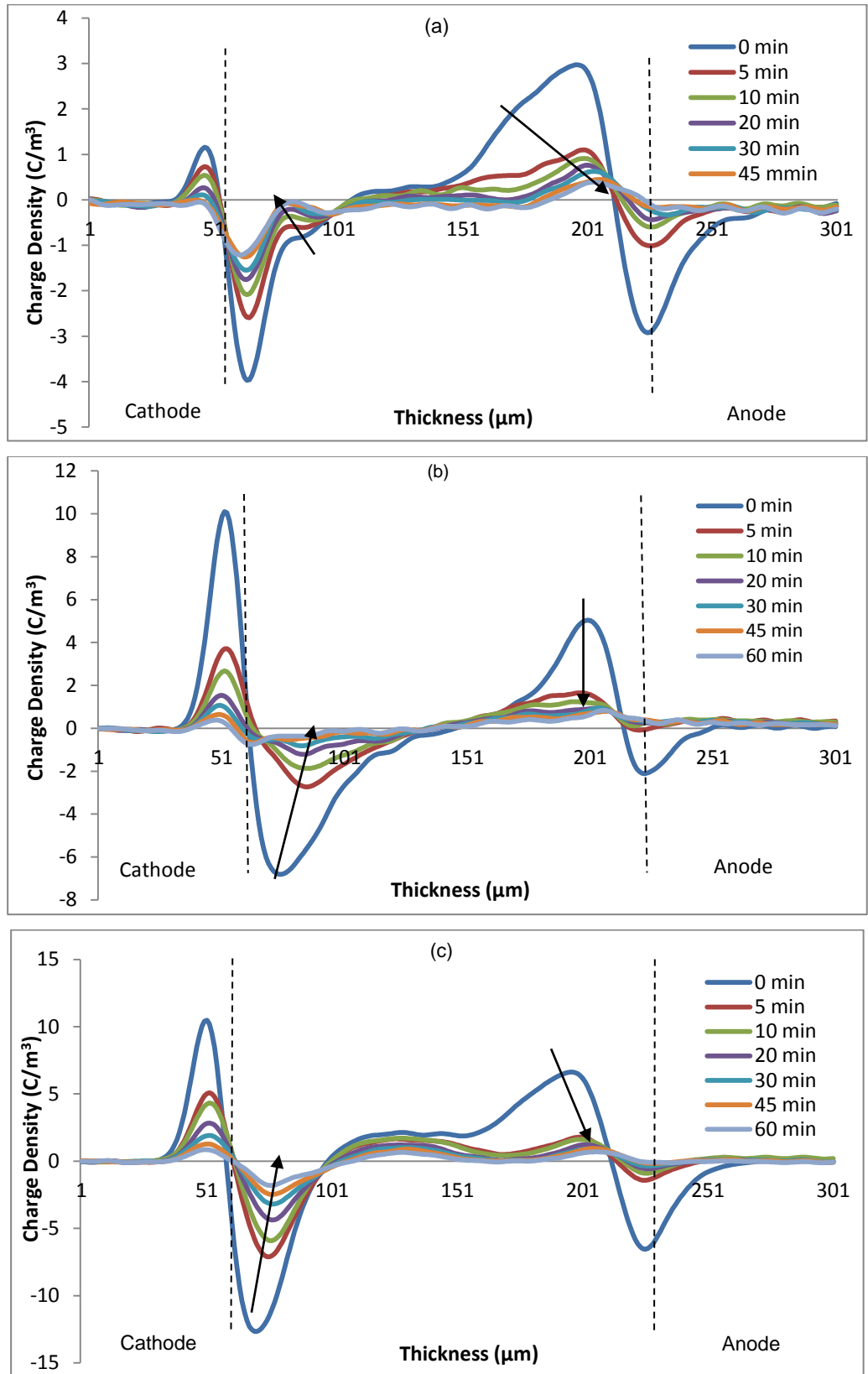
Figure 6-15: Charge Decay in 180µm α-methylstyrene soaked LDPE after; a) stressed at
5kV, b) stressed at 8kV, c) stressed at 10kV , for 1 hour
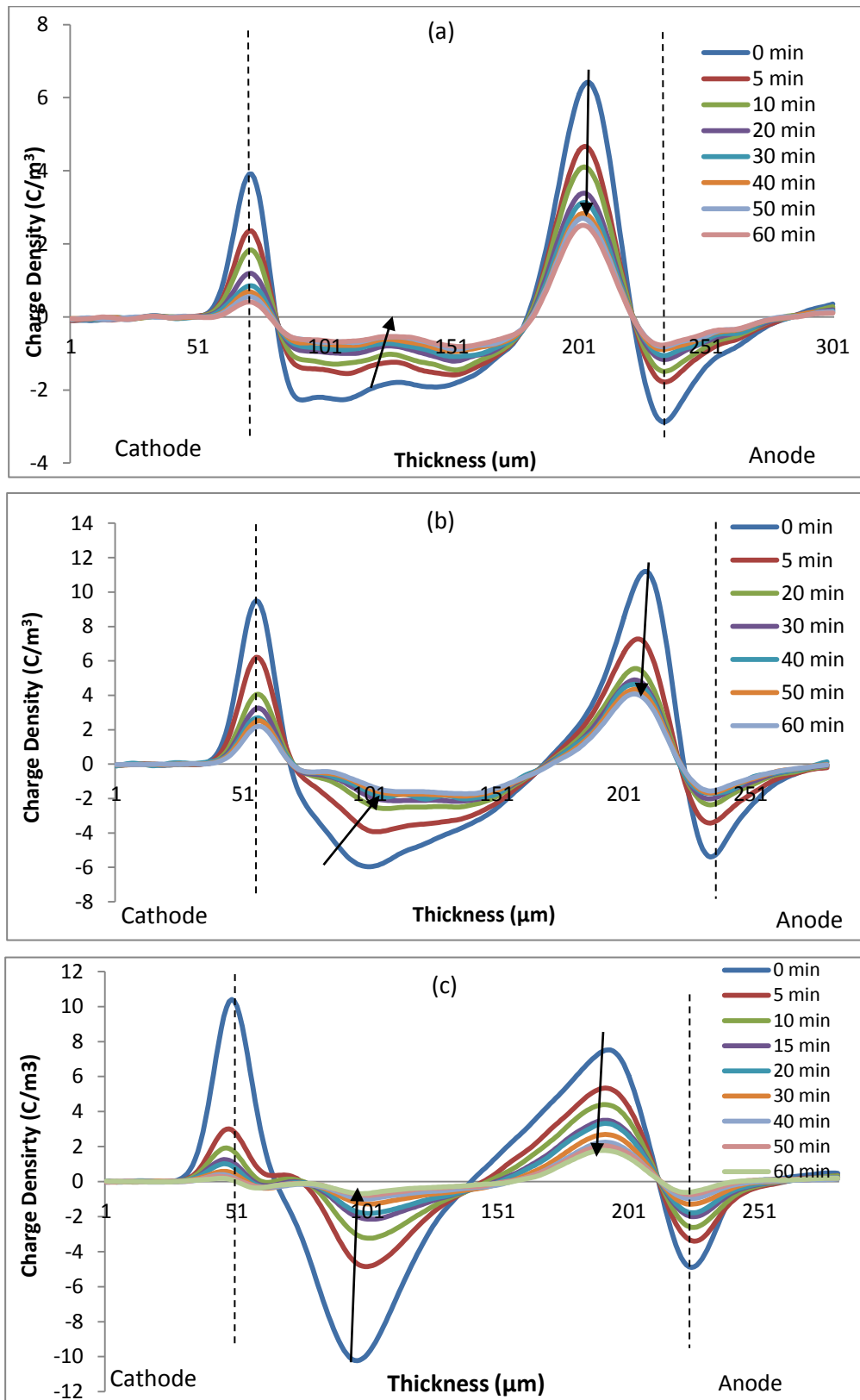
Figure 6-16: Charge Decay in 180µm cumyl alcohol soaked LDPE after; a) stressed at
5kV, b) stressed at 8kV, c) stressed at 10kV , for 1 hour

For acetophenone, α-methylstyrene and cumyl alcohol soaked samples, the decays are extremely fast especially in the first 10 minutes. As the decay results are referred, the byproducts assist the movement of the carriers in LDPE and reduce the number of charges trapped in the existing traps of the polymer. This argument is supported by the results from volt off measurement, where more charges could drift into the bulk instead of trapped at the adjacent of the electrodes.

By integrating the space charge density over the insulation thickness at a certain time t, ρ(x, t; E) the amount of charge in the sample, q(t; E) is obtained [87].

$$q(t; E) = \int_0^L |\rho(x, t; E)| \cdot S \cdot dx \qquad \text{Equation 6-1}$$

where 0 and L denote the position of the electrode excluding the charges at the electrodes, E is the electric field and S is the electrode area. The charge profile of the sample could be analysed as the total charge value during charging and decay is plotted over time. The results of this calculation are presented in Figure 6-17.

The effect of the chemicals on the total charge is the utmost at elevated voltage and no big difference is observed at lower voltage. This is shown in the left graphs in Figure 6-17. In samples charged at 5kV and 8kV, cumyl alcohol causes more charge accumulation as compared to that of the clean LDPE. Acetophenone and α-methylstyrene reduce the amount of total charge accumulated in the LDPE. At 10kV, acetophenone and cumyl alcohol introduce more charge accumulation to the clean LDPE.

After comparing all soaked samples and the clean LDPE, α-methylstyrene appears to cause the least effect on the charge accumulation in the insulator. In all three stressing voltages, the smallest amount of charges is found in α-methylstyrene soaked LDPE and the value is smaller than that of clean LDPE sample. This result is similar to the result reported in [88] where it was concluded that α-methylstyrene has no contribution to the space charge formation. On the other hand, cumyl alcohol and acetophenone show a clear contribution to the charge built up in the insulator, especially at high voltage.
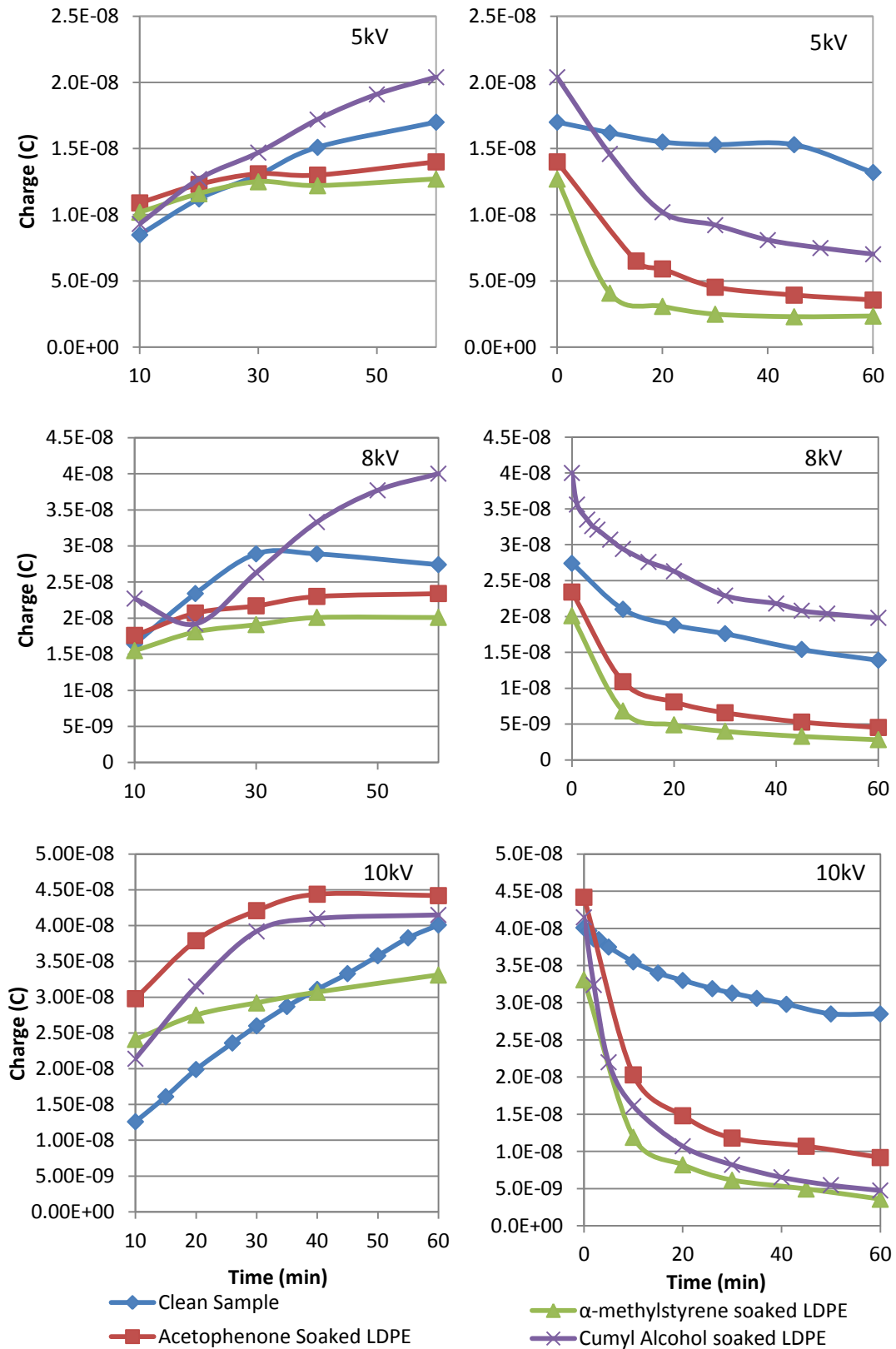
Figure 6-17: The total charge in the samples that stressed at 5kV, 8kV and 10kV during charging (LEFT) and decay (RIGHT) process.

6.3.3 *Rate of Charge Decay*

The rate of charge decay could give an indication of charge mobility and thus the trap depth. Despite the increase of charge injection and accumulation in the insulator, the byproducts speed up the decay process particularly in the first 15 minutes. From this point, the charge decay is comparable to the untreated LDPE. This decay could be seen in Figure 6-17. From the charge decay results, LDPE soaked in α-methylstyrene has the greatest rate of decay followed by acetophenone and cumyl alcohol. α-methylstyrene results in 80% of the original charges within a sample to decay. As the rate of decay is commonly associated with shallow and deep traps, where rapid decay is observed in the former [89], one can conclude that the chemical byproducts reduce the number of charges trapped in the deep traps. This is demonstrated by a slower rate of decay in a smaller number of charges, as seen in the decay curves. Based on the results one assumes that the charges will initially fill the shallow traps prior to the deep traps. This hypothesis has been verified recently [90]. It is reasonable to suggest that the byproduct chemicals modify the trapping characteristics of LDPE in two possible ways which are,

1) by increasing the population of the shallow traps, and
2) by reducing the number of deep traps in the LDPE, replacing them with the shallow traps.

In untreated LDPE, deep electron traps are often found in regions of reduced density, such as sub-microvoids with surrounded polymer chains [48]. These voids and naturally occurring spaces between the crystalline structures will fill with chemicals in the soaking process and result in a change in the charge trapping and de-trapping characteristics associated with the region. This is dependent on the type of bonding the chemical byproducts induce within the system such as benzene ring, carbonyl group, double bond, and hydroxyl groups [37].

It should be noted that the evaluation made here is contradict to the report in [91] which associates the crosslinking byproducts to deep traps. This report is based on the calculations of electron affinity and trap depth. This trap depth values however have been obtained without considering the polarisation that neighbouring molecules induced on the model molecule which is non negligible in general cases [92].

6.4   Two Chemicals In One Sample

The analysis made above is based on an assumption that the chemical function of the byproducts molecule act separately from each other. At this stage, it is difficult to achieve a similar mixture ratio to that in practice via soaking process. This is because of the difficulty to control the amount of byproducts in the soaked sample and at the same time have a uniform distribution across the film thickness. The main concern here is to examine potential interactions amongst different byproducts. As it is difficult to see these effects with a mixture of three byproducts, only two byproducts are mixed at one time. The results are compared to those obtained in the previous section.

Similar procedures as before, including the soaking, charging and decaying processes were applied to the samples. However in this part, the samples were stressed at one stressing voltage which is at 8kV. With 3 different chemicals, we have 3 different combinations of the chemicals, which have been simplified in Table 6-1 below. The volt off measurement results are presented in Figures 6-18 to 6-20.

Table 6-1: The mixture of byproduct chemicals

Sample	Chemical
a+α	acetophenone plus α-methylstyrene in LDPE
a+c	acetophenone plus cumyl alcohol in LDPE
α+c	α-methylstyrene plus cumyl alcohol in LDPE
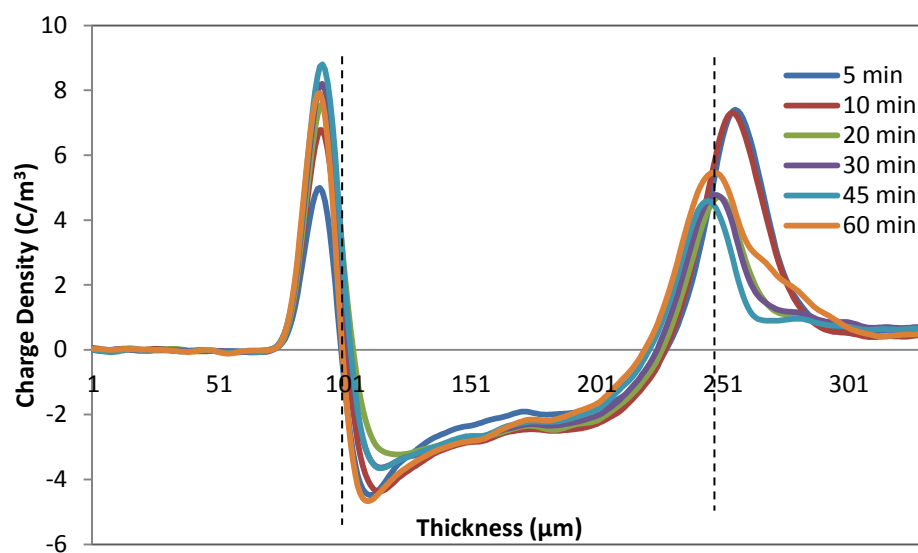
Figure 6-18: Volt off measurement for Sample a+α
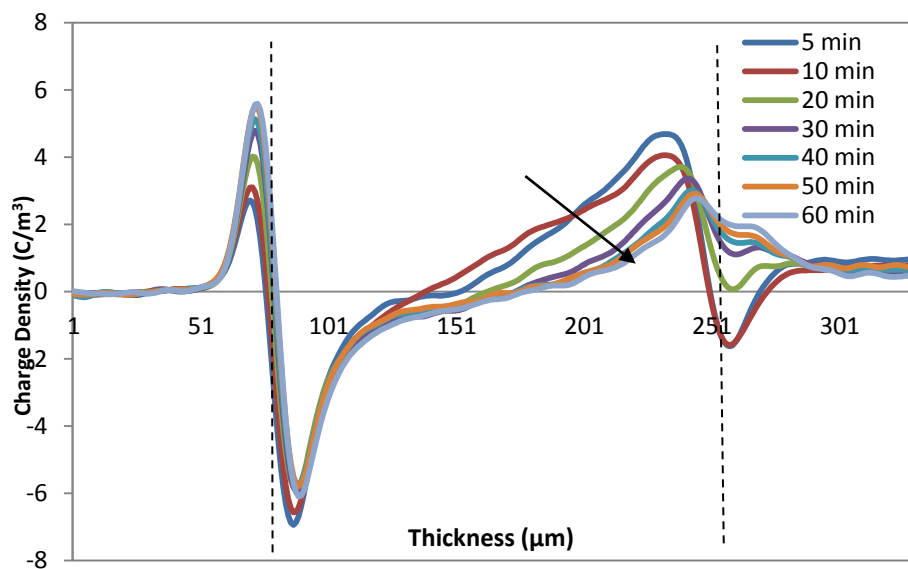
Figure 6-19: Volt off measurement for Sample a+c
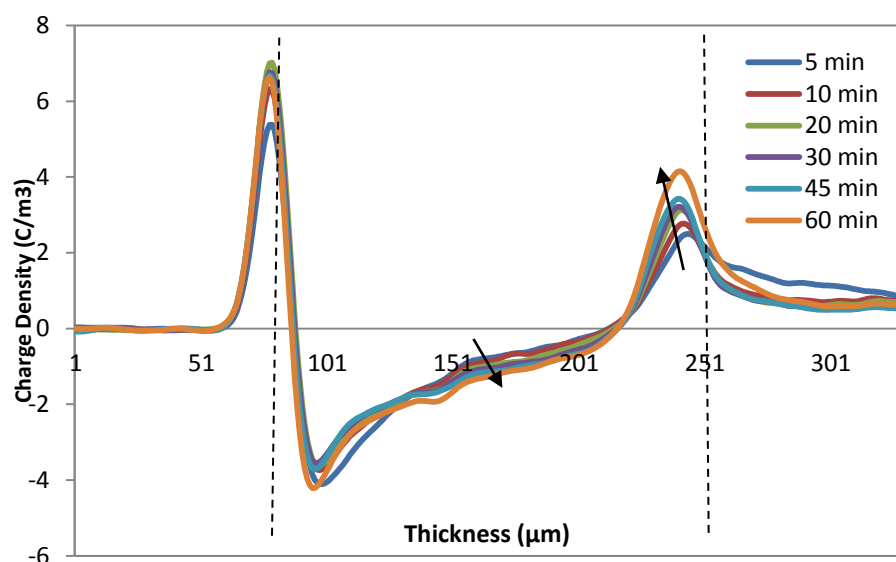
Figure 6-20: Volt off measurement for Sample α+c

For Sample a+α (Figure 6-18), the Volt off profile illustrates how negative charges dominate the sample bulk. This profile is similar to data obtained from acetophenone soaked LDPE, which suggests that acetophenone has a greater influence than α-methylstyrene in terms of controlling the charge build up. The former byproduct suppresses positive charge injection from the anode. Similar characteristic is observed in Figure 6-7(b).

In Figure 6-19, the domination of acetophenone over the other byproduct is also shown in Sample a+c. Although negative peak is only observed near to the cathode, the amount of positive charges that reduce with charging time and the positive peak moves towards the anode showed that the charges are suppressed. This observation is believed to be related to the existence of acetophenone in the sample.

No heterocharges appeared in Sample a+c and Sample α+c (Figure 6-20), although cumyl alcohol presents in the samples. In Sample α+c, positive charges are trapped in the vicinity of the anode and at the same time, the negative charges migrate from the cathode to the sample bulk. As a result, more negative charge is seen in the sample. It is believed that some positive charges are trapped in the vicinity of the anode, this is consistent with the space charge profile in α-methylstyrene and cumyl alcohol soaked LDPE. However, due to low resolution, these charges appear in only one positive peak. As the charge dynamics do

96

not show any distinctive pattern associated with any of the individual byproducts, a conclusion cannot be drawn as to which byproduct is the most dominant.

After one hour charging, the samples were left to decay. Again, the amount of charges in samples is calculated and the results are shown in Figure 6-21. The results for sample soaked into single chemical that stressed at 8kV are also included for comparison purpose.
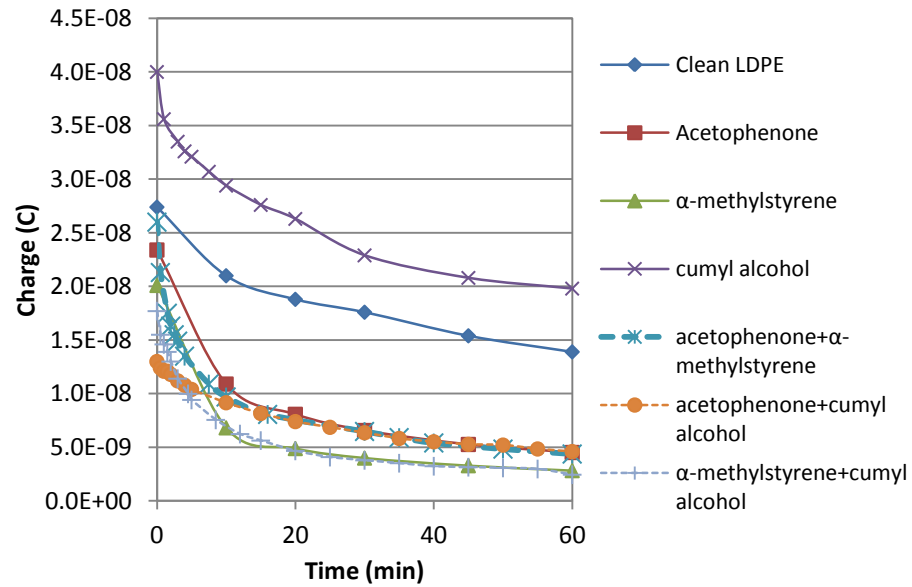
Figure 6-21: Total charge accumulated in sample during decay in samples.

After being stressed for an hour, the total charge accumulated in Sample a+α is the highest followed by Sample α+c and Sample a+c. Once again, we could observe the similar slow decay after about 20 minutes open circuit, which is due to the deep traps in the polymer. Despite having the least total charge, the rate of charge decay in Sample a+c is low relative to the other two samples. It is believed that the presence of α-methylstyrene in samples a-α and α+c cause a faster rate of decay. The result indicates that in terms of charge accumulation, it is rather difficult to see which byproduct causes the most charge injection into the insulator. However, α-methylstyrene maintains its characteristic as the charge decay accelerator while in the existence of other byproducts in the insulator.

6.5   AC Space Charge Profile

Similar to DC measurement semicon and aluminium were used as the top and bottom electrodes respectively. Samples were stressed at 4kV peak voltage which equivalent to $28kV_{rms}$/mm, for 4 hours at the frequency of 50Hz. Space charge profile of the sample was collected in every hour. This measurement is followed by 20 minutes of charge decay. 800V electric pulse at 2 kHz was applied to produce the acoustic signal. Due to very small data signal that will be obtained in this test especially for short circuit measurement, data need to be denoised before further analysis could be done.

Volt on results show no significant difference in the charge profile of the clean LDPE and the soaked samples. These results are included in the Appendix. Hence, the Volt off measurement results are referred to study their differences. Figure 6-22 shows the charge profile of all samples during volt off condition.
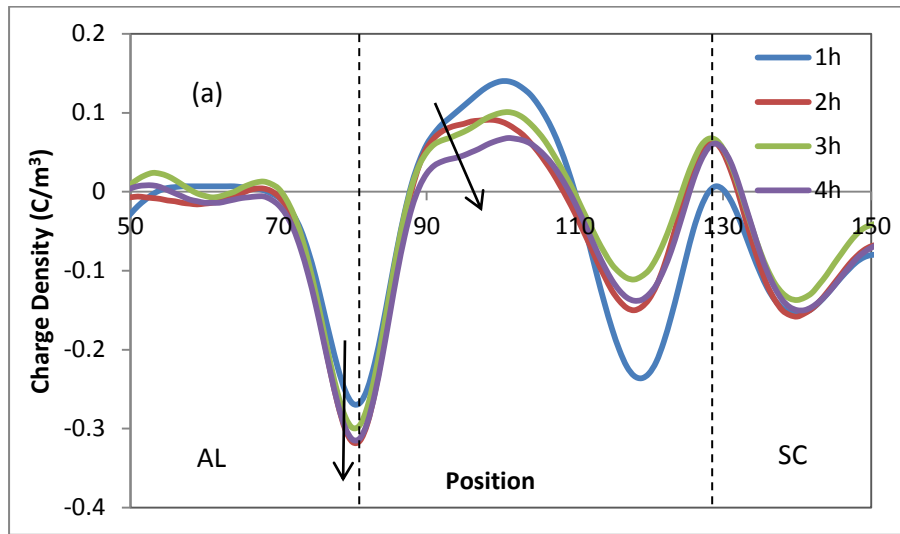
a) Clean LDPE,
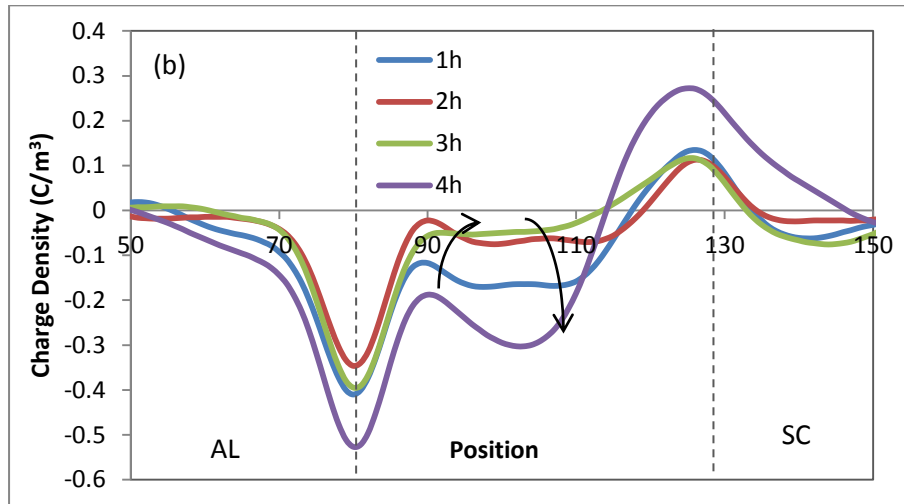
b) Acetophenone soaked LDPE,
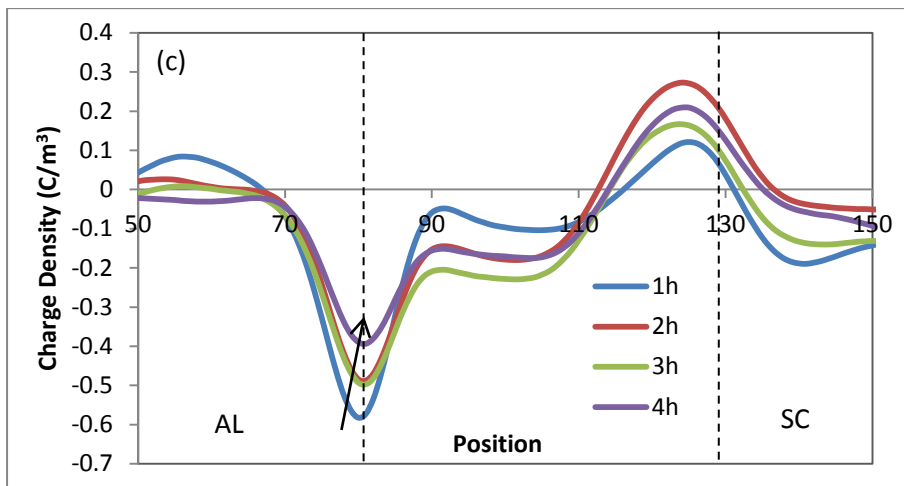
c) α-methylstyrene soaked LDPE
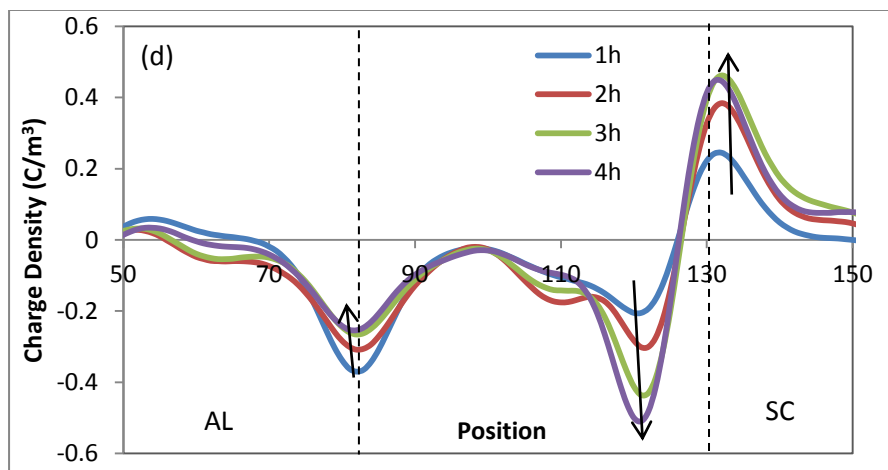
d) Cumyl alcohol soaked LDPE

Figure 6-22: Charge Density of a) Clean LDPE, b) acetophenone soaked LDPE, c) α-methylstyrene soaked LDPE and d) cumyl alcohol soaked LDPE during Volt off condition after 28 kV/mm ac.

In the clean LDPE sample, positive and negative charges are observed in the bulk. The positive peak is near to the aluminium electrode and negative peak is near to the semicon electrode. However the positive peak is wider than the negative peak. Both of these peaks amplitude reduce with stressing time. This reduction may due to more charges recombined during the second half cycle compared to the charge injected into the film. Meanwhile in acetophenone soaked LDPE, more negative charges reside in the bulk of the sample. The negative charge decreases with time within the first 3 hours of stressing. The charges suddenly get bigger after 4 hours. Positive and negative peak is also observed in the vicinity of semicon and aluminium electrodes respectively.

In α-methylstyrene soaked LDPE negative charge is also detected in the vicinity of aluminium electrode and penetrates into the sample bulk. Positive peak is observed near the semicon electrode. In the presence of α-methylstyrene, the negative charge in the bulk as well as the positive peak near the top electrode increase by time. On the other hand, negative charges near aluminium electrode become lesser by time. Cumyl alcohol soaked sample is the only sample that shows a total domination of negative charge in the sample. The negative peak near the semicon electrode gets higher as the charging time gets longer.

It is difficult to have a direct comparison between the samples that were stressed at ac and dc in term of charge density profile. Although both tests used similar electrode system, the difference on the material for top and bottom electrode making the analysis on the charge injection in samples during ac stress becomes very complicated. Hence, total charge in every sample was calculated by integrating the charge density over the sample thickness. Figure 6-23 shows the total charge decay in samples stressed at ac.
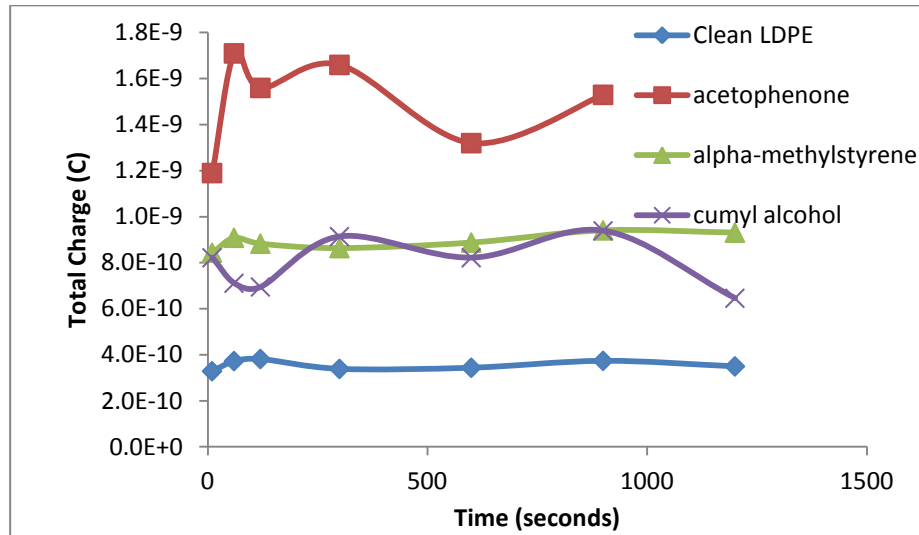
Figure 6-23: Total charge decay in clean LDPE, acetophenone, α-methylstyrene and cumyl alcohol soaked LDPE after been stressed at E_{RMS}=28 kV/mm for 4 hours.

The charge decay profiles for ac stressed samples were recorded up to 20 minutes (1200 s). The fluctuation that observed in acetophenone soaked LDPE and cumyl alcohol soaked LDPE is most likely due to noises that appear in the data. The total charge accumulated during ac stress is much lower compared to the total charge under dc condition. This is due to the recombination of the majority of electrons and holes alternately injected each half cycle [93]. Despite this small amount of charge, the accumulation of space charge under ac condition should not be neglected particularly at lower frequency where the formation of space charge is more severe [94].

Charge decay profile of ac stressed samples is not as direct as that of dc stressed samples. Overall, the results suggested that after a few hours stressed, the charges movement in the samples become very static. The rate of charge decay is very small. This observation proves that the charges left in the sample during decay process are the charges that were trapped in the deep traps.

During DC Stress

From dc space charge measurement, it was observed that the byproducts have contributed to very fast initial charge decay followed by slower decay. It is suggested that the byproducts either (a) increase the number of shallow traps in the samples, or (b) reduce the density of deep traps in the sample. With continuous current in one direction, the charges

will initially fill into the shallow traps and conduct through the dielectric to the opposite polarity electrode. Accordingly, the conduction current is higher for the byproduct soaked samples compared to the clean LDPE.

During AC Stress

In ac, charges will move back and forward due to the polarity change of the electrodes. It is in agreement with the results obtained in dc test that the byproducts introduce more shallow traps in the sample causing higher traps density in the sample.

During the first half cycle, the charges will be injected into the sample. Since higher shallow trap density found in byproducts soaked LDPE, there is higher probability of the charges to be trapped either in shallow or deep traps. However due to the polarity reverse, charges trapped in shallow traps can be easily extracted into the electrode. The remaining charges will shift further into the bulk, moving back and forward due to the polarity reverse and eventually trapped into the deep traps.

With more shallow traps, the crosslinking byproducts ease the movement of the charges further into the bulk and have higher probability to be trapped into the deep traps. As a result, samples with crosslinking byproduct posses more charges compared to the clean sample. The dependency of charges trapping dynamics on the total number of shallow and deep traps is mentioned by Chen et. al in [90] analysing the trapping and detrapping characteristics of polymer by using PEA technique. The analysis however does not consider the trapping process from shallow to deep traps. It is clear now, that this process should be taken into account when analysing the trapping and detrapping process especially during ac stress.

6.6 Chapter Summary

It was observed from comparison between the fresh XLPE and degassed XLPE that both samples have heterocharges accumulation near the electrodes. With more byproducts in the sample, fresh XLPE sample has more injected charge in the sample.

The homocharges are found in acetophenone and α-methylstyrene soaked LDPE. However, acetophenone causes negative charge to accumulate in the sample bulk, meanwhile α-methylstyrene allows the positive charge to dominate the sample bulk. Cumyl alcohol is the only byproduct that introduces heterocharges in the LDPE sample. These heterocharges become less after more charges injected into the sample and over cover the heterocharges. In term of total charge, α-methylstyrene soaked LDPE has shown the least charges accumulated in the sample.

With the existence of 2 byproducts in one sample, acetophenone is dominant in determining the profile of the charge accumulation. Any sample with α-methylstyrene has the fastest charge decay. Charge decay profiles from dc space charge measurement reveal that the crosslinking byproducts introduce shallow trap into the LDPE structure. During dc stress, these shallow traps assist the movement of charges across the polymer thickness causing fewer charges trapped in deep traps.

During ac stress, the shallow traps in crosslinking byproduct cause more charges to be trapped in the polymer. With more charges trapped and move further into the bulk, hence there is higher probability for the charges to be trapped in the deep traps due to the polarity reverse that happen through out the stressing period.

Chapter 7 Dielectric Spectroscopy Measurement

7.1 Introduction

The electrical properties are determined by the degree of polarity of a material. A dielectric like polyethylene which only consists of carbon and hydrogen or methylene chains is non-polar in nature. Such material has low conductivity value. If any polar component exists in the chain, the polymer will then become more polar and its characteristics are no longer as explained before. When a polymer is subjected to an electrical field, the polymer will become polarised where the polar parts of the chain will respond to the electric field applied. As a result, the polymer will be pulled into two directions due to two charge polarities in the chain. Although ideally polyethylene is a non-polar material, in real world compositions there are always small amount of polar components such as impurities, which present in the polymer structure. Under electric field application, these impurities will also experience polarisation [95].

In the case of ac, we will see that the polar chain will be shifting back and forth according to the polarity change. The rate of changes of the alignment of this chain is controlled by the frequency. As the frequency increases, it occurs at one point that the chain cannot 'keep up' with the changing frequency. With various functional groups in the polymer, different groups will be sensitive to different frequencies. As the frequency increases, no changes will be seen in real permittivity value (ε') provided that the dipole can respond. When the dipole could no longer rotate as fast as the changing field, charges cannot be held and the dielectric constant value changes with frequency. This phenomenon not only

occurs in a polar structure, but also occurs in other electrical polarisation such as electronic, atomic and orientational polarisation. Figure 7-1 and Figure 7-2 illustrate the frequency response of different dielectric mechanisms across the measured frequency.

HIGHER   FREQUENCY

Orientational Polarisation	Atomic Polarisation	Electronic Polarisation
• Any molecule with dipole moment will be alligned by the applied electric field so that the net polarisation will be pointing to the direction of electric field. • Can be brokendown to dipole, ionic and dielectric relaxation.	• This polarisation is due to the rearrangement of atomic nuclei in molecule or lattice. • Happens at lower frequency due to its bigger mass than elecron.	• Electric field causes small displacement to any electron relative to the inner positive nucleus. • Happens at high frequency and responsible for refrecting light.

Figure 7-1: Three main polarisations from lower to higher frequency [96].
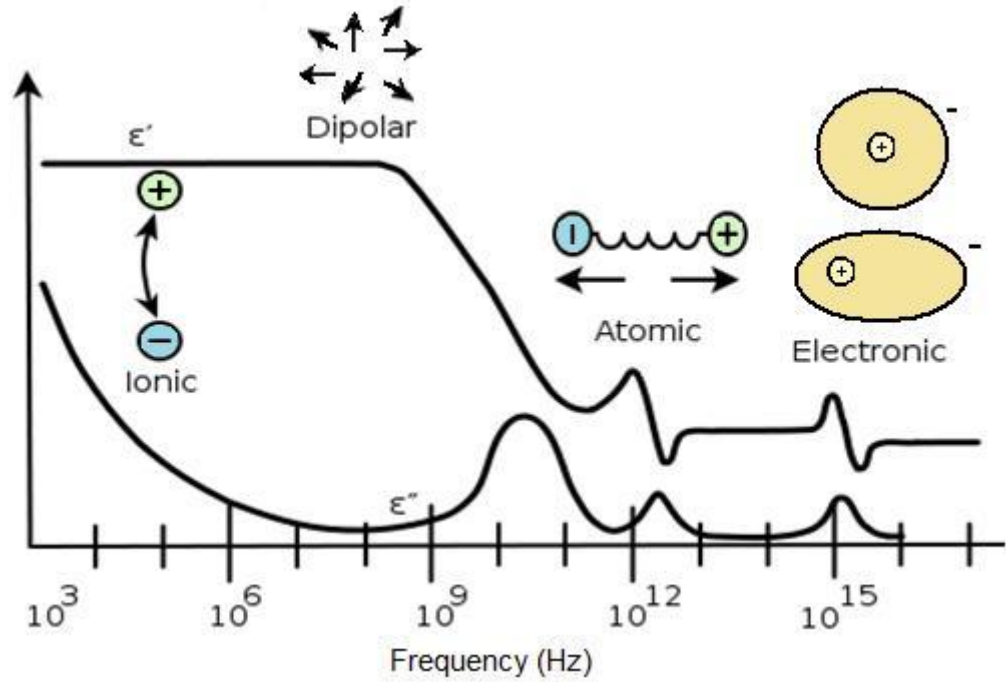
Figure 7-2: Frequency response of different dielectric mechanisms.

Permittivity (ε') represents the ability of the material to polarise by an electric field. Dissipation factor or dielectric loss (tan δ) is a measure of the amount of energy loss as heat rather than transferred as electrical energy. For a good insulator, the value of ε' and tan δ should be low. To understand the concept of permittivity, it is easier to first discuss a closely related property, capacitance (C). Consider a dielectric sandwiched between two parallel metal plates. The capacitance and conductance (G) for the dielectric are [97] :

$$C = \frac{\varepsilon' \varepsilon_0 A}{d}$$
Equation 7-1

$$G = \frac{\sigma A}{d} = \frac{1}{R}$$
Equation 7-2

where A in m^2 is the area of electrodes, d in m is the electrode separation, σ in $\Omega^{-1}m^{-1}$ and R in Ω is the resistance. However, in ac voltage waveform, the 'formulae' is not as simple as that in dc voltage. It is more convenient to use a vector diagram to describe these two properties with real and imaginary part as in Figure 7-3.

107
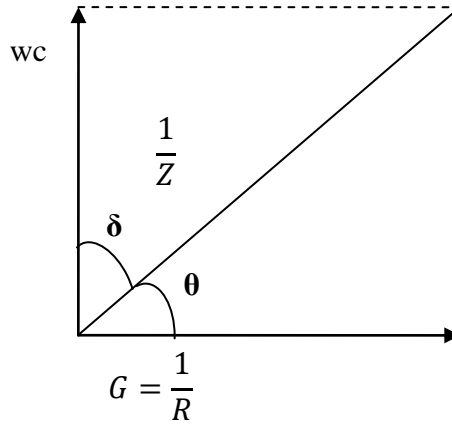
Figure 7-3: Vector diagram of the electrical response of a dielectric [97].

The phase angle θ represent the angle by which the current waveform leads the voltage waveform. The impedance Z of a dielectric is given by:

$$\frac{1}{Z} = \frac{1}{R} + j\omega C$$

Equation 7-3

The complex dielectric function ε*(ω) is determined from:

$$\varepsilon^*(\omega) = \varepsilon' - j\varepsilon''$$

Equation 7-4

where ω=2πf is the angular frequency. One could also express the complex capacitance C* of a dielectric as:

$$C^* = \varepsilon^* C_0$$

Equation 7-5

Where C_0 is the capacitance of the cell with air given by $C_0 = \varepsilon_0 A/d$ for a parallel plate capacitor and the impedance Z is given by:

$$Z = \frac{1}{j\omega C*} = \frac{1}{j\omega C_0(\varepsilon' - j\varepsilon'')} = \frac{R}{1 + j\omega CR}$$

Equation 7-6

From equation 7-6, equating the real and imaginary parts, we obtain the real permittivity as expected,

108

$$\varepsilon' = \frac{C}{C_0}$$

Equation 7-7

And

$$\varepsilon'' = \frac{1}{\omega C_0 R} = \frac{\sigma}{\omega \varepsilon_0}$$

Equation 7-8

And thus

$$\tan \delta = \frac{\varepsilon''}{\varepsilon\prime} = \frac{1}{\omega RC} = \frac{\sigma}{\omega \varepsilon\prime \varepsilon_0}$$

Equation 7-9

Cole-Cole plots has been introduced by Kenneth and Robert in 1941 [98]. Cole-Cole plot is produced by plotting the imaginary permittivity against real permittivity in log-log plot which produce a curve that normally in a semicircular shape (Figure 7-4) for a fully Debye relaxation process. This plots is used to determine the zero-frequency dielectric constant ε'_0 and the limiting high frequency value ε'_∞ [99]. Equation that defines the Cole-Cole plots is given by;

$$\varepsilon = \varepsilon_\infty + \frac{\varepsilon_s + \varepsilon_\infty}{1 + (i\omega\tau)^\alpha}$$

Equation 7-10

Here ε_s is the static permittivity (at 0Hz), ε_∞ is the permittivity at maximum frequency, τ is the relaxation time and α is the Cole exponent, which have a specific value for different material. Good background on Cole-Cole plots is described in [100].
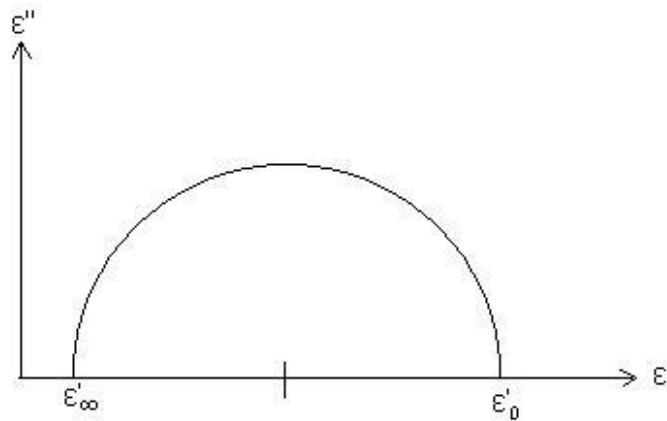
Figure 7-4: Semicircular Cole-Cole plot.

7.2 Measurement procedures

Dielectric measurement was performed on the liquid byproduct and the byproducts soaked LDPE. Hence different cells are required for the solid sample and liquid sample. Figure 7-5 shows the cells used for solid and liquid samples in this measurement. In both measurements, a Solartron 1296 Dielectric Interface and Schlumberger SI 1260 Impedance/phase gain analyser were used. Dielectric spectroscopy of the samples was measured at room temperature. During measurement, the dielectric cell is placed in a metal box to avoid any unwanted noise to interfere with the measurement. To have a good contact between the sample and electrode, the film samples are initially coated with gold prior to the soaking process. By applying 25mA current for 4 minutes, the samples are coated by 32nm thick of gold on each side. The parameters used in this test are shown in table 7-1.

Table 7-1 : Parameter of dielectric spectroscopy experiment for solid (S) and liquid (L) samples.

Parameter	Value/Range
Frequency	10mHz -10MHz
AC Bias	1V
DC Bias	0V
Integration	10 cycle
Sample Area	Circular. 25mm diameter (S) Circular, 30mm diameter (L)
Sample Thickness	0.18mm (S)
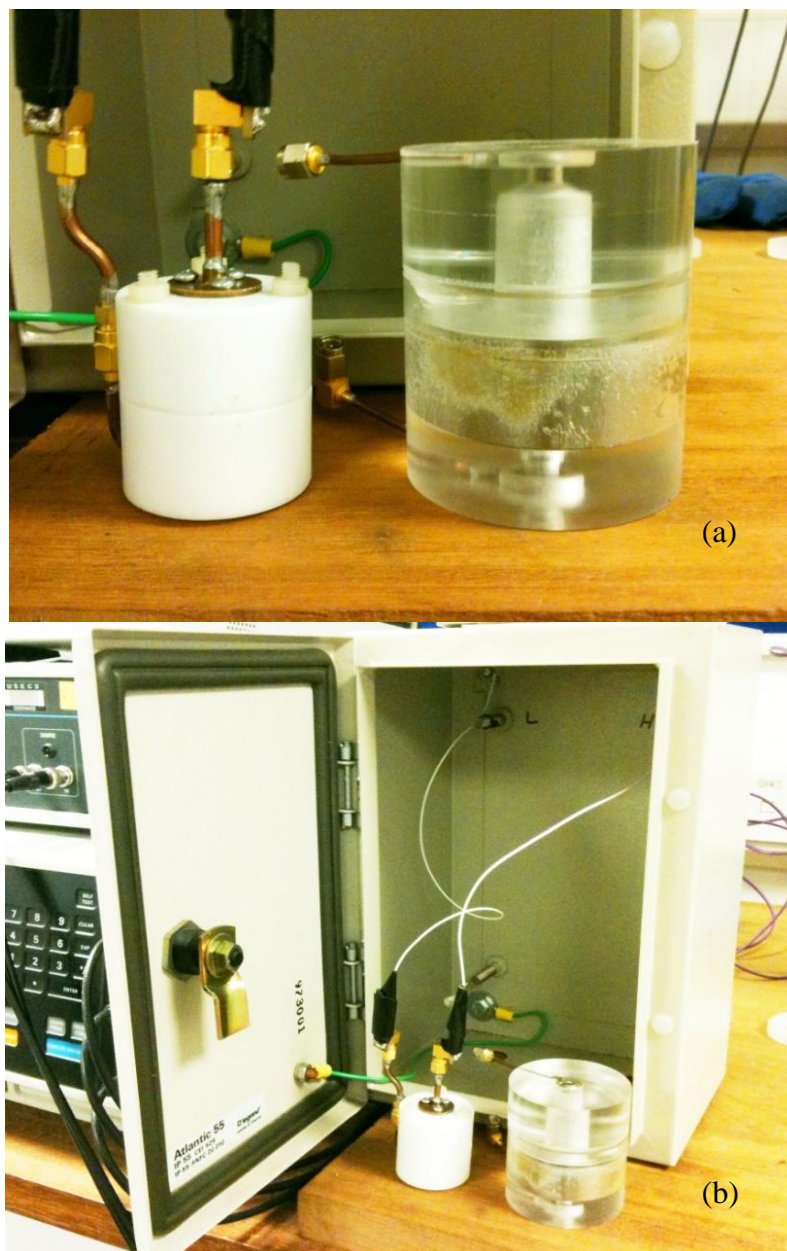
Figure 7-5: (a) The solid and liquid cells used in experiment and (b) metal box to avoid signal from noise.

7.3   Dielectric Measurement Results For Liquid Samples

The real and permittivity values for the liquid byproducts are calculated from equation 7-7 and the results as well as the imaginary permittivity values are shown in log-log plot in

Figure 7-6. At low frequency, the permittivity value of acetophenone is the highest ($\approx 10^6$) followed by cumyl alcohol ($\approx 10^2$) and last but not least α-methylstyrene (≈ 1). As the frequency increases, the real permittivity value is reduced rapidly. From the literature [101], the static permittivity values of acetophenone, α-methylstyrene and cumyl alcohol are 17.44, 2.28 and 5.61 respectively. It is clear from Figure 7-6 that the measured values are too high that are not acceptable at some frequencies. This enormous values are contributed by the combination effect of DC conductivity and the anomalous conductance due to the polarisation process [96]. As a result, the equipment that measured the impedance value which was largely contributed by the resistance had misinterpreted it as the capacitive value hence giving high dielectric constant. The dielectric constant values that are acceptable for acetophenone, cumyl alcohol and α-methylstyrene liquids from Figure 7-6 are from 50 Hz, 0.3 Hz and 0.01Hz onwards respectively. In these range of frequencies, the dielectric constant values are more acceptable and closer to theoretical values.

Figure 7-7 shows the tan δ values for the byproducts liquids. For the tan δ curve, after comparing the values to that of the empty cell, the relaxation peak for α-methylstyrene, cumyl alcohol and acetophenone are observed at frequency range of 10^{-2} to10^{-1} Hz, 10^{-1} to 1 Hz and $10^2$to 10^3 Hz respectively.
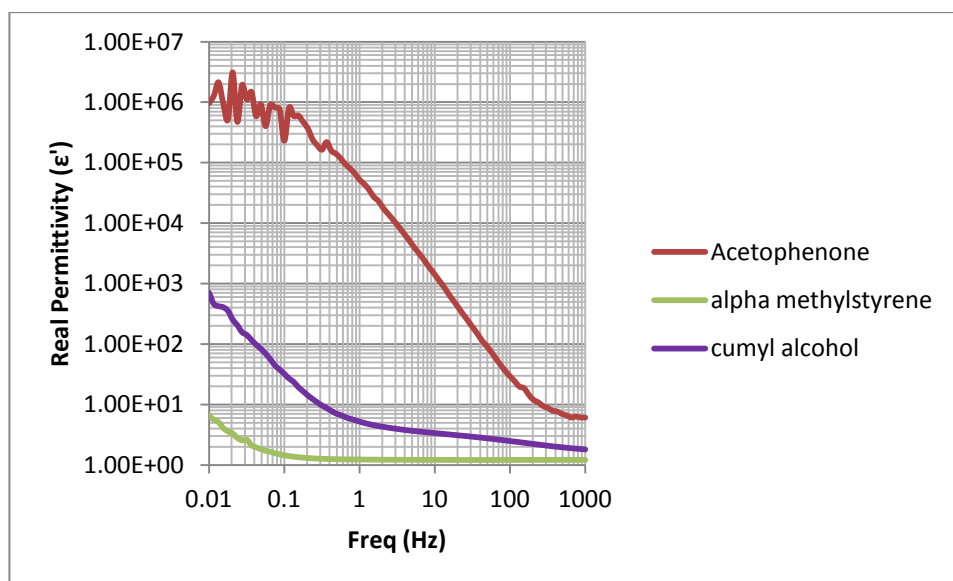
Figure 7-6: The real part of ε' of acetophenone, α-methylstyrene and cumyl alcohol.
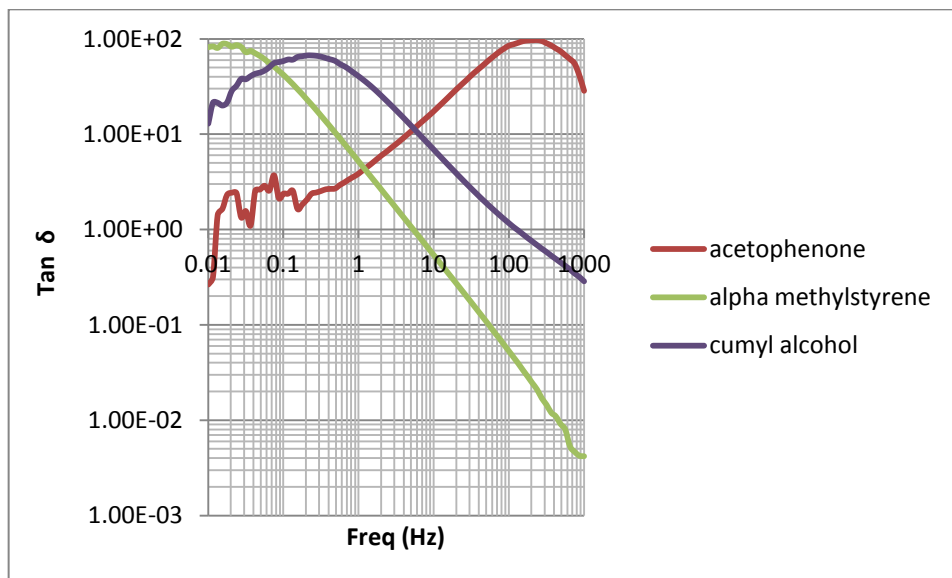
Figure 7-7: Frequency plot of tan δ of the byproducts liquids.

7.4 Dielectric Measurement Results For Solid Samples

The relative permittivity value obtained for the clean LDPE is ≈2.31. Similar measurement was conducted on uncoated LDPE sample. As a result, permittivity value that obtained is ≈2.1 which is quite low compare to the theoretical value which typically lies in the range of $2.25 < \varepsilon_r < 2.3$. Therefore, it is quite essential to gold coat the sample film in order to obtain a more accurate film.

The additional byproducts in the material cause small increment on the permittivity value. Among the three byproducts, acetophenone gives the highest permittivity value, followed by α-methylstyrene and cumyl alcohol. Despite this small effect, the tan δ curves show some changes when the byproducts exist in the LDPE film. The value of ε' and tan δ values are presented in Figure 7-8 and Figure 7-9 respectively.
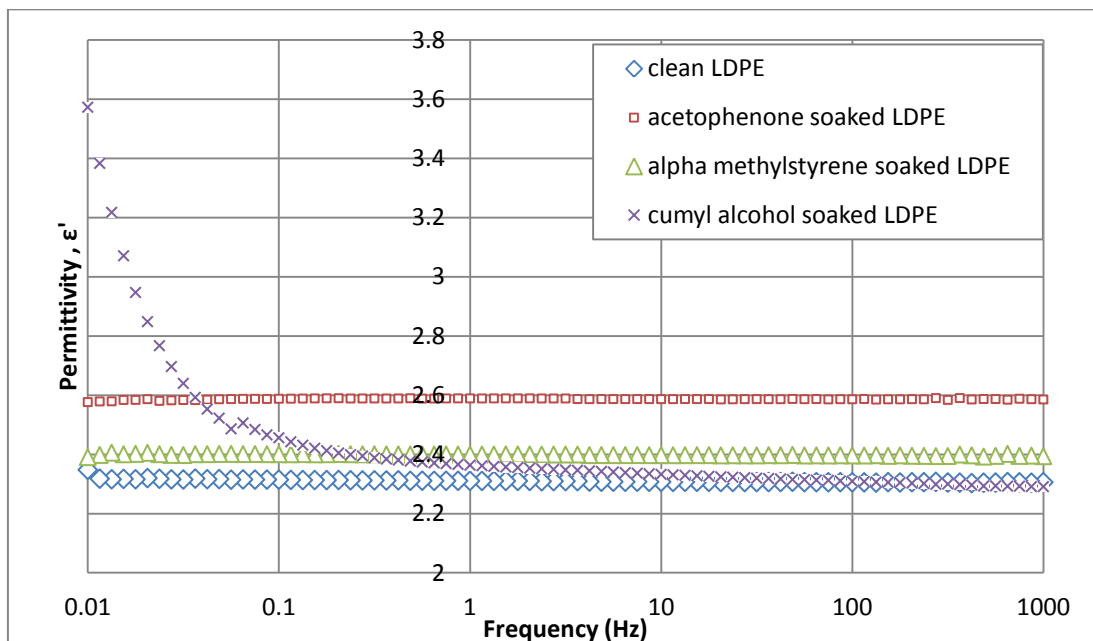
Figure 7-8: Permittivity values of the clean LDPE and the soaked LDPE.
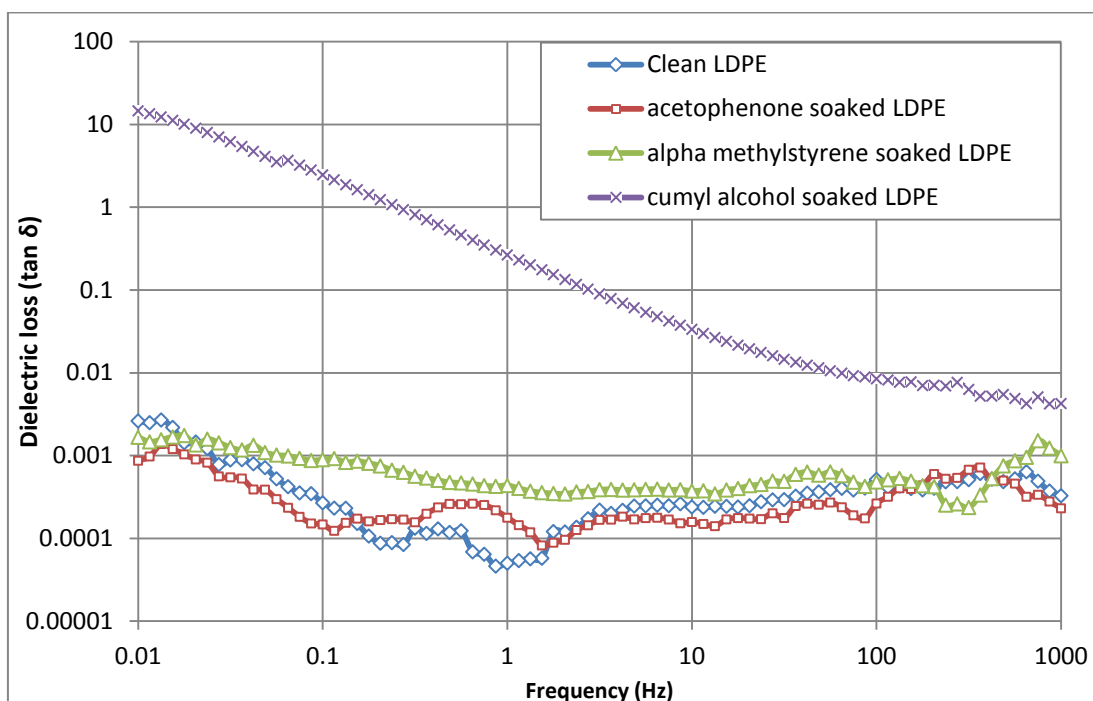
Figure 7-9: The dielectric loss values of the clean LDPE and the soaked LDPE.

It is observed that acetophenone have very similar tan δ values of that of the clean LDPE. α-methylstyrene increases the tan δ value in the range of 0.1Hz-10Hz. The increment is however very little. On the other hand, cumyl alcohol increases the ε' and tan δ values especially at lower frequency. This is obviously not the actual values corresponding to the

114

bulk dielectric permittivity characteristic of cumyl alcohol soaked LDPE but rather are due to the charge build up at interfaces between the bulk of the sample forming spurious boundary layers (interfacial or Maxwell-Wagner-Sillars (MWS) polarisation [96]) and between the sample-electrode interface (Space charge polarisation [102]). At lower frequency, there is more time for the charges to move in and build up at the sample-electrode interface within the half-cycle of the applied AC, giving rise to the measured capacitance and hence the effective dielectric permittivity values. On contrary, this will not happen at high frequency as very short time is available for the charge movement in one half-cycle, the charges could not keep up with the change of electric field and thus only bulk polarisation mechanism contribute to the electric polarisation. The Cole-Cole plots of the clean sample as well as the byproducts soaked sample is presented in Figure 7-10. The Cole-Cole plots do not form a semicircular shape indicating the samples do not undergo Debye relaxation process. However it is shown here that cumyl alcohol has a large increase in conduction compared to the other samples.
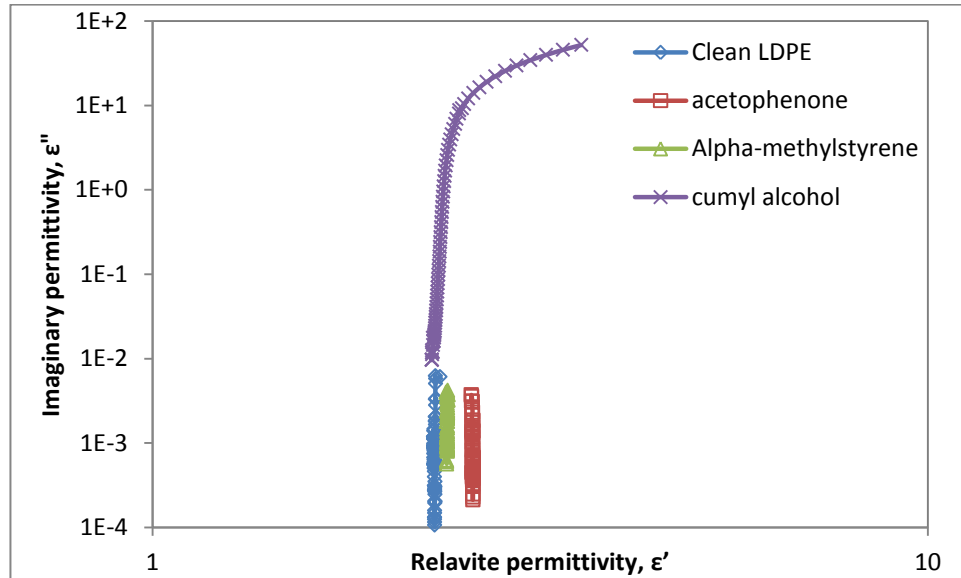
Figure 7-10: Cole-Cole Plots of the clean LDPE and the byproducts soaked LDPE.

With the results obtained in permittivity and dielectric loss spectrum, cumyl alcohol is proved to introduce either more mobile carriers into the insulator, or increase the charge mobility in the insulator [103]. The frequency-dependent real part of alternating current conductivity σ_{ac} of the dielectric is obtained from the relation [104]:

$$\sigma = \omega\varepsilon_0\varepsilon''$$
Equation 7-11

From this equation, the conductivity values are calculated and presented in Figure 7-11 below. Acetophenone and α-methylstyrene give almost no effect on the conductivity values. As expected cumyl alcohol increases the conductivity of LDPE film. This result however, shows the conductivity value when AC current is applied to the sample which may not be directly equal to the result obtained from DC conduction current measurement. Polarisation that might occur under the influence of AC current may delude the actual conductivity value of the samples. A DC characteristic may be obtained from dielectric spectroscopy at a very low frequency where the polarisation effect is minimal.
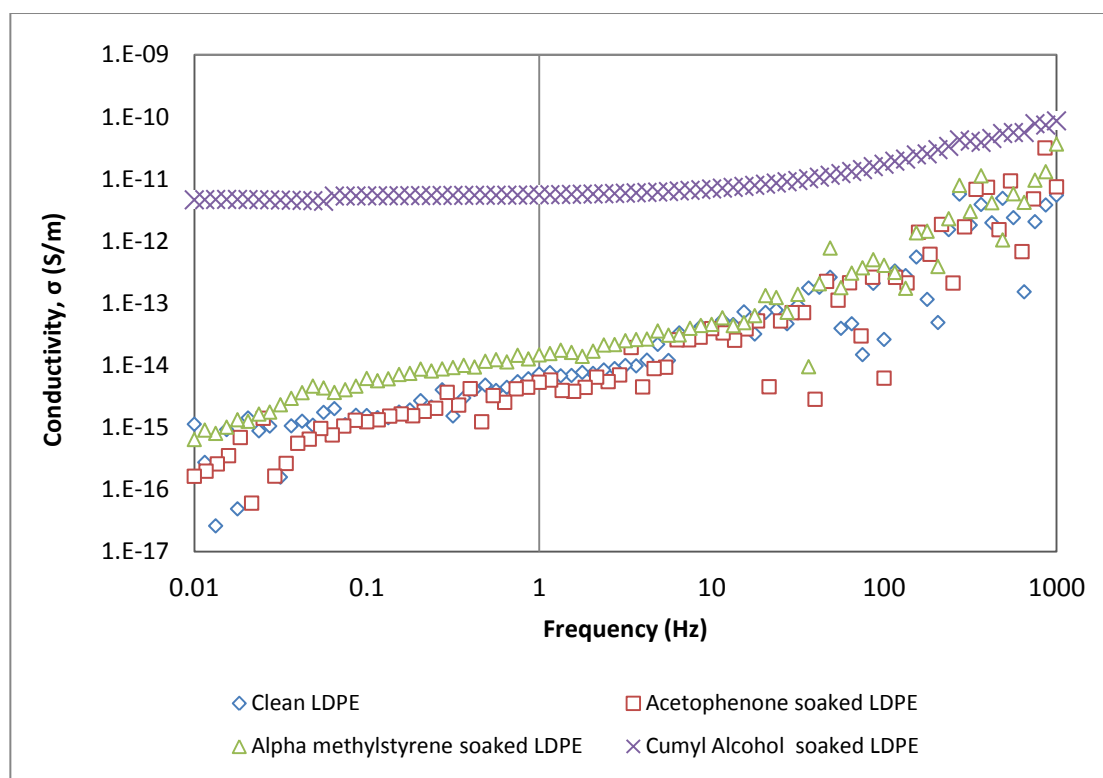
Figure 7-11: The conductivity of the clean LDPE and the soaked LDPE.

7.5   Chapter Summary

The dielectric spectroscopy measurements have been carried out on the liquid byproducts as well as the byproduct soaked LDPE. The value of permittivity and dielectric loss of the byproducts soaked LDPE films do not really resemble the measured values of the parent byproducts. It may possible to relate the small percentage weight of acetophenone in LDPE to its small effect on the dielectric constant and loss of LDPE. However, this relation is not true for α-methylstyrene sample. Thus, it is proposed that these differences may due to different polarisation effect of the byproducts in LDPE. In the future, it is worth to check the effects of several byproducts in one LDPE samples on dielectric spectroscopy.

Acetophenone soaked LDPE has the highest permittivity value followed by α-methylstyrene and cumyl alcohol soaked LDPE. Among the samples, only cumyl alcohol soaked LDPE exhibit the MWS polarisation and space charge polarisation effect at low frequencies. As a result, the dielectric loss and conductivity value of this sample is much higher than the rest of the measured samples.

On the other hand, the acetophenone soaked LDPE and α-methylstyrene soaked LDPE have very similar dielectric loss values to the clean LDPE. Last but not least, the Cole-Cole plots show that the soaked samples do not exhibit the Debye relaxation process.

Chapter 8   Conduction Current Measurement

8.1   Introduction

Generally, polymer has very low conductivity. Despite its high insulating properties, polymer could not stop some tiny flow of charges injected from the electrode at high voltage. Conductivity measurement has been a commercial interest because of the relation of cable aging or failure due to the local damage induced by charge flow and/or recombination. Due to the amount of traps in polymer, it is said that the polymer has a trap-controlled conductivity [105].

Conduction current consist of three components namely the leakage current, charging current and absorption current. The later two currents rise dramatically during the initial charging period but gradually reduce to a smaller value and eventually approaching zero. The charging current or also known as capacitive current becomes very high due to the electron rush into the negative electrode and be drawn from the positive electrode. Absorption current is due to the gradual change of polarisation of polymer (orientation of the polar side of the polymer chain by the electric field) [106] and accumulated charges under the influence of the electric field stress. This transient current is followed by a steady current which is the leakage.

8.2 Procedures

Samples for conduction current measurement have been coated with gold on both sides before they undergo the soaking process. 2 cm mask diameter was used to match the electrode size. Samples were stressed at 3, 5 and 8 kV which are equivalent to 16.7kV/mm, 27.8kV/mm and 44.4kV/mm respectively. The measurement took 3600 seconds (60 minutes) to be completed and readings were taken for every 20 seconds. Keithley 6487 picoammeter has been used to measure the current. The electrodes were placed in an oven to maintain the temperature through out the experiment. However, the temperature is limited to room temperature due to the nature of the byproducts that will evaporate at high temperature. It is crucial to maintain the same amount of byproducts in the sample through out the experiment. The circuit connection is illustrated in Figure 8-1.

180μm samples were used for the soaked sample measurement. The clean LDPE measurement however requires a thinner sample and larger electrode due to very small current flow in the sample. Here, 50μm LDPE film and 5cm electrode diameter are used. In addition, higher electric fields need to be applied for the measurement to obtain a higher signal to noise ratio.
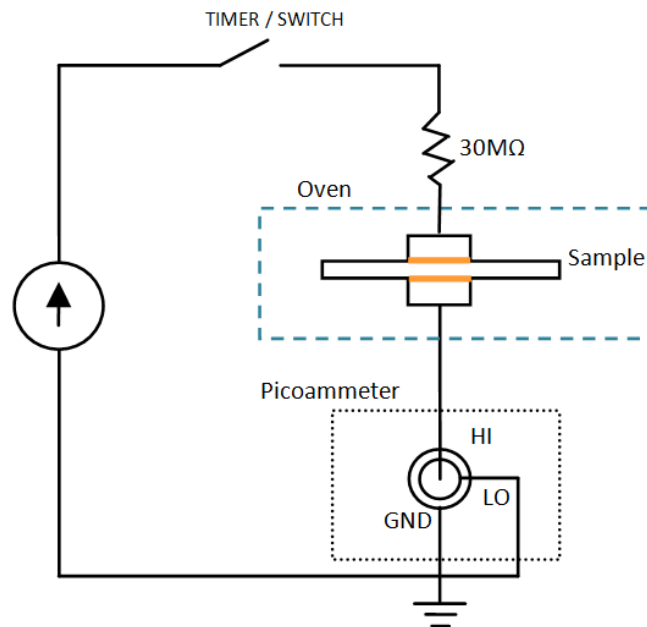
Figure 8-1: Circuit connection for conduction current measurement.

8.3 Conduction Current Result
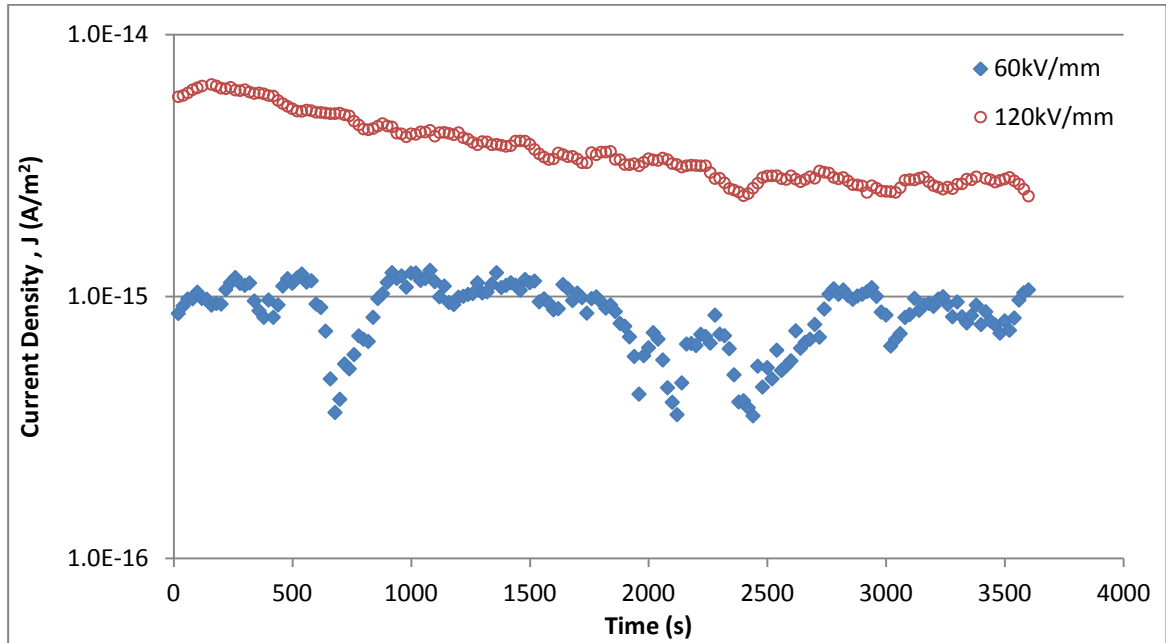
Figure 8-2: The current density-time characteristic of clean LDPE at 60kV/mm and 120kV/mm at room temperature.

To obtain the conduction current value without being deceived by the charging and absorption current, it is necessary to measure the current after a specified period of time. In this research, the conduction current reading is taken at 3500 seconds. Figure 8-2 shows the current density profile of the clean LDPE sample during charging. Although the field applied is very big, the current flow in the sample is very small. After 1 hour charging at 60kV/mm, the current density becomes as low as $\approx 1 \times 10^{-3} pA/m^2$ and $\approx 2.8 \times 10^{-3} pA/m^2$ at 120kV/mm. One can imagine that the current in clean LDPE at lower electric field is so much lower.

Comparing the current density of the soaked sample to that of the clean LDPE, it is quite obvious that the byproducts enhance the conduction current value in at least one order of magnitude. These values are presented in Figure 8-3 to Figure 8-5. From the results, cumyl alcohol causes the biggest jump to the current value followed by α-methylstyrene and then acetophenone.

Charged at 3kV, the current density in acetophenone soaked LDPE initially started at $\approx 5 \times 10^{-8}$ A/m^2 and this decreased to $\approx 3.5 \times 10^{-8}$ A/m^2 after 60 minutes charging. The reduction of the current is very little. The current density of acetophenone soaked LDPE after charged at 5kV and 8kV are 8×10^{-8} A/m^2 and 2.5×10^{-7} A/m^2 respectively. At higher charging voltage, the current reduction over the charging period becomes bigger.
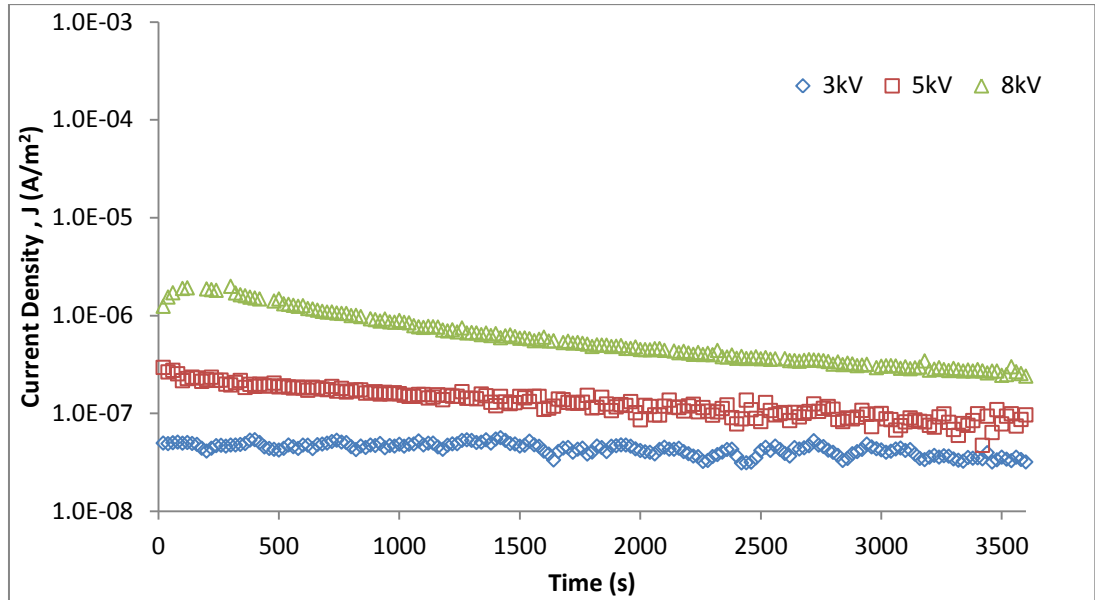
Figure 8-3: The current-time characteristic of acetophenone soaked LDPE at 3, 5 and 8kV at room temperature.
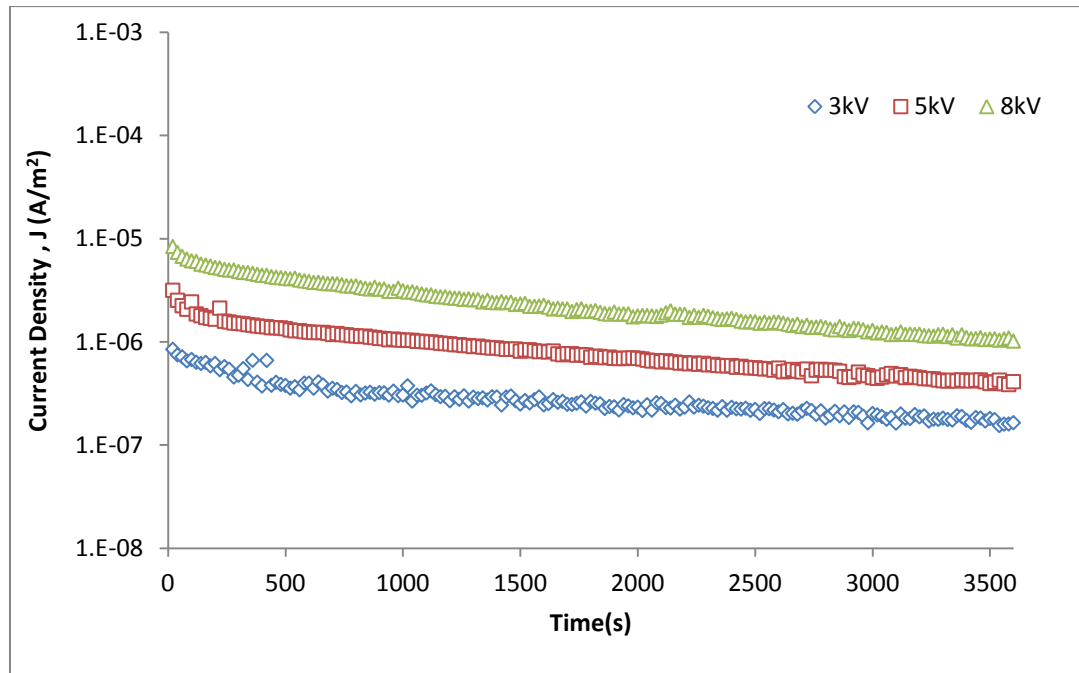
Figure 8-4: The current-time characteristic of α-methylstyrene soaked LDPE at 3, 5 and 8kV at room temperature.
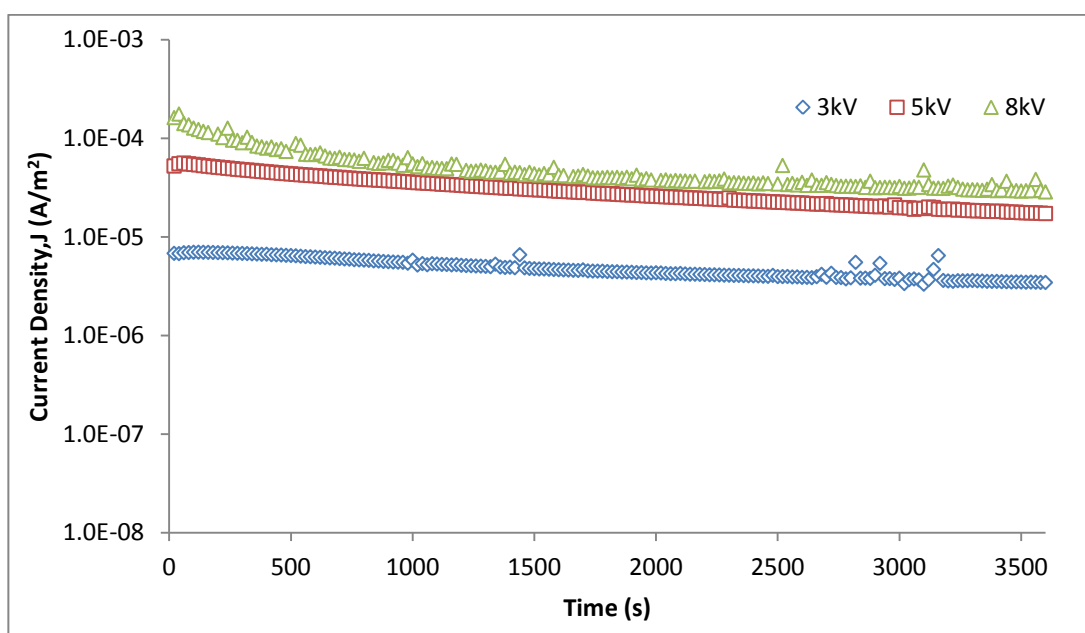
Figure 8-5: The current-time characteristic of cumyl alcohol soaked LDPE at 3, 5 and 8kV at room temperature.

For α-methylstyrene soaked LDPE, similar current decay is seen in the samples charged at different voltages. Cumyl alcohol soaked LDPE however shows a different result. Similar decay is seen in the current from samples charged at 3 and 5kV. Meanwhile sample that charged at 8kV has faster current decay. Table 8-1 shows the current density value of all samples at 3500s.

Table 8-1: Current density of samples at 3500s

Sample	Charging Voltage		
	3kV	5kV	8kV
Acetophenone soaked LDPE	3.5×10^{-8} A/m^2	8.0×10^{-8} A/m^2	2.5×10^{-7} A/m^2
α-methylstyrene soaked LDPE	1.8×10^{-7} A/m^2	4.0×10^{-7} A/m^2	1.1×10^{-6} A/m^2
Cumyl Alcohol soaked LDPE	3.5×10^{-6} A/m^2	1.8×10^{-5} A/m^2	3.0×10^{-5} A/m^2

8.4   The Correlation of DC Conductivity with space charge

This observation may be explained by the heterocharges that formed in cumyl alcohol soaked sample. Heterocharges enhance the electric field at the metal-insulator interface causing more charges to drift into the dielectric. Cumyl alcohol allows more charges pass through the LDPE leading to the increment of the current. Figure 6-12 in Chapter 6, demonstrates the fast growth of positive and negative charges both in bulk and near the electrodes.

The decaying transient current is proved to be bulk origin [105]. The accumulation of heterocharges reduce the electric field acting in the bulk and hence it explain the large current decay after the high initial current in cumyl alcohol soaked LDPE as seen in Figure 8-5.

Despite having the highest conductivity value, acetophenone ($1.8x\ 10^{-6}$ S/m) becomes less conductive compared to cumyl alcohol ($1.4\ x10^{-7}$ S/m) as it presence in LDPE [101]. This discrepancy might due to the small amount of acetophenone diffused in soaked LDPE compared to the other byproducts. Comparing a clean LDPE to the acetophenone as well as α-methylstyrene soaked LDPE, more charges injected from the electrode forming homocharge in the samples, and hence the diffusion of charges through the bulk may also increase. This is why bigger current was found in the soaked LDPE.

Conductivity (σ) values of the samples are calculated from the result of conduction current via equation:

$$\sigma = J/E$$
<div align="right">Equation 8-1</div>

and the values are plotted against electric field in Figure 8-6. The conductivity values for acetophenone and α-methylstyrene soaked LDPE increase linearly with the electric field. Meanwhile conductivity of cumyl alcohol soaked LDPE shows a different pattern in the relationship with electric field. Initially, the conductivity value increase dramatically but as the electric field increases, the slope of the graph start to decrease. It can be observed that cumyl alcohol amplifies the current that can pass through the dielectric with only small change of electric field.
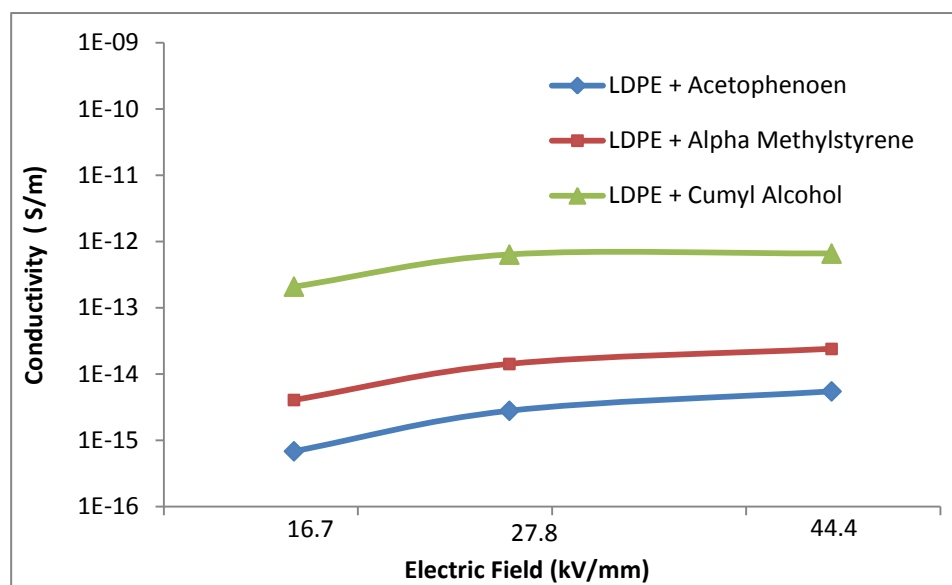
Figure 8-6: The conductivity of the soaked samples at 3, 5 and 8kV.

As presented in Table 8-2, each byproduct-soaked-LDPE has different amount of byproducts. This is due to the different diffusion rate of the byproducts into LDPE. R. Minami et.al reported in [107] that the conductivity increases with the soaking time, ie more byproducts chemical in the sample film. Hence, it is only justified to measure the influence of each byproduct on conductivity value relatively to the amount of these byproducts in the samples. Table 8-2 presented the conductivity gain by each percent of byproducts in LDPE. These values indicate the conductivity increment (in percent) caused by each percent of byproducts in the soaked sample and they are dependent on the electric field. These values show that with only small amount of crosslinking byproducts left in the insulator, particularly cumyl alcohol, the conductivity of the insulator could be magnified to a very big value that may damage the insulation.

Table 8-2: Conductivity Gain by each percent of byproduct in LDPE

Sample	Electric Field (kV/mm)		
	16.70	27.80	44.40
Acetophenone soaked LDPE	28.5%	88.5%	96.0%
α-methylstyrene soaked LDPE	93.8%	152.5%	137.5%
Cumyl Alcohol soaked LDPE	4957.26%	6736.4%	3750.3%

The effects of polar groups on conduction in polyethylene have been reported before [108]. Although the work done was on acetoxy group, similar effect could be observed from the polar groups that exist in the crosslinking byproducts. With the formation of heterocharges in cumyl alcohol soaked LDPE as well as a massive impact on the conductivity value, cumyl alcohol has a special feature that does not exist in acetophenone and α-methylstyrene. It is necessary to associate the unique characteristic with the existence of the hydroxyl group that exists in cumyl alcohol.

In addition, it was found that the conductivity values are thickness dependent. Extra measurements were conducted on 50μm byproducts soaked LDPE samples. Figure 8-7 plots the conductivity values for the samples at different electric filed. Result shown in figure 8-6 also included for comparison. Thinner sample has lower conductivity. Notice the 50μm cumyl alcohol soaked LDPE at field around 20 and 40kV/mm. The conductivity values are two orders smaller than that of 180μm samples around the same electric field.

Comparing the conductivity values for the 50μm samples, cumyl alcohol still acquires the highest conductivity value. Acetophenone and α-methylstyrene soaked LDPE have almost similar conductivity value, two order lower than that of cumyl alcohol soaked LDPE. Last but not least is the clean LDPE. The conductivity value of LDPE is as low as 10^{-17}. It is seen from Chapter 6 before, although the total charge that injected into clean LDPE is comparable with the total charge in byproducts, most of the charges are trapped in deep traps. As a result, very little charge contributes to conduction in clean LDPE.
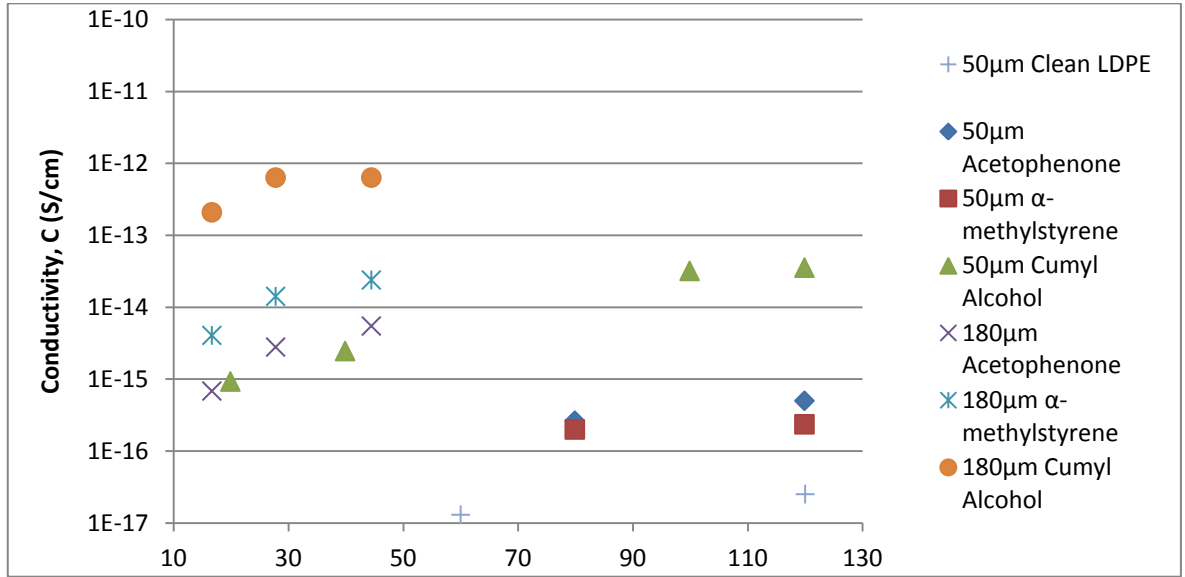
Figure 8-7: The conductivity of the 50μm and 180μm clean and soaked samples at different electric field.

8.5 Carriers Mobility

The power law dependency of current density to electric field is often found in many research of electrical conduction of dielectric polymer. The power law is given by [109];

$$J = aE^n \qquad \text{Equation 8-2}$$

And can be written as

$$ln\,J = ln\,a + n\,ln\,E \qquad \text{Equation 8-3}$$

This gives a straight line with slope n of ln J vs. ln E plot. Different n value indicates different conduction mechanism. In the case of ohmic conduction, where n = 1, it is usually as the result of electric field independency of carrier concentration and mobility [110]. In the case of space-charge-limited-conduction (SCLC), Equation 3-18 is referred, which give the value of n ≈ 2. For a combination effect of non-ohmic contact, e.g. Schottky barrier with the effect of space charge, the values of lie in the range of 2 to 4 [111]. Montanari in his work [110,112] uses this relation to distinguish the electrical degradation threshold of PE.
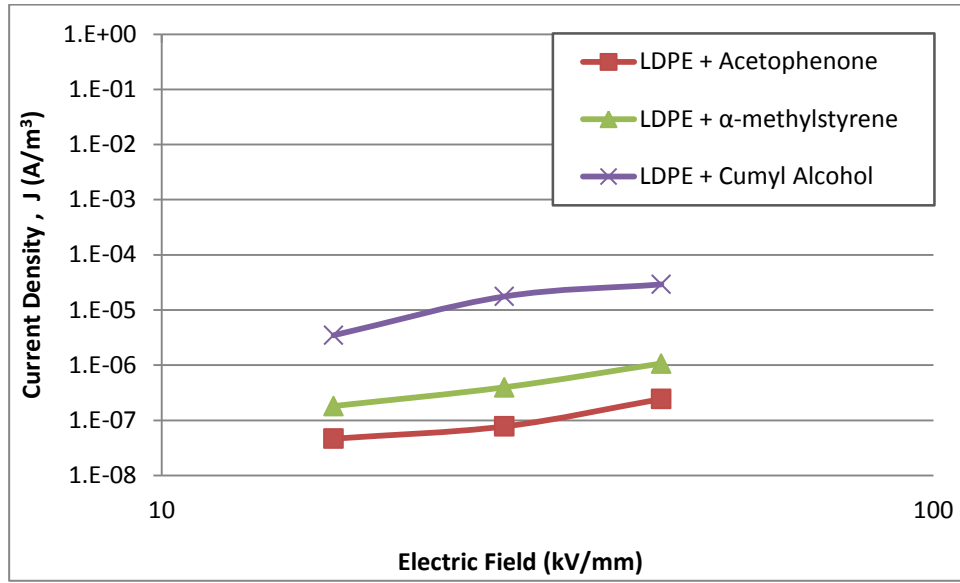
Figure 8-8: J-E characteristic of soaked LDPE samples.

J-E characteristic of the soaked samples are presented in Figure 8-8. The J-E curves of three byproducts-soaked samples are almost similar. The slope values for acetophenone, α-methylstyrene and cumyl alcohol soaked LDPE are 1.68, 1.81, and 2.19 respectively. According to [113] current distributions with such *n* values could be described by the SCLC theory. It may however be expressed by the Schottky laws as well as the ionic conduction. However SCLC plot can effectively display the space charge accumulation process on the basis of charging current.

Mobility could be obtained from SCLC theory from equation 3-19, which is $\mu = \frac{8Jd^3}{9V^2\varepsilon_0\varepsilon_r}$. The relative permittivity of the samples is taken from the measured value presented in Chapter 7. Since permittivity value for cumyl alcohol soaked sample increase at lower field due to the ionic conduction, the permittivity value used for the calculation is taken at 10Hz before the ionic conduction just started to affect the permittivity value. Figure 8-8 plots the charge mobility values against electric field.
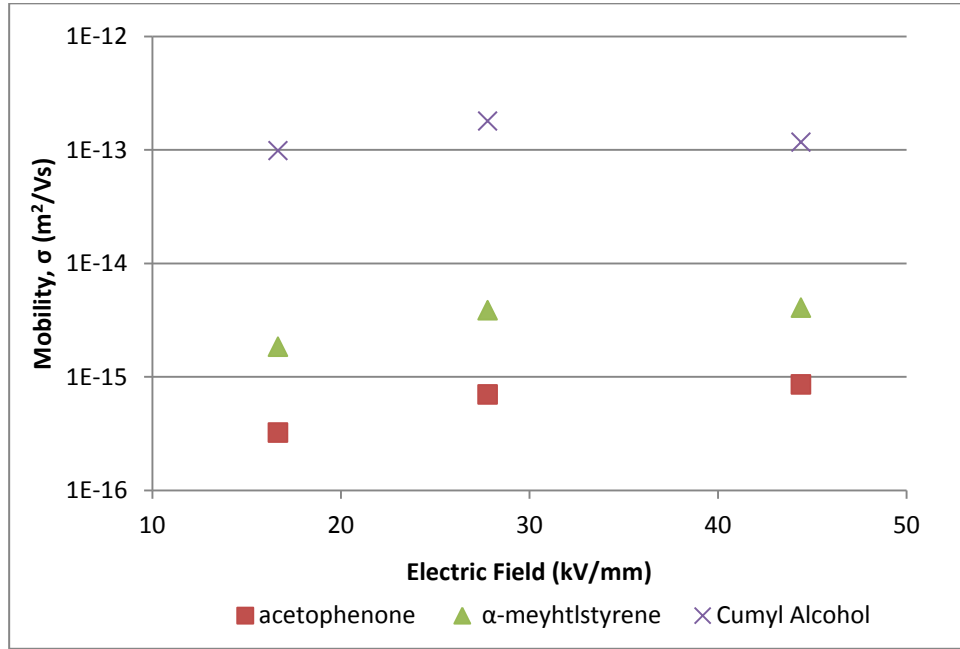
Figure 8-9: The charge mobility value calculated using SCLC theory

It must be pointed out, regarded Figure 8-9, the mobility values calculated by the derivation from SCLC theory refer properly to the mobility of free charge carrier where $\theta = n_c/n_t$ is assumed to be equal to one. Hence, in a dielectric with traps such as the samples measured, the mobility values should be expected to be lower than the plotted values.

8.6 Chapter Summary

The conductivity of the clean LDPE is very low and hence the conduction current measurement can only be conducted at a very high electric field. The conductivity of the byproducts soaked LDPE is so much higher in at least 8 times higher than the conductivity of the clean LDPE.

This finding is different from the total accumulated charges calculated from the space charge measurement. From Figure 6-16, it is clear that the charge in LDPE is considered in the equivalent range of that of the byproducts soaked sample. Thus, we can say that the ratio of the free charge carrier to the trapped charges (n_c/n_t) is very small and hence very little charges contribute to conduction.

Cumyl alcohol soaked LDPE has the highest conductivity which is 2 times bigger than α-methylstyrene soaked LDPE and 3 times bigger than the acetophenone soaked LDPE. This observation could be linked to the hydroxyl group that appear in cumyl alcohol as well as the heterocharge formation in the cumyl alcohol soaked LDPE.

Chapter 9   AC Breakdown

9.1   Introduction

Breakdown in dielectric insulation occurs when the insulation can no longer insulate and forced to conduct electricity. Dielectric breakdown in polymer is very complicated due to its complex structure. Breakdown mechanism is always associated with the internal field. In term of mechanical breakdown theory, internal field causes electromechanical force to be sufficient enough to break the material [114]. Meanwhile for thermal theory, internal field is related to electrical conductivity which increases the temperature up to the melting point of the material [43]. Last but not least, in the electronics breakdown theory, breakdown happens when the internal field reaches its critical value. The summary of breakdown process that occurs in solid dielectric is presented in Figure 9-1.

Electronic breakdown Theories	Thermal breakdown Theories	Mechanical Breakdown Theories
• intrinsic breakdown • Electronic thermal breakdown • Electron avalanche breakdown field emission breakdown • Space charge-enhance critical field breakdown	• Steady state thermal breakdown • Impulse thermal breakdown	• Electromechanical breakdown

Figure 9-1: Electrical breakdown theories of solid dielectrics.

Electronics breakdown theory can be classified into three mechanisms which are intrinsic, avalanche and space charge-enhanced critical field. During the application of very high electric field, some electrons from the valance band cross the band gap into the conduction band. As more and more electrons become available for conduction, conduction current across the insulation becomes huge and this phenomenon is called intrinsic breakdown. Avalanche theory was initially developed for a dielectric that is considered as a polar crystal. Avalanche happens when an electron from cathode with sufficient energy collide with another atom/molecule producing more electron and hole. If these electrons produce further two electrons, an avalanche of n electron will be produced in n generation. The process will be repeated and propagate across the insulation thickness.
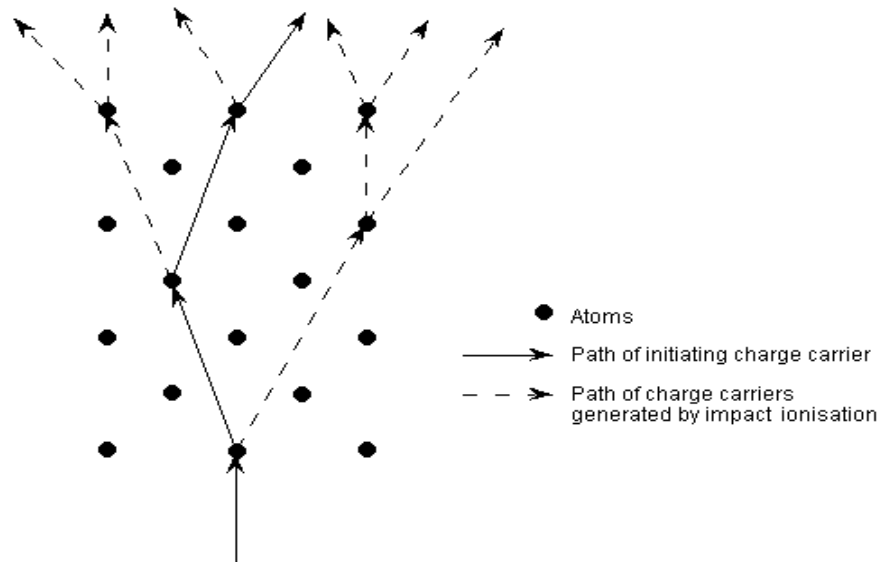
Figure 9-2: Avalanche process

Electrons injection in voids is controlled by the space charge that accumulated on the surface of void. Electrons (injected from the electrode or from the polymer) get trapped on the void surface as they travel to the opposite electrode. Negative electron affinity of polyethylene promotes surface state of the electron under the bottom of conduction band. The electrons that travel in polymer will get trapped on the surface of void and the process continues until the Coulombic repulsion between them is high enough to increase their energy level to de-trap by Schottky effect or thermal activation. In the void, the energy

barrier is much lower than in the PE. Electrons injected into the void are accelerated by applied electric field and if the field is high enough, it could cause avalanche in the void.

It is agreed that breakdown strength is defined as the voltage at which beyond this value, the dielectric can no longer maintain its ability to insulate. This value however is not an absolute number. This value varies depending on several factors that may influence the breakdown mechanism. These factors need to be reviewed so the limitation of dielectric strength value could be understood better. Some of the factors that have a big influence to breakdown strength values are;

- Dielectric thickness
- Temperature
- Electrode shape and size
- Rate of voltage increase

Other than the obvious reason that thinner sample will have less chance for defects to exist, the dependency of breakdown strength on thickness could also be explained by Maxwell stress [115,116]. Breakdown strength of dielectrics decreases with its thickness. Temperature control is important as the dielectric strength is related to the temperature of the specimen at the time of breakdown. The temperature dependent of dc breakdown field is usually decreased with temperature however this relation is non-linear. The electrode shape and size will determine the electric field distribution on the test sample. This factor is very important for small sample testing. Rogowski type electrode and ball bearing electrode could provide a uniform stress gradient which is important in order to obtain a reliable result. However, needle tests are also performed to investigate the breakdown phenomenon under divergent field. Rate of voltage increase may also affect the breakdown strength value. As the breakdown is performed at a constant ramp-rate (in which the electric field increases from zero at a predetermined rate), the breakdown value obtained will normally be greater than the value that obtained in step-rise test procedure (field increase at every set rise time). The impulse breakdown strength is reported to increase as the ramp rate is increase[117]. Hence, it is important to state the conditions together with the breakdown strength value since different condition may give different breakdown value.

9.2   Weibull Distribution Of AC Breakdown

Two-parameter Weibull Distribution is most commonly used for characterizing the time of failure for solid insulation. This distribution has been accepted as IEEE 930/IEC 62539 standard. The cumulative probability of failure for two parameter Weibull distribution can be expressed by:

$$P_F(t) = 1 - \exp\left(-\frac{t}{\alpha}\right)^\beta \qquad \text{Equation 9-1}$$

where t is the measured variable (t or E), α (eta) is the scale parameter, and β (beta) represent the shape parameter. The higher the value of β, the narrower the spread of times (or fields) to failure. From another perspective, the value of β shows the reliability of such material to insulate the HV cable before the material breakdown. The probability density function (PDF) of equation 9-1 is given by:

$$g(t) = \frac{dP_F(t)}{dt} = \beta\alpha^{-\beta}t^{\beta-1}\exp\left\{\left(\frac{t}{\alpha}\right)^\beta\right\} \qquad \text{Equation 9-2}$$

Figure 9-3(a) and (b) show the plot of cumulative probability of failure and probability density function respectively for the cases of β=0.5, 1.0, 1.5, 2.0 and β=3.0. At a constant value of α, which in this case α=1, various value of β will result to different slope.

In order to calculate the cumulative probability of failure, it is necessary first to rank the breakdowns in order of time (or field) and then estimate the true probability of failure for each point from i=1 to i=n for n samples. This probability of failure is best obtained at the median, in which the estimation proposed by Bernard and Bos-Levenbach [118] given by:

$$F(i,n) = \frac{i-0.3}{n+0.4} \qquad \text{Equation 9-3}$$
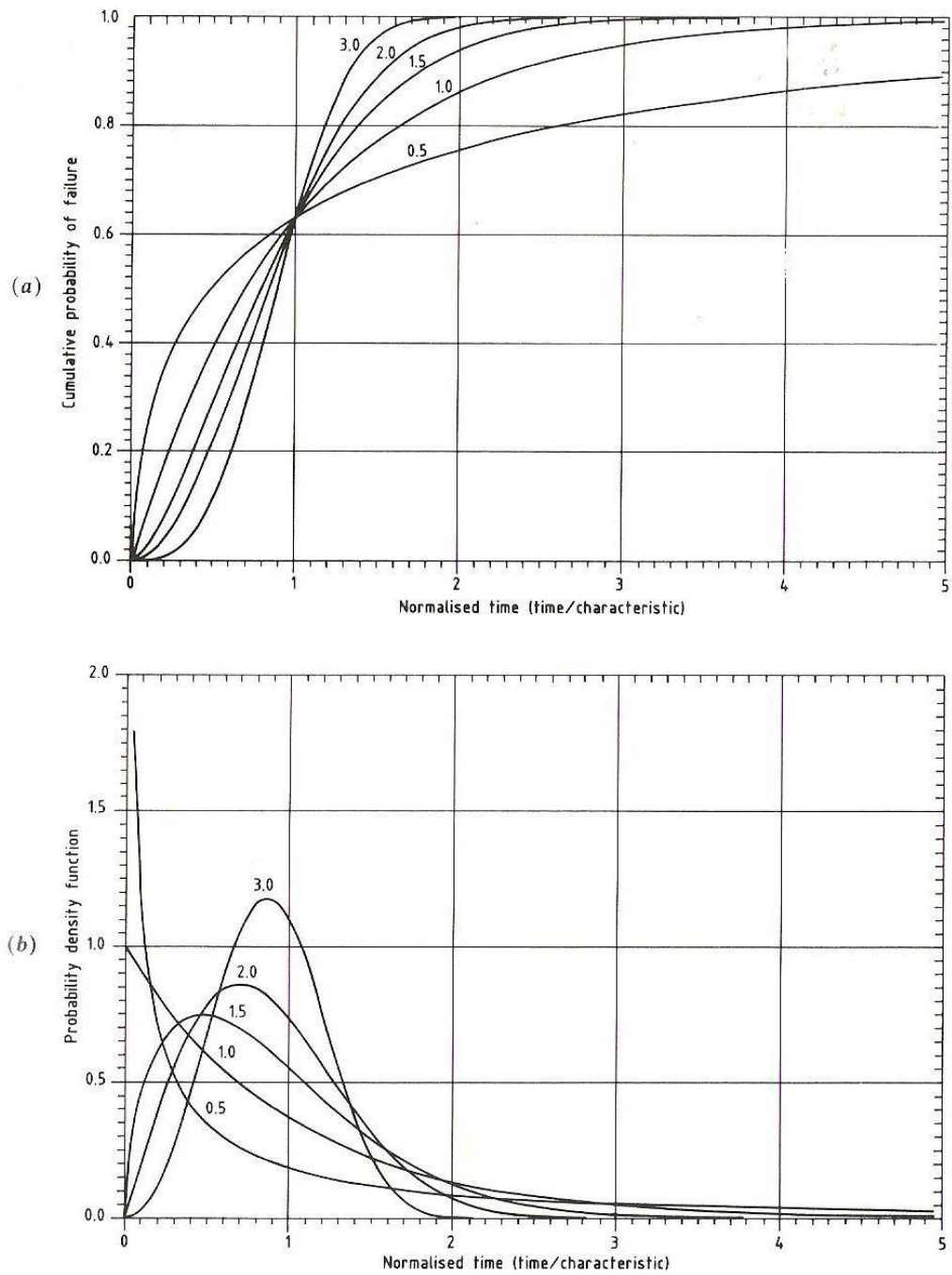
Figure 9-3: (a) The cumulative probability of failure and (b) probability density function
for the cases of β=0.5, 1.0, 1.5, 2.0 and β=3.0. [43]

Obtaining Weibull parameters is possible by rearranging equation 9-1 as a linear function;

$$\log_{10}\{-\log_e[1 - P_F(t)]\} = \beta.\log_{10}(t) - \beta.\log_{10}(\alpha) \qquad \text{Equation 9-4}$$

135

Plotting $\log_{10}\{-\log_e[1 - P_F(t)]\}$ versus $\log_{10}(\alpha)$ will result in a straight line of slope β. This linear regression however will be bias at the extreme of distribution. Therefore, maximum likehood (ML) estimation is used to approximate the values of α and β which is the product of PDF at each data point.

$$L(p) = g(x_1\alpha, \beta) \text{ x } g(x_2\alpha, \beta) \text{ x } \dots \dots \text{ x } g(x_n\alpha, \beta) \qquad \text{Equation 9-5}$$

In practice, log L(p) is used rather than L(p) (likehood function) and the relevant equation of two-parameter Weibull distribution becomes;

$$\frac{1}{\beta_{ML}} = \frac{\sum_{i=1}^{n}\left(x_i^{\beta_{ML}}\right) \ln x_i}{\sum_{i=1}^{n}\left(x_i^{\beta_{ML}}\right)} - \frac{1}{n}\sum_{i=1}^{n} \ln x_i \qquad \text{Equation 9-6}$$

$$\alpha_{ML} = \left[\frac{1}{n}\sum_{i=1}^{n} x_i^{\beta_{ML}}\right]^{\frac{1}{\beta_{ML}}} \qquad \text{Equation 9-7}$$

where β_{ML} and α_{ML} are the shape and scale parameters obtained from maximum likehood estimation. Nevertheless, this estimation is known to be biased to the value of β for small n and the value α become more bias for small β.

In this study, Weibull software supplied by ReliaSoft® was used to perform the Weibull distribution.

9.1   Experiment Procedures

LDPE films of 50μm thick were soaked into acetophenone and α-methylstyrene at room temperature meanwhile into cumyl alcohol at 80°C. The samples were used to perform the breakdown strength (E_b) of the LDPE with the byproducts chemical reside in the sample. The AC breakdown measurements were conducted at a ramp rate of 50V/s at room temperature. Ball-bearing electrodes were used. Weibull distribution is used to analyse the AC breakdown result. Figure 9-4 shows the equipment setting in the breakdown rig.
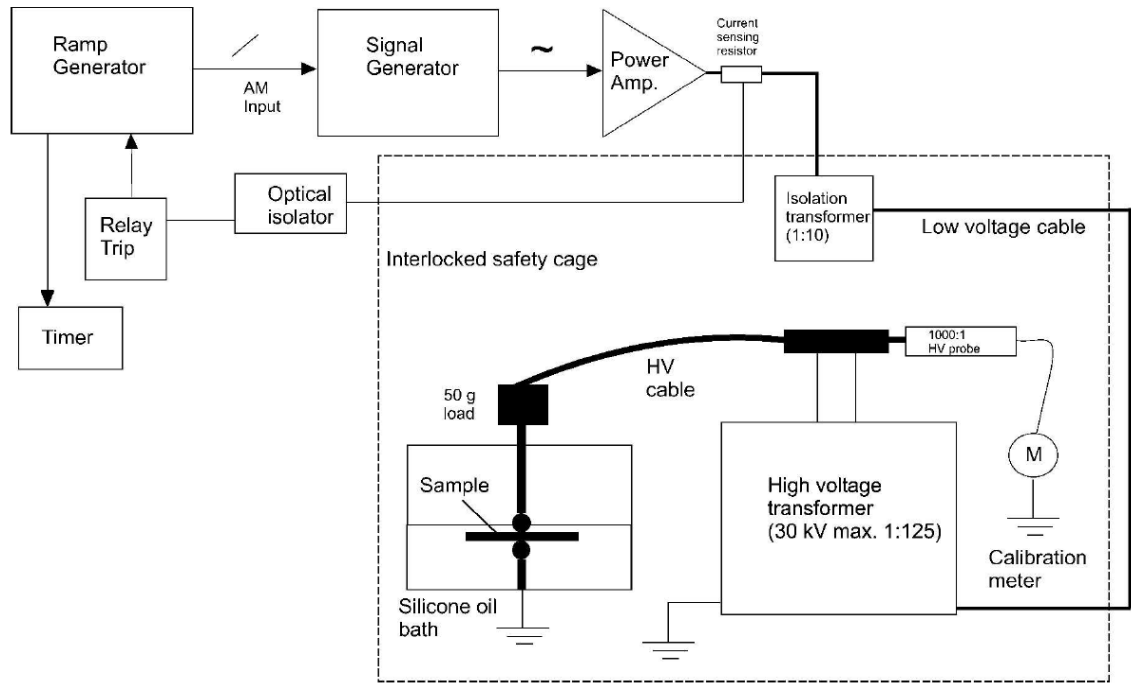
Figure 9-4:   Schematic diagram of the breakdown rig. [119]

9.2   AC breakdown test result

Figure 9-5 shows the plot of probability of failure, $F(i , n)$ versus the breakdown strength for all samples. The Weibull parameters, shape and scale parameters are estimated from these plots by using special software. The dotted lines drawn in the figures are the estimates value of 90% confidence intervals for each measurement.

Looking at the α value, which is the scale parameter of the breakdown strength, these values shows that some of the byproducts increase the AC breakdown strength. Acetophenone and cumyl alcohol increase the breakdown strength for about 10kV/mm. This result is in agreement with result reported in [120,121]. Meanwhile it is shown here that α-methylstyrene reduces the scale parameter value for about 10kV/mm lower than the clean LDPE. These values are presented in Table 9-1. The results obtained here is in agreement with [121] due to resistance of the byproducts impregnated samples to partial discharge. Nevertheless, the breakdown increment in the samples reported in the paper is much higher than the values obtained in our experiment. Overall, the breakdown strengths
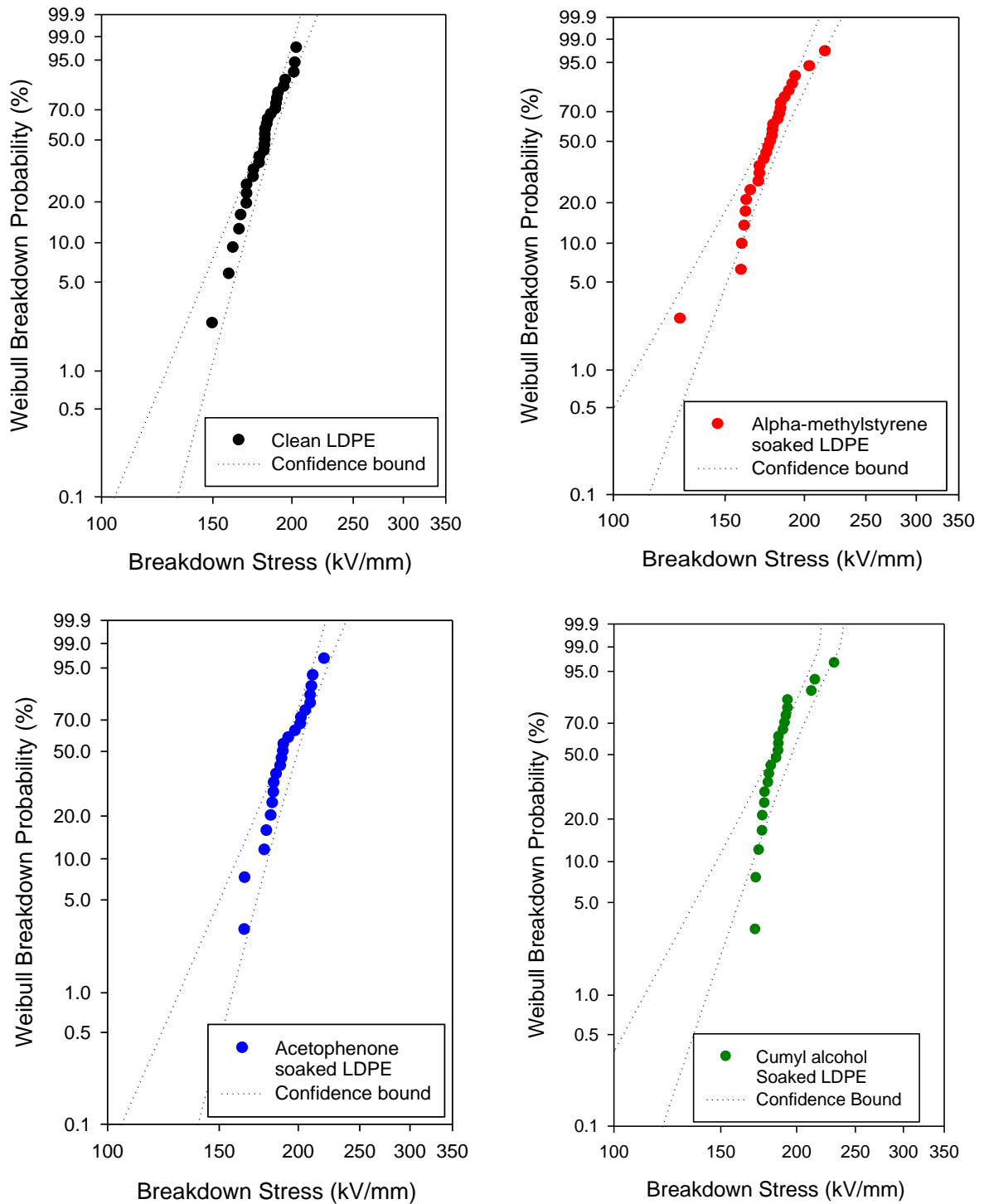
Figure 9-5: The Weibull Breakdown probability plot of a) Clean LDPE , b) acetophenone soaked LDPE, c) α-methylstyrene soaked LDPE and d) cumyl alcohol soaked LDPE

of all samples fall in the same range of values. Thus the byproducts have no effect on the ac breakdown strength of LDPE and similar observation seen in [28].

The exact breakdown mechanisms of the samples are difficult to be confirmed since it may involve more than one mechanism in the breakdown process. However it is worth to mention here that author like Fukuma reported breakdown measurement in conjunction with the space charge measurement [122]. Here, the role of space charge is observed as the space charge dynamics in the sample is captured just before breakdown happens. Nevertheless, most of the works that link space charge and breakdown strength are mainly related to direct field where the effect of space charge is much more severe. The results in Chapter 6 have shown the different impact of ac and dc field on the accumulation of space charge. Hence, it is believed that the effect of byproducts on dc breakdown strength will be more severe. With the breakdown process governed by the maximum electric field in the sample, space charge effect on dc field will play the utmost role to cause breakdown to happen.

Table 9-1: Weibull analysis of breakdown strength test result

Sample	% added crosslinking byproducts (%)	Eta, α (kV/mm)	Beta, β	Range of E_b (kV/mm)
LDPE	0	192.2 ± 6.2	11.9	148-226
LDPE + Acetophenone	2.42	198.8 ± 5.2	14.6	165-220
LDPE + α-Methylstyrene	13.20	183.5 ± 5.6	11.3	127-216
LDPE + Cumyl Alcohol	14.36	195.1 ± 6.8	11.0	171-231

9.3 Chapter Summary

AC breakdown test has been performed on the clean LDPE and crosslinking byproducts soaked LDPE. Weibull distribution is used to give the statistical features of the breakdown phenomena of the byproducts soaked LDPE.

By referring to the α values from the distribution, acetophenone and cumyl alcohol slightly increase the ac breakdown strength of LDPE. On contrary, α-methylstyrene slightly reduces the breakdown strength value.

In term of β, this value is very similar between the soaked sample and the clean LDPE, except for the acetophenone soaked LDPE which shows a higher β value. The overall ac breakdown characteristic of the soaked samples are very much similar to that of the clean LDPE. The breakdown values for each sample fall in the same range. Thus the byproducts have no effect on the ac breakdown strength of LDPE.

The small effect of crosslinking byproducts on ac breakdown is also observed in ac space charge measurement. In the latter, although the byproducts increase the total charge accumulated in the LDPE sample, the increment is very small compared to dc case. Hence, it is believe that the crosslinking byproducts may also have greater effect on dc breakdown strength due to high charge mobility in the soaked sample in dc condition as seen in Chapter 6 and Chapter 8. This hypothesis is also based on the report on the influence of the byproducts towards impulse breakdown [123].

Chapter 10 Conclusions and Future Works

10.1 Conclusions

This thesis provides a report on the research done on the crosslinking byproducts that remain in XLPE after the crosslinking process. Three main byproducts were investigated here which are acetophenone, α-methylstyrene and cumyl alcohol. To obtain a single product in each measured sample, LDPE was used as the base material for the soaking process. Through this research, consequences of crosslinking byproducts towards space charge accumulation across the polymeric insulation and their effect towards the charge conduction, permittivity and ac breakdown strength are realised. Some conclusions can be made.

1. Space Charge Accumulation in byproducts soaked LDPE

The presence of byproducts in XLPE cable is mostly associated with space charge formation in the cable insulator. Here, the individual effects of the byproducts on the formation of space charge were investigated. The presence of the byproducts changes the space charge pattern in the samples. Homocharges are seen in the vicinity of the electrodes for acetophenone and α-methylstyrene soaked samples. Although the clean sample also possesses similar homocharge, the charge pattern is different. Acetophenone ease the movement of negative charges in LDPE causing more negative charge accumulation in the sample bulk. On contrary, α-methylstyrene causes more positive charge build up in the sample bulk. Dissimilar to the former two byproducts, cumyl alcohol introduces

heterocharges near both electrodes. The formation of heterocharges is believed due to the hydroxyl group that presence in cumyl alcohol.

We were also able to calculate the total charge in each sample and compared with the total charge in clean LDPE. Cumyl alcohol has the highest total charge followed by clean LDPE, acetophenone and α-methylstyrene. However at higher field, acetophenone introduces more charges compare to clean LDPE. α-methylstyrene on the other hand consistently reduces the amount of total charge introduced into the insulator. This characteristic is also observed in samples with 2 byproducts, where any samples with α-methylstyrene have low total charge.

The charge decay process reveals the ability of the byproducts to speed up the charge reduction in samples. 2 different charge decay rates leads us to 2 different traps depth in polymer. Hence, the influence of the byproducts on each population of traps could be determined. It was found that the byproducts increase the number of shallow traps in the samples and reduce the number of charges that are trapped in deep traps. α-methylstyrene soaked LDPE have the fastest charge decay followed by acetophenone and then cumyl alcohol.

An improved PEA system enables us to measure the space charge property of the samples in ac condition. It was found that the byproducts once again increase the total charge in the sample although the amount is so much smaller than that in dc. This time however, the charges that trapped in the samples are identified as the charges in deep traps due to their very slow charge decay. These findings together with the results obtained in dc condition lead us to another conclusion. The shallow traps that exist in crosslinking byproducts increase the number of charges trapped in the sample. As they move further into the bulk, the probability of the charges to be trapped into deep traps is higher and hence we see more charges in deep traps in the byproducts soaked sample. This conclusion is significant in determining the trapping probability of deep traps in any model. From this research, it is found that this value depends on the concentration of shallow traps in the dielectrics.

2. Dielectric Spectroscopy Measurement

In applying a material as the cable insulation, the dielectric constants (permittivity) as well as the dielectric loss tangents are two important parameters that need to be considered. As we measure the byproducts soaked LDPE, it was found that acetophenone give a small increase of the dielectric constant value of LDPE. The other byproducts do not affect much on this value.

Cumyl alcohol soaked LDPE shows a gradual increase of the permittivity value as the spectrum shifted to lower frequency. The dielectric loss value for this sample is also very high particularly at lower frequency. This result may be due to the MWS polarisation effect and electrode polarisation effect as well as the ionic conduction in the sample. This phenomenon however was not observed in acetophenone and α-methylstyrene soaked LDPE. Hence it is believe that the hydroxyl group in cumyl alcohol plays the main role in causing such behaviour.

The conductivity values were calculated using the imaginary part of permittivity. As expected, cumyl alcohol has the highest conductivity value.

3. DC Conductivity measurement

Conductivity values of the sample are measured at room temperature. DC conductivity of clean LDPE is very low. The influence of electric field on conductivity is observed. Cumyl alcohol has the biggest effect on the conductivity of the soaked LDPE followed by α-methylstyrene and acetophenone. This result may be explained by the formation of heterocharges in the vicinity of electrode which observed in space charge measurement, enhancing the electric field near the metal-dielectric interface and lead to the increment of the current value. Cumyl alcohol is proven to be more conductive in LDPE compared to the other byproducts even at low electric field.

Through the experiment, we were able to calculate the mobility values of the carriers in the samples by using SCLC theory.

4. Dielectric breakdown on AC field

AC breakdown test was conducted using ball-bearing electrodes which were placed in silicon oil. The result reveals that the breakdown strength of the byproduct soaked LDPE is almost similar to that of the clean LDPE. Although acetophenone and cumyl alcohol slightly increase the α value, also α-methylstyrene slightly reduces the α value, the breakdown strength for each samples fall in the same range.

In other words, the crosslinking byproducts have little effect on ac breakdown strength. By relating the ac breakdown strength with ac space charge measurement result, one could agree that the little difference on space charge formed in byproducts soaked LDPE and LDPE samples that were stressed in ac field may lead to small difference on ac breakdown strength among the samples.

Since the effect of the crosslinking byproducts on space charge formation at dc field is more severe, we believe that the byproducts will also influent the dc breakdown strength value of LDPE.

5. Byproducts

After comparing the influence of acetophenone, α-methylstyrene and cumyl alcohol on the electrical properties that discussed above, it could be concluded that the total amount of byproducts in each sample is not one of the factors that contribute to the different observation on each tested sample. We believe that these differences are related to the polar group that exist in each byproduct molecule. The hydroxyl group in cumyl alcohol may cause the heterocharge in the stressed sample due to the ionisation process in the sample. The O-H bond may also causes ionic conduction as well as MWS and electrode polarisation during the dielectric spectroscopy measurement. As a result, cumyl alcohol has the biggest dielectric loss compared to the other samples.

The carbonyl group (C=O) in acetophenone and conjugate double bond (C=C) in α-methylstyrene have lead to the formation of homocharges in stressed samples. They however are observed to assist the movement of different type of charge carriers. Both of

144

these byproducts do not change the dielectric loss of LDPE and their charge mobility values are only one order of magnitude differ.

The three crosslinking byproducts have very small effect on electrical properties of LDPE during ac condition. This is observed from the ac space charge measurement as well as the ac breakdown measurement. In term of charge decay, we could conclude that the byproducts particularly α-methylstyrene leave a positive effect on the process. With the fastest charge decay, α-methylstyrene could remove all of the charges in the sample much faster than other samples. The byproducts however have affected the total amount and distribution of space charge as well as the charge dynamics of the sample. The effects of the byproducts become much severe at higher electric field. With very high DC conductivity, the byproducts have proved to be the drawback to the insulation material. Cumyl alcohol has shown its ability to introduce more charges into the LDPE with the formation of heterocharge. It also has the highest dielectric loss and dc conductivity which leads to the highest charge mobility value. Based on these results, we could conclude that cumyl alcohol is the most dangerous crosslinking byproduct compared to the others.

10.2 Future Work

Several areas of this investigation have the potential to be continued by further research and experimentation, some of which is detailed below.

1. Much knowledge could be gained by studying the space charge profile of the polymer. One big advantage that could contribute to this research is by measuring the conduction current simultaneously with the space charge profile. By obtaining the current values, the carrier mobility could be calculated without applying any ambiguous assumption to simplify the equation. With this, the carriers' mobility value could be attained accurately.

2. In this thesis, we were trying to link the space charge profile to the breakdown result that obtained from a different system. This comparison however will be much more accurate if the breakdown test could be conducted on the PEA system.

145

By having this system, we will be able to monitor the space charge and electric field in the sample just before breakdown happens. DC breakdown measurement of the byproduct soaked LDPE could also be done to verify the contribution of the byproduct.

3. It is also an interest of this research to relate the electrical properties that are measured to the chemical structure of the byproducts such as the molecule size, since they are both related to each other. The trapping characteristic might be influenced by the chemical groups in the byproducts. One thing that could be done is to use various chemicals with similar group to confirm their effects on electrical properties.

4. The influence of space charge on the electrical performance of a material depends on several factors such as the amount and distribution of space charge and charge dynamics. These are affected by the magnitude and duration of the applied electric field, temperature and electrode material. The works that reported in this thesis present the short-term effects of the byproducts. These results may be different from the samples that are stressed for a longer duration. Thus, a long-term effect of the byproducts should also be studied to reveal the hazardousness of these byproducts on the electrical properties. By doing this, along with selecting the right experiment variables, the results obtained will be closer to the actual condition in the real insulation cable.

References

[1]   K.C. Agrawal. *Electrical Power Engineering: Reference & Applications Handbook*,Taylor and Francis, 2007. 1125 pages.

[2]   G.F. Moore, *Electric Cables Handbook*. Third Edition ed: well Publishing 1997, 1098 pages.

[3]   T. Andrews, R. N. Hampton , A. Smedberg, D. Waldm, V. Waschk, W. Weissenberg. *The Role of Degassing in XLPE Power Cable Manufacture* IEEE Electrical Insulation Magazine, December 2006 pp. 5-16.

[4]   T. William A, *Electrical Power Cable Engineering* Volume 2. New York , USA: Marcel Dekker, 417 pages.

[5]   Y. Ohki, N. Hirai, K. Kobayashi, R. Minami, M. Okashita, T. Maeno. *Effects of Byproducts of Crosslinking Agent on Space Charge Formation in Polyethylene-Comparison Between Acetophenone and α-methylstyrene*, in Conference on Electrical Insulation and Dielectric Phenomena, 2000, Victoria, BC, Canada, pp. 535 - 538

[6]   K.S. Suh, S.J. Hwang, J.S. Noh, T. Takada. *Effects of Constituents of XLPE on the Formation of Space Charge*, in IEEE Transactions on Dielectrics and Electrical Insulation, 1994, Vol. 1 (6), pp.1077-1083.

[7]   N. Hirai , Y. Maeno , T. Tanaka, Y. Ohki, M. Okashita, T. Maeno. *Effect of Crosslinking on Space Charge Formation in Crosslinked Polyethylene*, in Conference On Properties and Applications of Dielectric Materials, 2003, June 1-5, Nagoya, Japan, pp. 917-920.

[8]   Y. Sekii, A. Taya, T. Maeno. *Effect of Antioxidants on Space Charge Generation in Crosslinked Polyethylene and EPR*, in Conference on Electrical Insulation and Dielectric Phenomena, 2006,Kansas City, MO, United states, pp. 133-137.

[9]   Y.L. Chong, G. Chen, Y.F.F. Ho. *The Effect of Degassing on Morphology and Space Charge*, in IEEE International Conference on Solid Dielectrics, 5-9 July 2004,Toulouse, France, pp. 162-165.

[10]   *Polymers in General*, available from http://lww.kt.dtu.dk/~vigild/2005_06_hempel/Theory/Polymers%20in%20general.htm, access on 20 May 2008

[11]   *Polyethylene*, available from http://en.wikipedia.org/wiki/Polyethylene, access on 20 Jun 2009

[12]   A. Barlow. *The Chemistry of Polyethylene Insulation*, in Electrical Insulation Magazine, IEEE, 1991, Vol. 7 (1), pp.8-19.

[13]   GoodFellow, *GoodFellow ,Polyethylene - Low Density (LDPE)- Material Information*, available from http://www.goodfellow.com/csp/active/STATIC/E/Polyethylene_-_Low_Density.HTML, access on 15 july 2008

[14]   T. S. Yeong, S. L. Jia, K.C. Tzung. *An Investigation of Water Crosslinking Reactions of Silane-Grafted LDPE*, in Journal of Applied Polymer Science, 19 August 2000, Vol. 81 (No 1), pp.186-196.

[15]   T. S. Yeong, C. C. Hui, M.L. Chih. *Water Crosslinking Reactions of Silane-Grafted Polyolefin Blends*, in Journal of Applied Polymer Science, 10 January 2001, Vol. 81 (No 7), pp.1799-1807.

[16]   Y. Zhu, H.G. Yoon, K.S. Suh. *Electrical Properties of Silane Crosslinked Polyethylene in Comparison with DCP Crosslinked Polyethylene*, in IEEE Transactions on Dielectrics and Electrical Insulation, 1999, Vol. 6 (2), pp.164-168.

[17]   R. Anbarasan, O. Babot, B. Maillard. *Crosslinking of High-Density Polyethylene in the Presence of Organic Peroxides*, in Journal of Applied Polymer Science, 2004, Vol. 93 (1), pp.75-81.

[18]   *Curing Agent Dicumyl Peroxide*, Liuyang Sanji Chemical Trade Co., Ltd. , on http://lysjhg.en.alibaba.com/product/431238914-209675510/Curing_agent_dicumyl_peroxide.html

[19]   G. A. Cartwright, A. E. Davies, S. G. Swingler, A.S. Vaughan. *Effect of An Antioxidant Additive on Morphology and Space-Charge Characteristics of Low-Density Polyethylene*, in IEE Proceedings - Science Measurement and Technology, 1996, Vol. 143 (1), pp.26.

[20]   M. Goshowaki, I. Endoh, K. Noguchi, U. Kawabe, Y. Sekii. *Influence of Antioxidants on Electrical Conduction in LDPE and XLPE*, in Journal of Electrostatics, 2007, Vol. 65 (9), pp.551-554.

[21]   Y. Sekii, T. Maeno. *Generation and Dissipation of Negative Heterocharges in XLPE and EPR*, in IEEE Transactions on Dielectrics and Electrical Insulation, 2009, Vol. 16, pp.668-675.

[22]   G.C. Montanari, C. Laurent, G. Teyssedre, A. Campus, U.H. Nilsson. *From LDPE to XLPE: Investigating the Change of Electrical Properties. Part I: Space charge, Conduction and Lifetime*, in IEEE Transactions on Dielectrics and Electrical Insulation, 2005, Vol. 12 (3), pp.438-446.

[23]   G. Teyssedre, C. Laurent, G.C. Montanari, A. Campus, D.H. Nilsson. *From LDPE to XLPE: Investigating the Change of Electrical Properties. Part II: Luminescence*,

in IEEE Transactions on Dielectrics and Electrical Insulation, 2005, Vol. 12 (3), pp.447-454.

[24] F. Aida , G. Tanimoto, M. Aihara, E. Hosokawa. *Influence of Curing Byproduct on Dielectric Loss in XLPE Insulation* in Conference on Electrical Insulation and Dielectric Phenomena, Oct 1990 Pocono Manor, PA, USA, pp. 465-473.

[25] T. Nakatsuka, T. Takahashi, H. Miyata, A. Yokoyama, I. Ishikawa , T. Niwa. *The Effect on Dielectric Loss of Polyethylene Caused by Acetophenone and Cumyl Alcohol* in IEEE International Symposium on Electrical Insulation 1994, June 5-8, Pittsburgh, PA USA, pp. 574-577.

[26] S.T. Hagen. *Improving the AC Breakdown Strength of XLPE Cable Insulation by Impregnation*, in Proceedings of Nordic Insulation Symposium, 1994,Vaasa, Finland.

[27] D.H. Damon, S.J. Huang, J.F. Johnson. *Electrical Strength of XLPE Cable Insulation Containing Controlled Amounts of the Volatile Products of the Crosslinking Reaction*, in IEEE Conference on Electrical Insulation and Dielectric Phenomena, October 1990,Pocono Manor, PA, USA, pp. 398-403.

[28] N. Amyot, S.Y. Lee, E. David, I.H. Lee. *Effect of Residual Crosslinking Byproducts on the Local Dielectric Strength of HV Extruded Cables*, in Annual Report Conference on Electrical Insulation and Dielectric Phenomena, Oct. 2000 Vol. 2 (No 2), pp.743 - 746

[29] K. S. Suh , C. R. Lee , M.K. Han. *Electrical Conduction of XLPE with Vacuum Degassed Semiconductive Electrodes*, in Conference On Electrical Insulation and Dielectric Phenomena, Oct 1992, Victoria, BC, Canada, pp. 130 -135.

[30] M. Fu, G. Chen, L.A. Dissado, J.C. Fothergill. *Influence of Thermal Treatment and Residues on Space Charge Accumulation in XLPE for DC Power Cable Application*, in IEEE Transactions on Dielectric and Electrical Insulation February 2007, Vol. Vol 14 (No. 1).

[31] Y. Sekii, T. Ohbayashi, T. Uchimura, U. Mochizuki, T. Maeno. *The Effects of Material Properties and Inclusions on The Space Charge Profiles of LDPE and XLPE*, in IEEE Conference on Electrical Insulation and Dielectric Phenomena, 2002, Cancun, Mexico, pp. 635-9.

[32] N.Nibbio, T.Uozumi, N.Yasuda, T.Fukui. *The Effects of Additives on Space Charge in XLPE Insulation - Crosslinking Reagent and Antioxidant -*, in IEEE International Symposium on Electrical Insulation, , June 1994, 5-8 June, Pittsburgh, PA USA,, pp. 559-562.

[33] Y. Sekii, T. Ohbayashi, T. Uchimura, T. Hukuyama, T. Maeno. *A Study On the Space Charge Formation in XLPE.*, in Conference on Electrical Insulation and Dielectric Phenomena, 2001, Kitchener, Ont. , Canada, pp. 469 - 472.

149

[34] H. Miyata , A. Yokoyama , T. Takahashi , S. Yamamaoto. *Effect of Water on the Space Charge Formation in XLPE*, in IEEE International Symposium on Electrical Insulation, 1996, 16-19 Jun 1996, Montreal, Que. , Canada pp. 670 - 673.

[35] T. Ohara, K. Kobayashi, Y. Ohki, T. Maeno. *Effect of Acetophenone on Space Charge Formation in LDPE and LLDPE*, in International Symposium on Electrical Insulating Materials, 1998,Toyohashi, Japan, pp. 231 - 234

[36] N. Hirai, R. Minami, Y. Ohki, M. Okashita, T. Maeno. *Effect of Byproducts of Dicumyl Peroxide on Space Charge Formation in Polyethylene* in IEEE 7th International Conference on Solid Dielectrics, 25-29 June 2001, Eindhoven, The Netherlands.

[37] N. Hirai, R. Minami, T. Tanaka, Y. Ohki, M. Okashita, T. Maeno. *Chemical Group in Crosslinking Byproducts Responsible for Charge Trapping in Polyethylene*, in IEEE Transactions on Dielectrics and Electrical Insulation, 2003, Vol. 10 (2), pp.320-330.

[38] T. Doi, Y. Tanaka , T. Takada. *Short Interval Measurement of Space Charge Distribution in Acetophenone Coated Low Density Polyethylene* in 5th Internal Conference on Properties and Applications of Dielectric Materials, 1997,May 25-30,Seoul , Korea, pp. 810-813.

[39] N. Hirai, Y. Maeno, T. Tanaka, Y. Ohki, M. Okashita, T. Maeno. *Roles of Cumyl Alcohol and Crosslinked Structure in Homocharge Trapping in Crosslinked Polyethylene*, in Conference on Electrical Insulation and Dielectric Phenomena, 19–22 October 2003, Albuquerque, NM, USA, pp. 213-16.

[40] Y. Zhang, J. Lewiner, C. Alquie, N. Hampton. *Evidence of Strong Correlation Between Space Charge Buildup and Breakdown in Cable Insulation*, in IEEE Transactions on Dielectrics and Electrical Insulation, 1996, Vol. 3 (6), pp.778-783.

[41] G.C. Montanari. *Bringing An Insulation to Failure: The Role of Space Charge*, in IEEE Transactions on Dielectrics and Electrical Insulation, 2011, Vol. 18 (2), pp.339-363.

[42] L.A. Dissado, G. Mazzanti, G.C. Montanari. *Role of Trapped Space Charges in the Electrical Aging of Insulating Materials*, in IEEE Transactions on Dielectrics and Electrical Insulation, 1997, Vol. 4 (5), pp.496-506.

[43] L.A. Dissado, J.C. Fothergill, *Electrical Degradation and Breakdown in Polymer* London , United Kingdom: Peter Peregrinus Ltd. , 1992, 601 pages.

[44] K.J.B. Kao. *Thermally Stimulated Discharge Current Study of Surface Charge Release in Polyethylene by Corona-Generated Excited Molecules, and the Crossover Phenomenon*, in Journal of Applied Physics, 1979, Vol. 50 (12), pp.8181-8185.

[45] W.S. Lau. *Simultaneous Space Charge and Current Measurement in Polyethylene Under HVDC Condition*, A PhD. thesis of University of Southampton, 2003.

[46] R. Patsch. *Space Charge Phenomena in Polyethylene at High Electric Fields*, in Journal of Physics D: Applied Physics, 1990, Vol. 23 (12), pp.1497-1505.

[47] F. Zakopoulos. *A Report on the Modelling of Space Charge Dynamics*, A PhD. thesis of University of Southampton, Southampton, May 2002.

[48] J. P. Jones, J. P. Llewellyn, T.J. Lewis. *The Contribution of Field-Induced Morphological Change to the Electrical Aging and Breakdown of Polyethylene*, in IEEE Transactions on Dielectrics and Electrical Insulation, 2005, Vol. 12 (5), pp.951-966.

[49] S. Takeshita. *Modeling of Space-Charge-Limited Current Injection Incorporating an Advanced Model of the Poole-Frenkel Effect*, A Master thesis of Clemson University, South Carolina, 2008, 154 pages.

[50] Y. Ouyang, F.D. Xu, X.S. Xie, D.H. Zhu. *Hopping Current and Charge Storage in Polymer Electret*, in 9th International Symposium on Electrets, 25-30 Sep 1996,Shanghai, China, pp. 54-59.

[51] P. Morshuis, M. Jeroense. *Space Charge Measurement on Impregnated Paper: A Review of the PEA Method and a Discussion of Result* IEEE Electrical Insulation Magazine 1997, pp. 26-35.

[52] A. Cherifi, M.A. Dakka, A. Toureille. *The Validation of the Thermal Step Method*, in IEEE Transactions on Electrical Insulation, 1992, Vol. 27 (6), pp.1152-1158.

[53] A. Cernomorcenco, P. Notingher. *Application of the Thermal Step Method to Space Charge Measurements in Inhomogeneous Solid Insulating Structures: A Theoretical Approach*, in Applied Physics Letters, 2008, Vol. 93 (19), pp.192903 - 192903-3

[54] A. Toureille, Y. Saito, C. Le Gressus. *Space Charge Measurement in 'R.F. Ceramic Windows' by the Thermal Step Method*, in IEEE Conference on Electrical Insulation and Dielectric Phenomena, 23-26 Oct 1994,Arlington, TX, USA, pp. 379-384.

[55] D. Malec. *Technical Problems Encountered with the Laser Induced Pressure Pulse Methode in Studies of High Voltage Cable Insulator*, in Meas. Sci. Technol. , 2000, Vol. 11 (5), pp.76-80.

[56] G. Chen , M. A. Brown , A. E. Davies, C. Rochester , I. Doble. *Investigation Of Space Charge Formation at Polymer Interface using Laser Induced Pressure Pulse Technique*, in 9th International Symposium on Electrets, 25-30 Sep 1996, Shanghai, China, pp. 285-290.

[57] G.T. O Gallot-lavallee. *Space Charge Measurement in Solid Dielectric by the Pulse Electroacoustic Technique*, in IEEE International Conference on Solid Dielectric 2004, pp. 268-271.

[58] Y. Tanaka, Y. Li, T.Takada, M. Ikeda. *Effect of Supression Layer on Space Charge Formation in Low Density Polyetylene*, in IEEE Anual Report Conference on Electrical Insulation and Dielectric Phenomena, 17-20 Oct 1993, Pocono Manor, PA, USA, pp. 174-179.

[59] T. Takada. *Acoustic and Optical Methods for Measuring Electric Charge Distributions in Dielectrics*, in IEEE Transactions on Dielectrics and Electrical Insulation, 1999, Vol. 6 (5), pp.519-547.

[60] Y. Li, M. Yasuda, T. Takada. *Pulsed Electroacoustic Method for Measurement of Charge Accumulation in Solid Dielectrics*, in IEEE Transactions on Dielectrics and Electrical Insulation, 1994, Vol. 1 (2), pp.188-195.

[61] M. Fu, G. Chen, A. E. Davies, J. Head. *Space Charge Measurements in Cables using PEA Method: Signal Data Processing Considerations*, in IEEE 7th International Conference on Solid Dielectrics, June 25-29, 2001, Eindhoven, The Netherlands, pp. 219-222.

[62] Y. Zhu, D. Tu, T. Takada. *Mathematical Analysis and Interpretation of Pulsed Electro-acoustic System*, in IEEE International Conference on Properties and Applications of Dielectric Materials, 21-26 Jun 2000,Xi'an, China, pp. 63-66.

[63] G. Chen , Y. L. Chong , M. Fu. *Calibration of Pulse Electroacoustic Technique in the Presence of Trapped Charge*, in Measurement Science and Technology, 2006, Vol. 17 (7), pp.1974-1980

[64] Y. L. Chong, G. Chen, H. Miyake, K. Matsui, Y. Tanaka, T. Takada. *Space Charge and Charge Trapping Characteristics of Crosslinked Polyethylene Subjected to AC Electric Stresses*, in Journal of Physics and Dielectric Application, 2006, Vol. 39 (8), pp.1658-1666.

[65] M. Fu, G. Chen, A.E. Davies, J.G. Head. *Space charge measurements in power cables using a modified PEA system* in Eighth International Conference on Dielectric Materials, Measurements and Applications, 2000,Edinburgh , UK pp. 74 - 79

[66] W. Choo, G. Chen. *Electric field determination in DC polymeric power cable in the presence of space charge and temperature gradient under dc conditions*, in 2007,Beijing, China, pp. 321-324.

[67] J. Zhao, Z. Xu, G. Chen, P.L. Lewin. *Numeric Description of Space Charge in Polyethylene Under AC Electric Fields*, in Journal of Applied Physics, 2010, Vol. 108 (12), pp.124107-1 -124107-7.

[68]   X. Wang, N. Yoshimura, Y. Tanaka, K. Murata, T. Takada. *Space Charge Characteristics in Crosslinking Polyethylene Under Electrical Stress from DC to Power Frequency* in Journal of Physics D: Applied Physics, 1998, Vol. 31 (16), pp.2057.

[69]   Z. Xu, J. Zhao, G. Chen. *An Improved Pulsed Electroacoustic System for Space Charge Measurement under AC Conditions*, in UHVnet, 18-19 January 2011, Winchester, UK, pp. 75.

[70]   Z. Xu, J. Zhao, G. Chen. *An Improved Pulsed Electroacoutic System for Space Charge Measurement Under AC Conditions*, in Proceedings of the 2010 IEEE International Conference on Solid Dielectrics, 4-9 July 2010,Potsdam, Germany, pp. 1-4.

[71]   A. See, J. C. Fothergill, L. A. Dissado, J.M. Alison. *Measurement of Space-Charge Distributions in Solid Insulators Under Rapidly Varying Voltage Vsing the High-Voltage, High-Speed Pulsed Electro-Acoustic (PEA) Apparatus*, in Measurement Science and Technology, 2001, Vol. 12 (8), pp.1227-1234.

[72]   Z. Xu. *Space Charge Measurement and Analysis in Low Density Polyethylene Film*, A PhD. thesis of University Of Southampton, Southampton, 2009, 195 pages.

[73]   Y.F.F. Ho. *Space Charge Measurement of XLPE-A Comparison of AC and DC Stressing*, A   Ph.D thesis of   University Of Southampton,   Southampton, September 2001, 202 pages.

[74]   N. L. Dao, P. L. Lewin, I. L. Hosier, S. G. Swingler. *A Comparison Between LDPE and HDPE Cable Insulation Properties Following Lightning Impulse Ageing*, in IEEE International Conference on Solid Dielectrics, 4 - 9 July 2010, Potsdam, Germany, pp. 72-75.

[75]   Y.L. Chong, G. Chen, I.L. Hosier, A.S. Vaughan, Y.F.F. Ho. *Heat Treatment of Crosslinked Polyethylene and its Effect on Morphology and Space Charge Evolution*, in IEEE Transactions on Dielectrics and Electrical Insulation, 2005, Vol. 12 (6), pp.1209-1221.

[76]   J.V. Gulmine, L. Akcelrud. *Correlations Between Structure and Accelerated Artificial Ageing of XLPE*, in European Polymer Journal, 2006, Vol. 42 (3), pp.553-562.

[77]   *Goodfellow Cambridge Ltd.* , available from   http://www.goodfellow.com/about-us/, access on 20 September 2011

[78]   E.W.   Weisstein,   *Fourier   Transform   Spectrometer*   available   from http://scienceworld.wolfram.com/physics/FourierTransformSpectrometer.html, access on 31 May 2009

[79]   *Fourier Transform Infrared Spectroscopy* available from http://www.wcaslab.com/TECH/TBFTIR.HTM, access on 31 May 2009

[80]   J.M. Garcia-Martinez, O. Laguna, S. Areso, E.P. Collar. *FTIR Quantitative Characterization of Chemically Modified Polypropylenes Containing Succinic Grafted Groups*, in Journal of Applied Polymer Science, 1999, Vol. 73 (14), pp.2837-2847.

[81]   J. Hanson, *Introduction to Interpretation of Infrared Spectra*, available from http://www2.ups.edu/faculty/hanson/Spectroscopy/IR/IRInterpretation.htm, access on 27 June 2009

[82]   G. Herzberg. *Molecular Spectra and Molecular Structure, Volume 3: Electronic spectra and electronic structure of polyatomic molecules*,New York: Van Nostrand, Reinhold, 1966.

[83]   J.V. Gulmine, L. Akcelrud. *FTIR Characterization of Aged XLPE*, in Polymer Testing, 2006, Vol. 25 (7), pp.932-942.

[84]   M. Fu, G. Chen, A. Dissado, J.C. Fothergill. *Influence of Thermal Treatment and Residues on Space Charge Accumulation in XLPE for DC Power Cable Application*, in IEEE Transactions on Dielectrics and Electrical Insulation, 2007, Vol. 14 (1), pp.53-64.

[85]   N. Nibbio, T. Uozumi, N. Yasuda, T. Fukui. *Effects of Additives on Space Charge in XLPE Insulation Crosslinking Reagent and Antioxidant*, in IEEE International Symposium on Electrical Insulation, 5-8 June 1994,Pittsburgh, PA, USA, pp. 559-562.

[86]   N. Hirai, R. Minami, Y. Ohki, M. Okashita, T. Maeno. *Effects of Byproducts of Dicumyl Peroxide on Space Charge Formation in Low Density Polyethylene*, in IEEE International Conference on Electrical Insulation and Dielectric Phenomena, 14-17 Oct 2001,Kitchener, Ont, Canada, pp. 478 - 483

[87]   G.C. Montanari, D. Fabiani. *Evaluation of DC Insulation Performance Based on Space Charge Measurements and Accelerated Life Tests*, in IEEE Transactions on Dielectrics and Electrical Insulation, 2000, Vol. 7 (3), pp.322-328.

[88]   Y. Maeno, N. Hirai, Y. Ohki, T. Tanaka, M. Okashita, T. Maeno. *Effects of Crosslinking Byproducts on Space Charge Formation in Crosslinked Polyethylene*, in IEEE Transactions on Dielectrics and Electrical Insulation, 2005, Vol. 12 (1), pp.90-97.

[89]   T. Mizutani, C. Zhang, M. Ishioka. *Space Charge Behavior in LDPE and Its Blend Polymers*, in 11th International Symposium on Electrets, 2002,Melbourne, Australia, pp. 147-150.

[90]   G. Chen, Z. Xu. *Charge Trapping and Detrapping in Polymeric Materials*, in Journal of Applied Physics, 2009, Vol. 106 (12), pp.123707 - 123707-5.

[91]   G. Teyssedre, C. Laurent, A. Aslanides, N. Quirke, L.A. Dissado, G.C. Montanari, A. Campus, L. Martinotto. *Deep Trapping Centers in Crosslinked Polyethylene Investigated by Molecular Modeling and Luminescence Techniques*, in Dielectrics and Electrical Insulation, IEEE Transactions on, 2001, Vol. 8 (5), pp.744-752.

[92]   G. Teyssedre , C. Laurent. *Charge Transport Modeling in Insulating Polymers: From Molecular to Macroscopic Scale* in IEEE Transactions on Dielectrics and Electrical Insulation, October 2005, Vol. 12 (5), pp.857 - 875.

[93]   O. Fanjeau, D. Mary, D. Malec. *A Note on Charge Recombination in Low Density Polyethylene Under A Moderate ac 50 Hz Field*, in Journal of Physics D: Applied Physics, 2000, Vol. 33 (8), pp.L61.

[94]   C. Thomas, G. Teyssedre, C. Laurent. *Space Charge Dynamic in Polyethylene: from DC to AC Stress*, in Journal of Physics D: Applied Physics, 2011, Vol. 44 (1), pp.015401.

[95]   R.W. Sillars. *Electrical Insulating Materials and Their Application*,Peter Peregrinus Ltd., 1973.

[96]   A.R. Blythe. *Electrical Properties of Polymer* Chambridge University Press, 1979. 191 pages.

[97]   P.J. Harrop. *Dielectrics*. Bathgate, West Lothian,London Butterworths, 1972. 155 pages.

[98]   K.S. Cole, R.H. Cole. *Dispersion and Absorption in Dielectrics. 1. Alternating Current Characteristics*, in J. Chem. Phys., 1941, Vol. 9 (4), pp.341-351.

[99]   J.G. Powles. *The Interpretation of Dielectric Measurement using the Cole-Cole Plot*, in Proc. Phy. Soc. B, 1951, Vol. 64, pp.81-82.

[100]   Y.Z. Wei, S. Sridhar. *A new Graphical Representation for Dielectric Data*, in J. Chem. Phys.,, 1993, Vol. 99 (4), pp.3119-3124.

[101]   N. Hirai, R. Minami, T. Tanaka, Y. Ohki. *Chemical Group in Crolsslinking Byproducts Responsible for Charge Trapping in Polyethylene*, in IEEE Transactions on Dielectrics and Electrical Insulation, April 2003, Vol. Vol. 10 (Issue 2), pp.320-330.

[102]   E. Neagu, P. Pissis, L. Apekis, J.L. Gomez Ribelles. *Dielectric Relaxation Spectroscopy of Polyethylene Terephthalate (PET) Films*, in Journal of Physics D: Applied Physics, 1997, Vol. 30 (11), pp.1551-1560.

[103]   M. Fu, G. Chen, L.A. Dissado, J.C. Fothergill, C. Zou. *The Effect of Gamma Irradiation on Space Charge Behaviour and Dielectric Spectroscopy of Low Density Polyethylene*, in International Conference on Solid Dielectrics, 8-13 July 2007,Winchester, United kingdom, pp. 442-445.
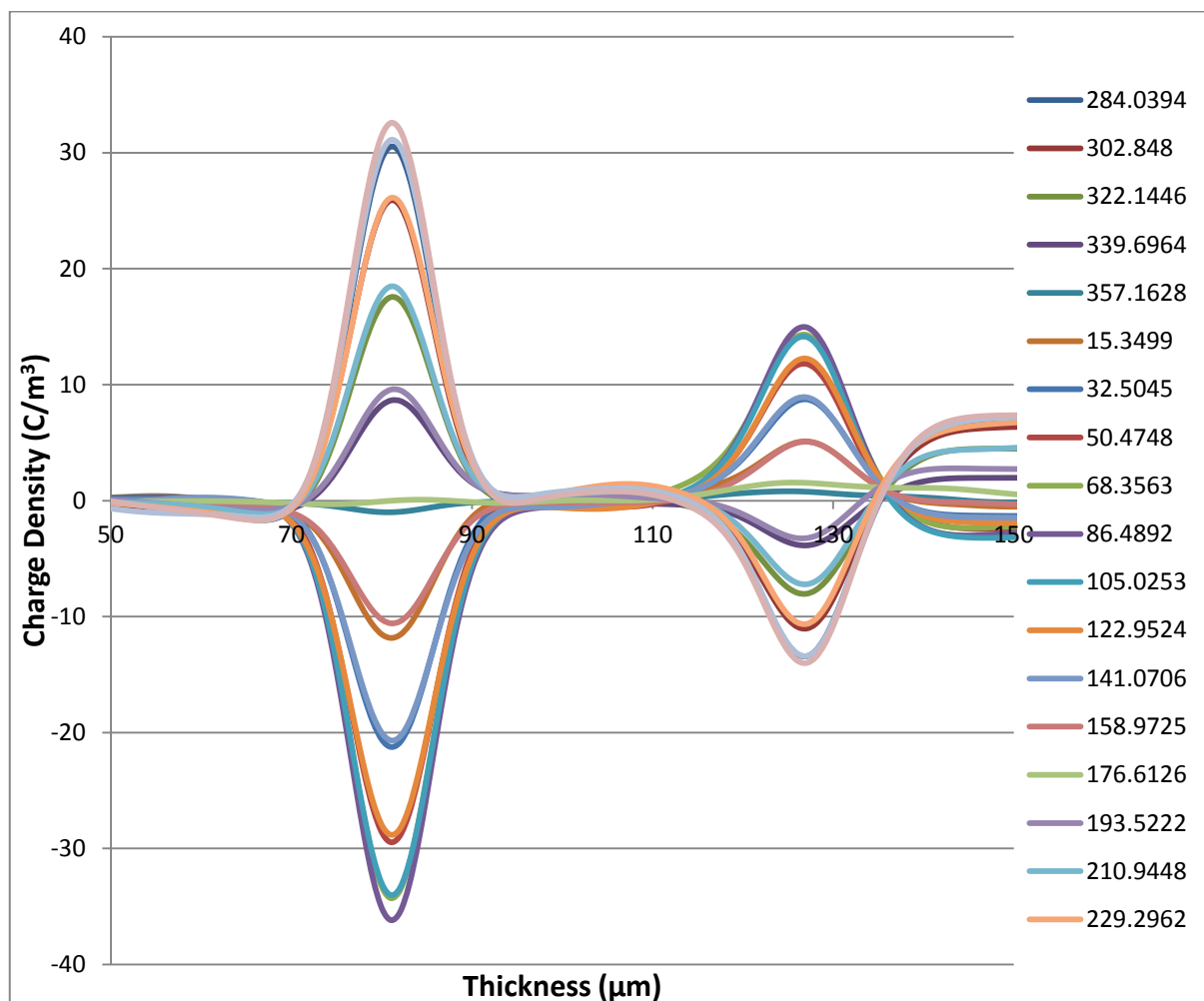
[104]   R.J. Sengwa, S. Choudhary, S. Sankhla. *Dielectric Spectroscopy of Hydrophilic Polymers-Montmorillonite Clay Nanocomposite Aqueous Colloidal Suspension*, in Colloids and Surfaces A: Physicochemical and Engineering Aspects, 2009, Vol. 336 (1-3), pp.79-87.

[105]   V. Adamec, J.H. Calderwood. *Electrical Conduction And Polarisation Phenomena In Polymerics at Low Fields*, in Journal of Physics D: Applied Physics, 1978, Vol. 11 (6), pp.781-800.

[106]   J. Lowell. *Absorption And Conduction Currents in Polymers: A Unified Model*, in Journal of Physics D: Applied Physics, 1990, Vol. 23 (2), pp.205-210.

[107]   R. Minami, N. Hirai, Y. Ohki, M. Okashita, T. Maeno. *Effects of Liquid Chemicals on Space Charge Evolution in Low Density Polyethylene*, in International Symposium on Electrical Insulating Materials, 19-22 Nov. 2001,Himeji, Japan, pp. 87-90.

[108]   Y. Suzuoki, H. Muto, G. X. Cai, T. Mizutani, M. Ieda. *Effects of Polar Groups on Electrical Conduction in Polyethylene*, in Japanese Journal of Applied Physics, 1984, Vol. 23 (1), pp. 91-92.

[109]   K.S. Suh, C.R. Lee, J.S. Noh, J. Tanaka, D.H. Damon. *Electrical Conduction in Polyethylene with Semiconductive Electrodes*, in IEEE Transactions on Dielectrics and Electrical Insulation, 1994, Vol. 1 (2), pp.224-230.

[110]   G.C. Montanari. *Electrical Degradation Threshold of Polyethylene Investigated by Space Charge and Conduction Current Measurements*, in IEEE Transactions on Dielectrics and Electrical Insulation, 2000, Vol. 7 (3), pp.309-315.

[111]   J.J. O'Dwyer. *Model for High Field Conduction in a Dielectric* in IEEE transactions on Electrical Insulation, 1986, Vol. EI-21 (2), pp.121-127.

[112]   G.C. Montanari, P.H.F. Morshuis. *Space Charge Phenomenology in Polymeric Insulating Materials*, in IEEE Transactions on Dielectrics and Electrical Insulation, 2005, Vol. 12 (4), pp.754-767.

[113]   G.C. Montanari, G. Mazzanti, F. Palmieri, A. Motori, G. Perego, S. Serra. *Space Charge Trapping and Conduction in LDPE, HDPE and XLPE*, in Journal of Physics D: Applied Physics, 2001, Vol. 34 (18), pp.2902-2911.

[114]   J. Li, Y. Zhang, Z. Xia, X. Qin, and Z. Peng. *Action of Space Charge on Aging and Breakdown of Polymers*. Chinese Science Bulletin,2001, pp. 796-800.

[115]   S. Diaham, S. Zelmat, M.L. Locatelli, S. Dinculescu, M. Decup, T. Lebey. *Dielectric Breakdown of Polyimide Films: Area, Thickness and Temperature Dependence*, in IEEE Transactions on Dielectrics and Electrical Insulation, 2010, Vol. 17 (1), pp.18-27.

[116] M. Ieda, M. Nagao, M. Hikita. *High-field Conduction and Breakdown in Insulating Polymers. Present Situation and Future Prospects*, in IEEE Transactions on Dielectrics and Electrical Insulation, 1994, Vol. 1 (5), pp.934-945.

[117] I.L. Hosier, A.S. Vaughan, S.G. Swingler. *The Effects of Measuring Technique and Sample Preparation on the Breakdown Strength of Polyethlyene*, in IEEE Transactions on Dielectrics and Electrical Insulation, 2002, Vol. 9 (3), pp.353-361.

[118] J.C. Fothergill. *Estimating the Cumulative Probability of Failure Data Points to be Plotted on Weibull and Other Probability Paper*, in IEEE transactions on Electrical Insulation, 1990, Vol. 25 (3), pp.489-492.

[119] G. Gherbaz. *Nanostructured Polymers: Morphology and Properties*, A PhD. thesis of University Of Southampton, Southampton, March 2009, 189 pages.

[120] S. Yan, K. Sheu, D.H. Damon, S.J. Huang, J.F. Johnson. *Electric Strength of XLPE Containing Acetophenone and Other Volatile Substances*, in IEEE International Symposium on Electrical Insulation, 3-6 Jun 1990,Toronto, Canada, pp. 305-308.

[121] S.T. Hagen, E. Ildstad. *Reduction of AC-Breakdown Strength Due to Particle Inclusions in XLPE Cable Insulation*, in Third International Conference On Power Cable and Accessories, 23-25 Nov 1993,London, England, pp. 165-168.

[122] M. Fukuma, K. Fukunaga, T. Maeno. *Space Charge Dynamics in LDPE Films Immediately Before Breakdown*, in IEEE Transactions on Dielectrics and Electrical Insulation, 2001, Vol. 8 (2), pp.304-306.

[123] D.H. Damon, S.J. Huang, J.F. Johnson. *Dielectric Breakdown of XLPE Containing Actophenone and Cumyl Alcohol*, in Conference on Electrical Insulation and Dielectric Phenomena, 1991, 20-23 Oct. 1991, Knoxcille, Tennessee, pp. 381 - 385.
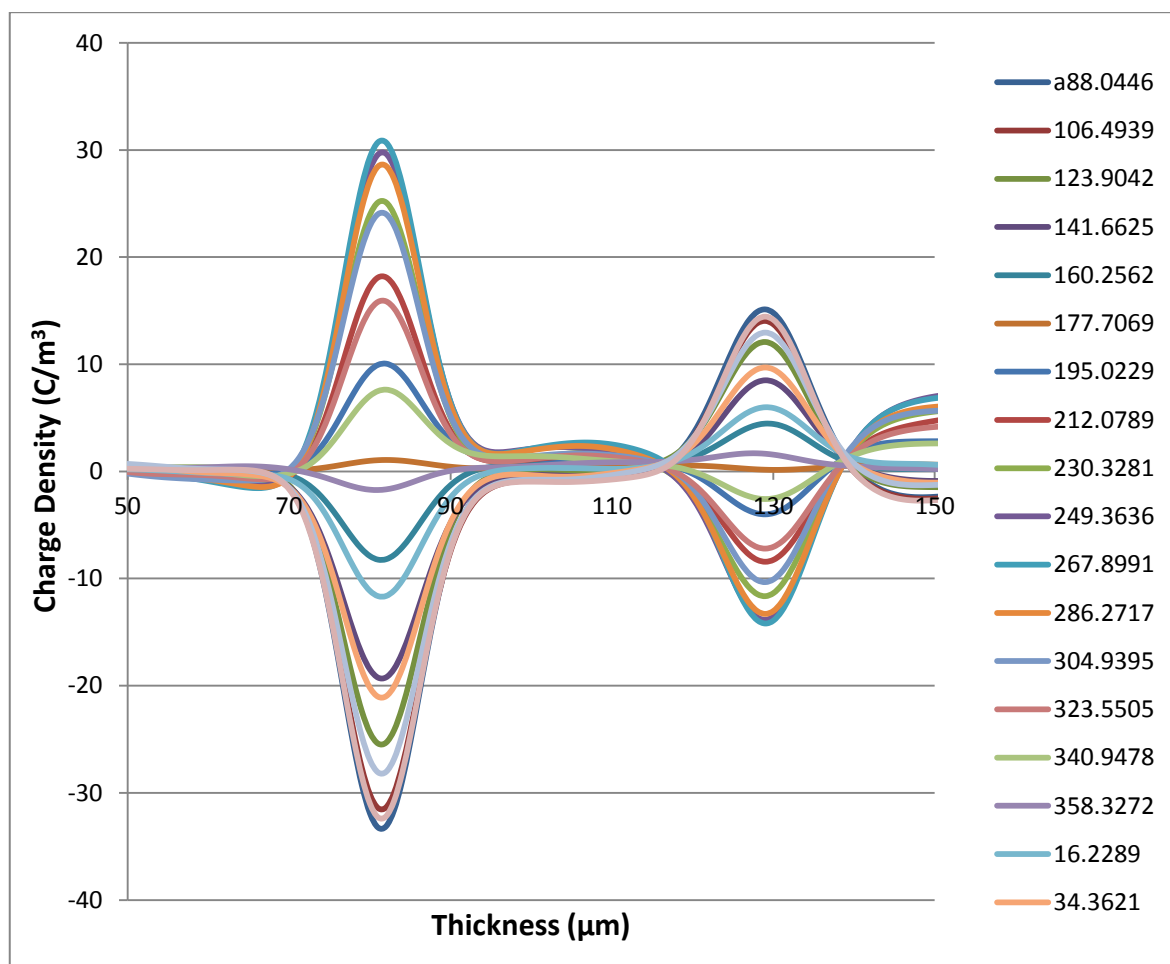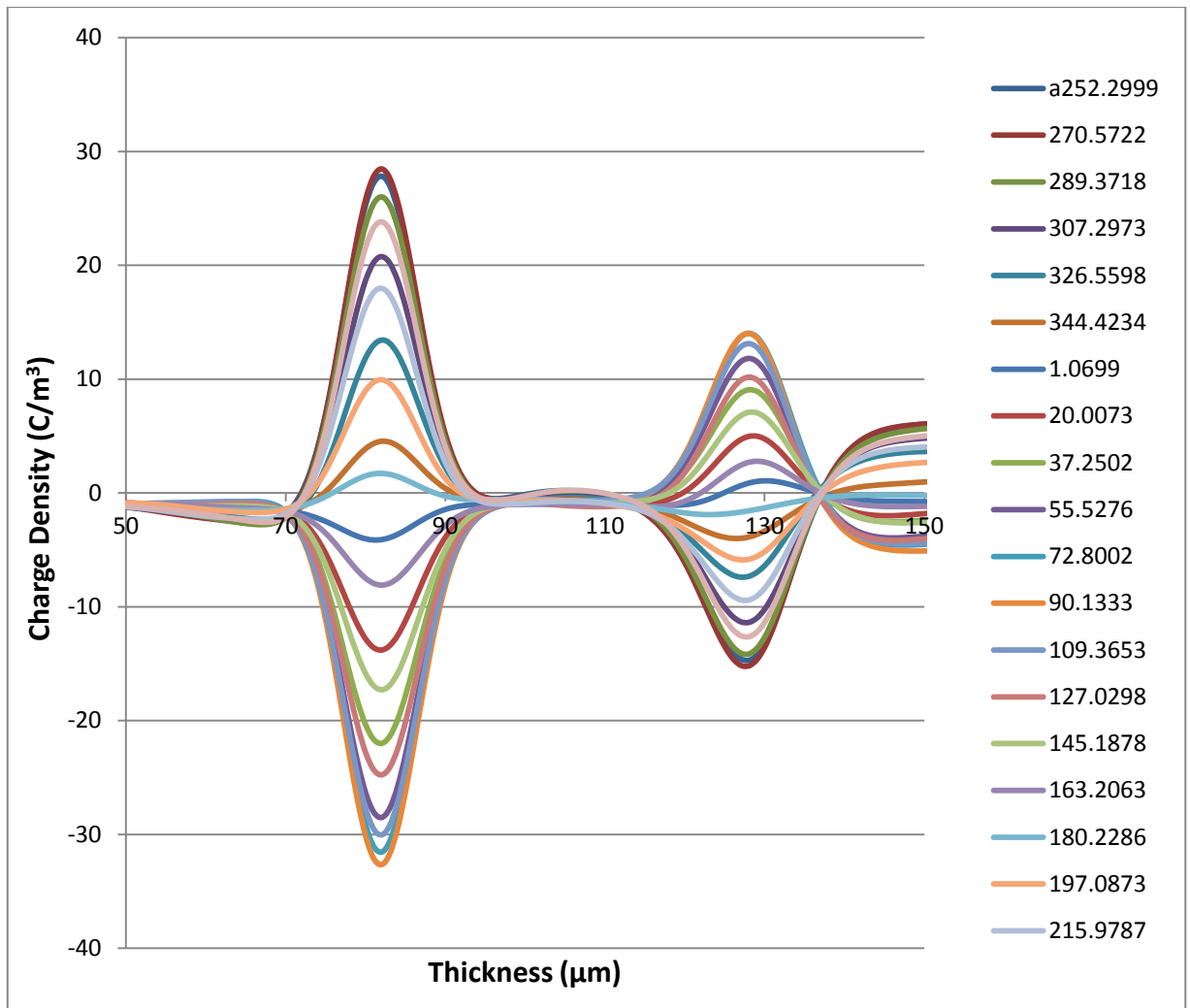
Appendix: AC Volt On result
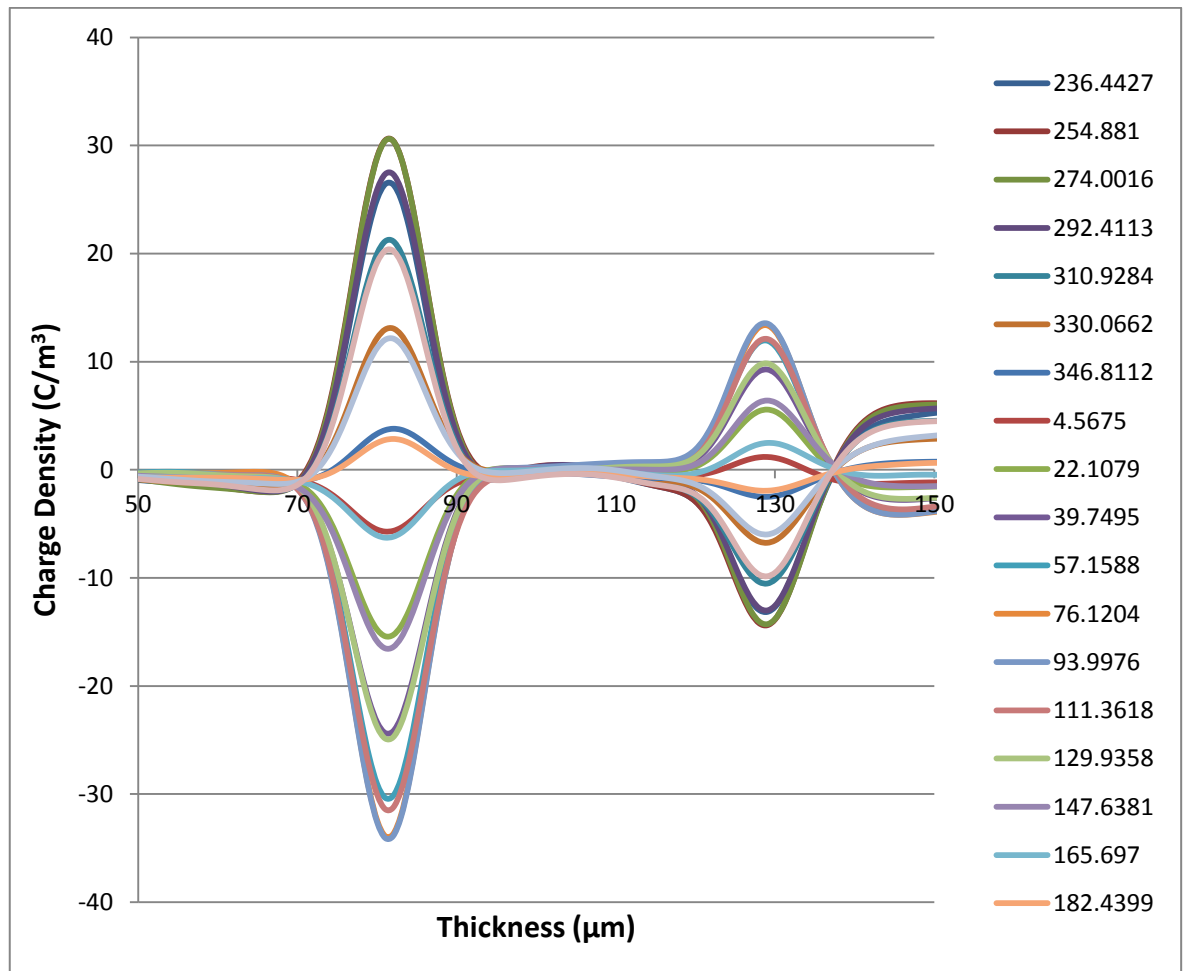
Charge Density of 180μm clean LDPE during Volt on condition after 4 hours stress at 28 kV/mm ac.

Charge Density of 180µm acetophenone soaked LDPE during Volt on condition after 4 hours stress at 28 kV/mm ac.

Charge Density of 180μm α-methylstyrene soaked LDPE during Volt on condition after 4 hours stress at 28 kV/mm ac.

Charge Density of 180µm cumyl alcohol soaked LDPE during Volt on condition after 4 hours stress at 28 kV/mm ac.